Reionization History of the Universe and the 21cm Background

Paul R. Shapiro

University of Texas at Austin

"The Standard Model of the Universe,"

13th Paris Cosmology Colloquium, Ecole Internationale Daniel Chalonge,

Observatoire de Paris

July 23, 2009

Reionization History of the Universe and the 21cm Background

Paul R. Shapiro

University of Texas at Austin

Collaborators:
Ilian Iliev (U. Sussex), Garrelt Mellema (Stockholm U.),
Ue-Li Pen, J. Richard Bond, Patrick McDonald (CITA/U.Toronto),
Hugh Merz (U. Waterloo), Kyungjin Ahn (Chosun U./Korea),
Leonid Chuzhoy (U.Chicago), Marcelo Alvarez (KIPAC/Stanford),
Eiichiro Komatsu, Jun Koda, Elizabeth Fernandez, Yi Mao (U. Texas),
Benedetta Ciardi (MPA), Rennan Barkana (Tel Aviv U)

The Epoch of Reionization

- Absorption spectra of quasars have long shown that the intergalactic medium at redshifts $z < 6$ is highly ionized, with a residual neutral H atom concentration of less than 1 atom in 10^4 .

  ===> universe experienced an “epoch of reionization” before this.

The Epoch of Reionization

- Absorption spectra of quasars have long shown that the intergalactic medium at redshifts $z < 6$ is highly ionized, with a residual neutral H atom concentration of less than 1 atom in 10^4 .

  ===> universe experienced an "epoch of reionization" before this.

- Sloan Digital Sky Survey quasars have been observed at $z > 6$ whose absorption spectra show dramatic increase in the H I fraction at this epoch as we look back in time.

  ===> epoch of reionization only just ended at $z \gtrsim 6$.

SDSS quasars show Lyman α opacity of intergalactic medium rises with increasing redshift at z = 6 ➔ IGM more neutral ➔ reionization just ending?

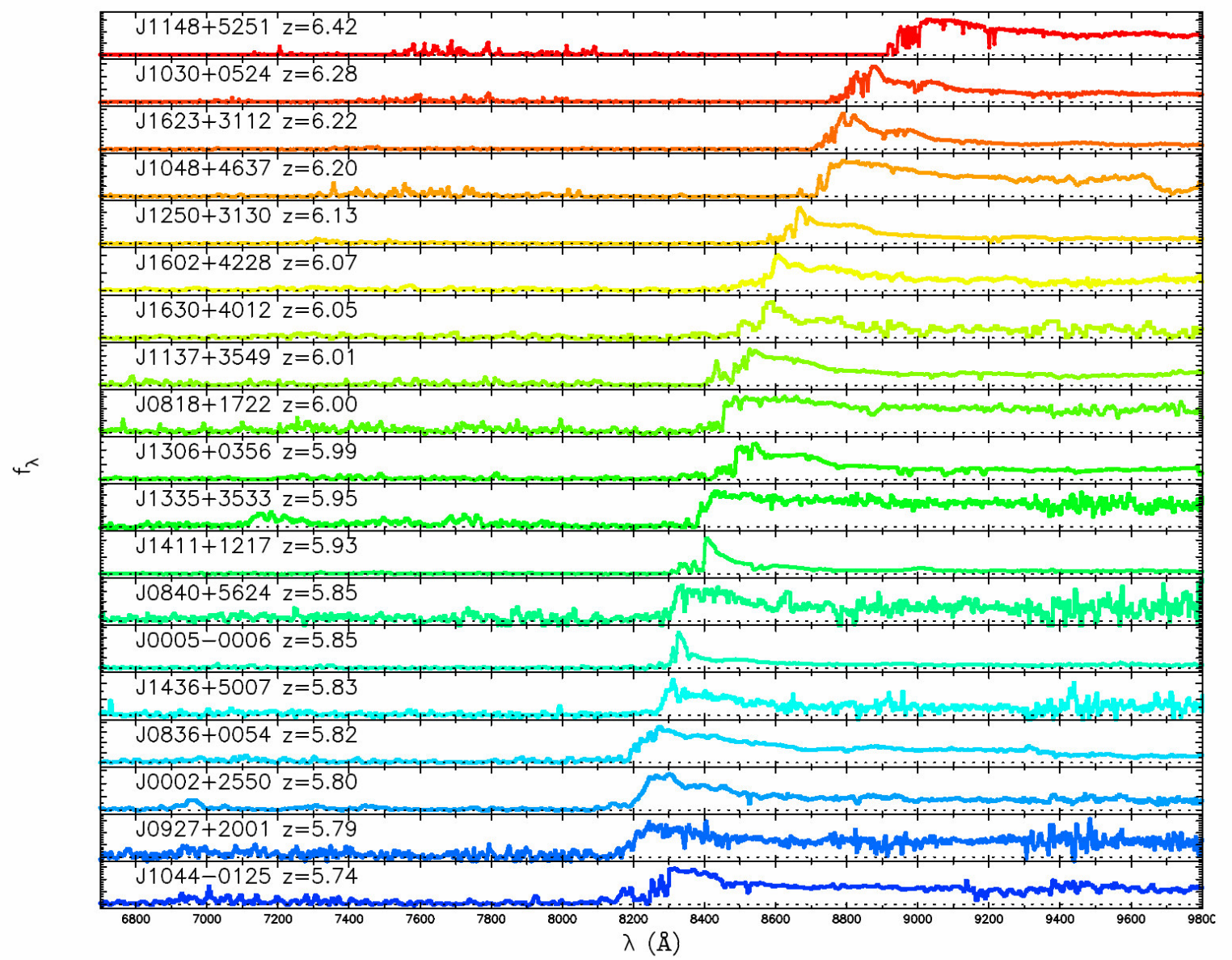

Fan et al (2005)

SDSS quasars show Lyman α opacity of intergalactic medium rises with increasing redshift at z = 6 ➔ IGM more neutral ➔ reionization just ending?

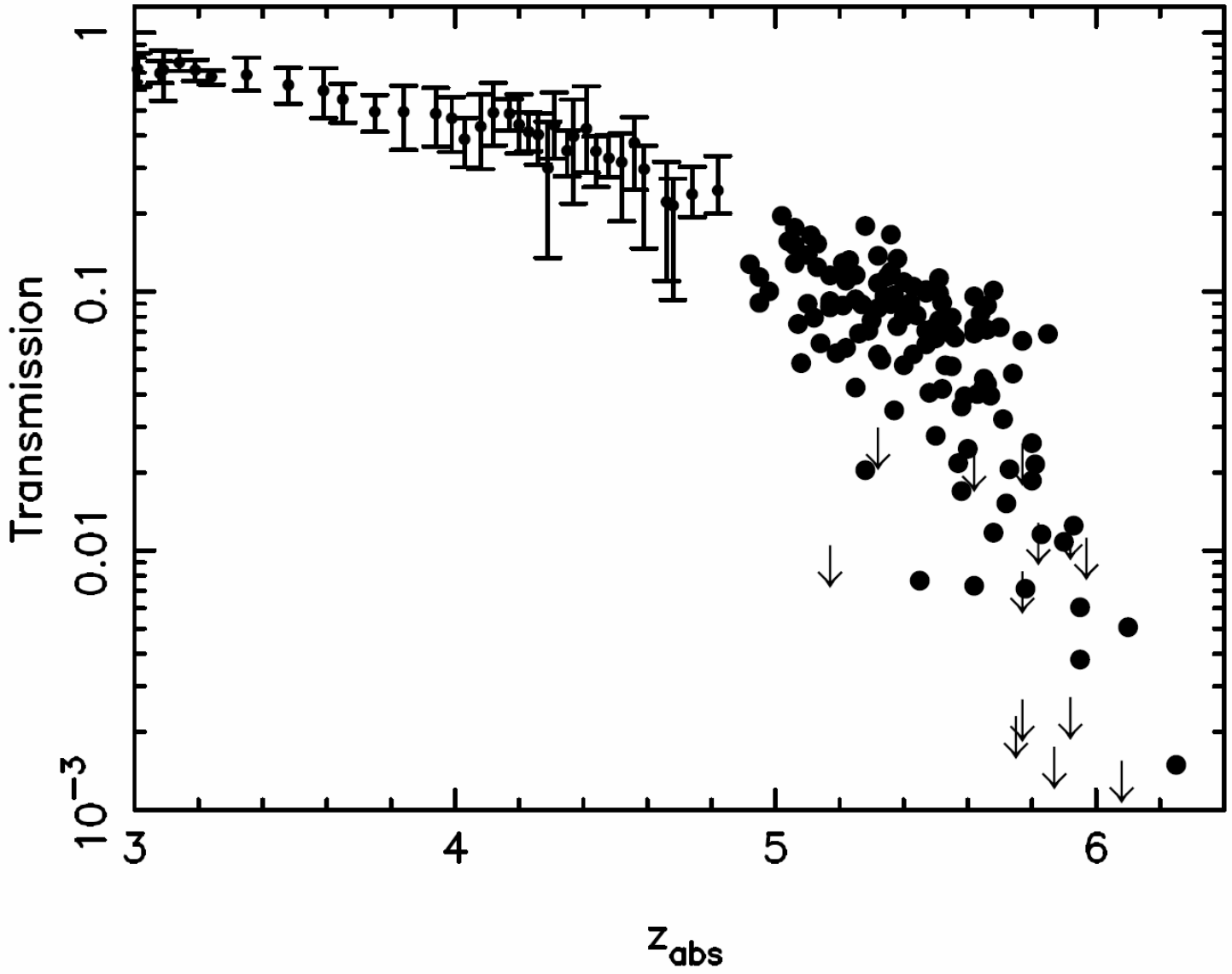

Fan et al (2006)

The Epoch of Reionization

- Absorption spectra of quasars have long shown that the intergalactic medium at redshifts $z < 6$ is highly ionized, with a residual neutral H atom concentration of less than 1 atom in 10^4 .

  ===> universe experienced an "epoch of reionization" before this.
- Sloan Digital Sky Survey quasars have been observed at $z > 6$ whose absorption spectra show dramatic increase in the H I fraction at this epoch as we look back in time.

  ===> epoch of reionization only just ended at $z \gtrsim 6$.
- **The cosmic microwave background (CMB) exhibits polarization which fluctuates on large angular scales; WMAP finds that almost 9% of the CMB photons were scattered by free electrons in the IGM, but only 4% could have been scattered by the IGM at $z < 6$.**

  ===> IGM must have been ionized much earlier than $z = 6$ to supply enough electron scattering optical depth

  ===> reionization already substantial by $z \gtrsim 11$

EoR Probes the First Billion Years of Cosmic Star Formation

Observations of galaxies and quasars as far back in time as currently available suggest that galaxies dominated the production of the ionizing photons necessary to finish reionization by z > 6, while quasars were not numerous or luminous enough

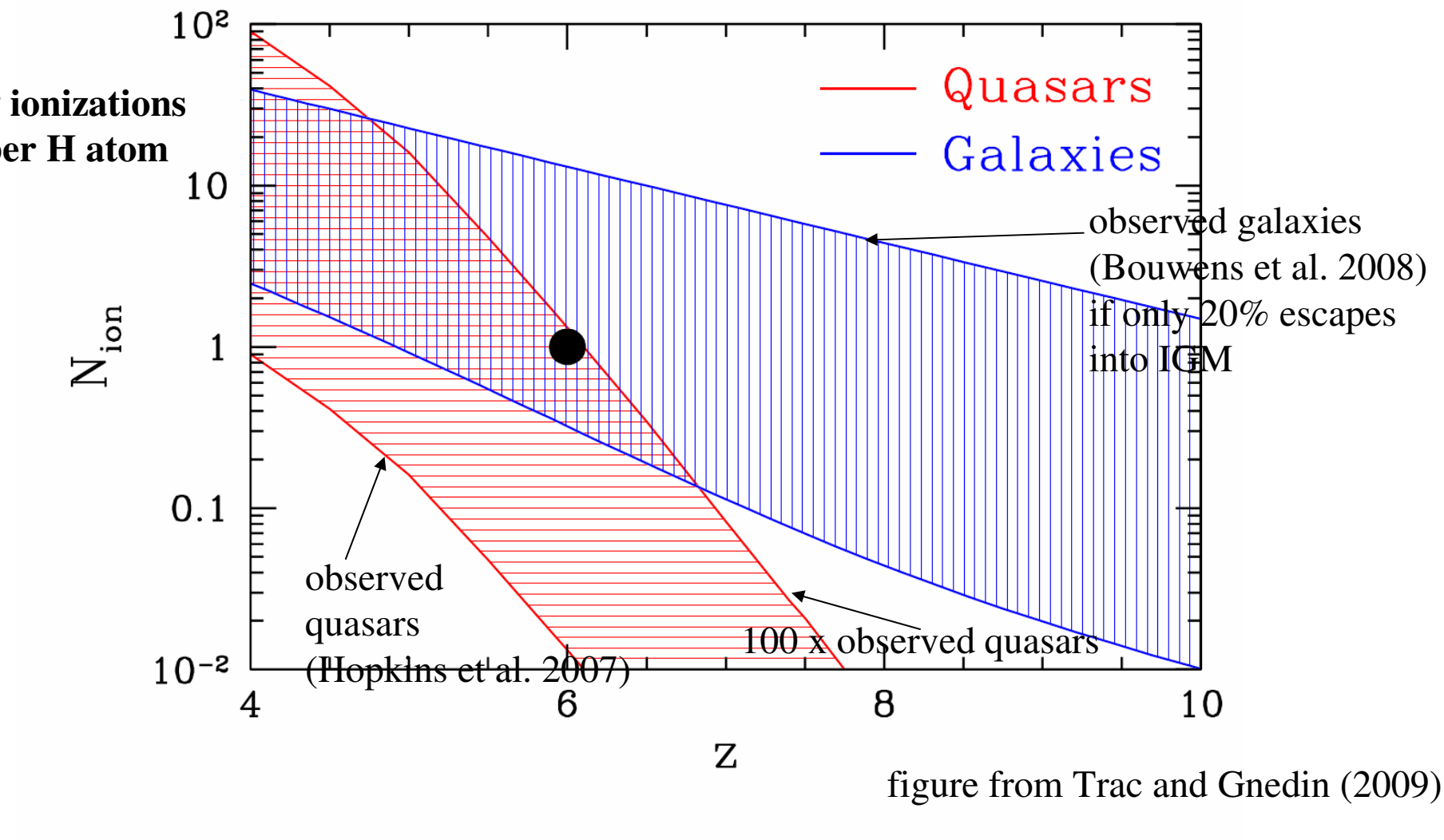

figure from Trac and Gnedin (2009)

EoR Probes the Primordial Power Spectrum Down to Very Small Scales

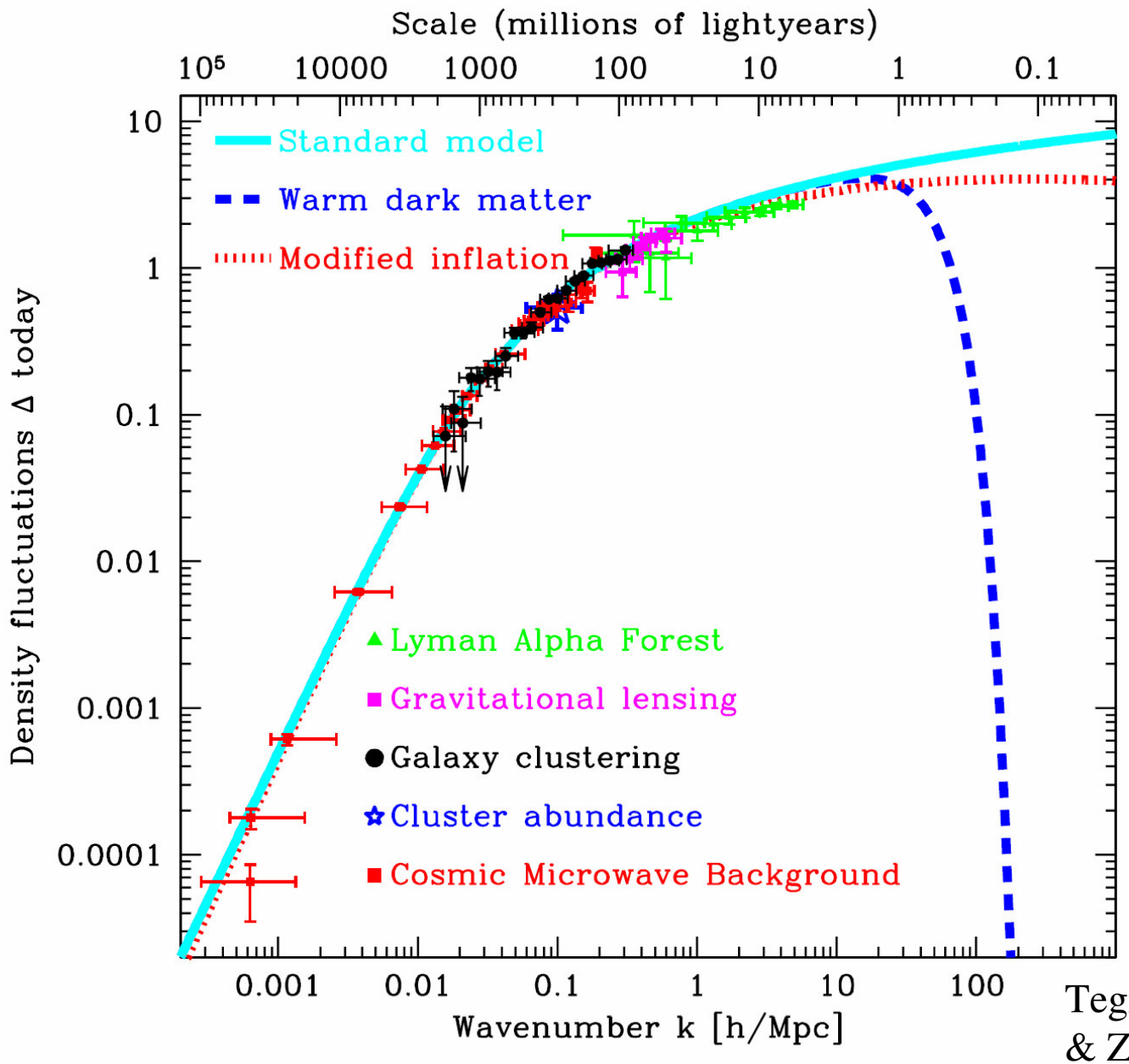

Tegmark
& Zaldarriaga (2008)

EoR Probes the Nature of Dark Matter

e.g. neutralino DM annihilations can partially ionize and heat the IGM ===>

CMB polarization observations of electron scattering optical depth

+

quasar absorption line Ly α forest observations of the IGM

===> limits allowed " m_X (DM particle mass) - ‹σv› (annihilation cross section)" parameter space

e.g. recent suggestions of large m_X + large ‹σv› into leptons suggested to explain anomalous charged-cosmic-ray signals reported by PAMELA, FERMI, & HESS experiments are ruled out; *too many free electrons produced*

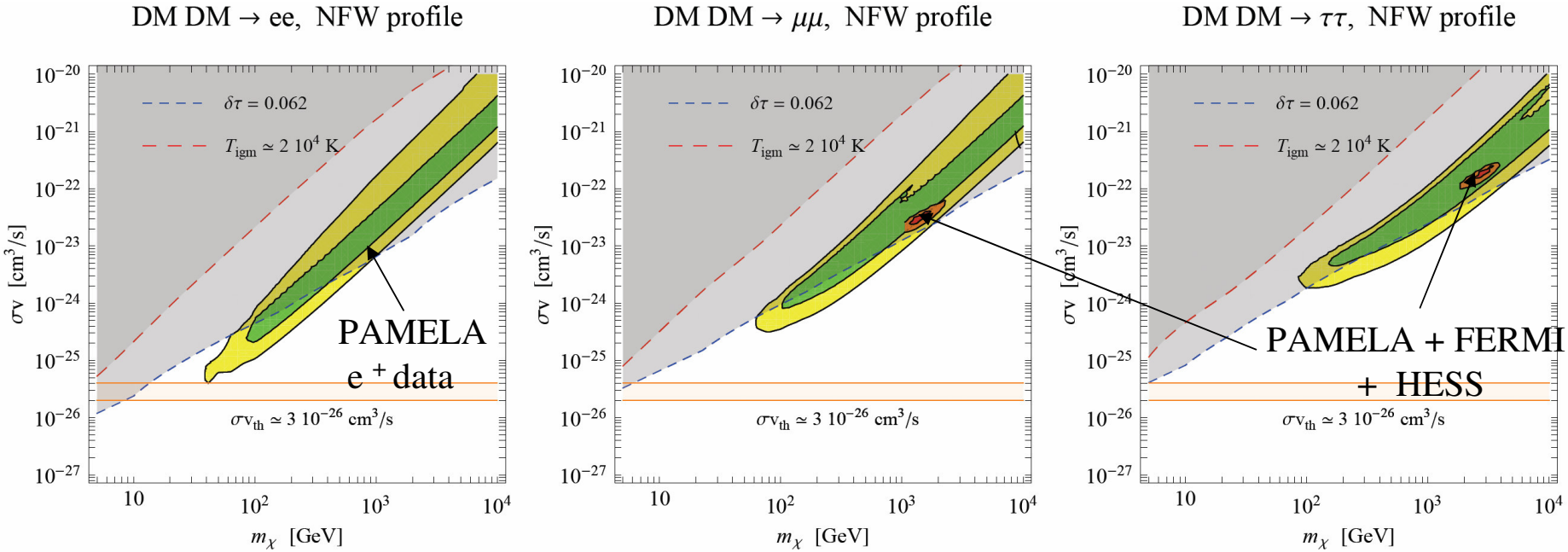

Cirelli, Iocco & Panci (2009)

Structure formation in ΛCDM at z = 10

simulation volume = $(100\ h^{-1}\mathrm{Mpc})^3$, comoving

1624^3 particles on 3248^3 cells

Projection of cloud-in-cell densities of 20 Mpc slice

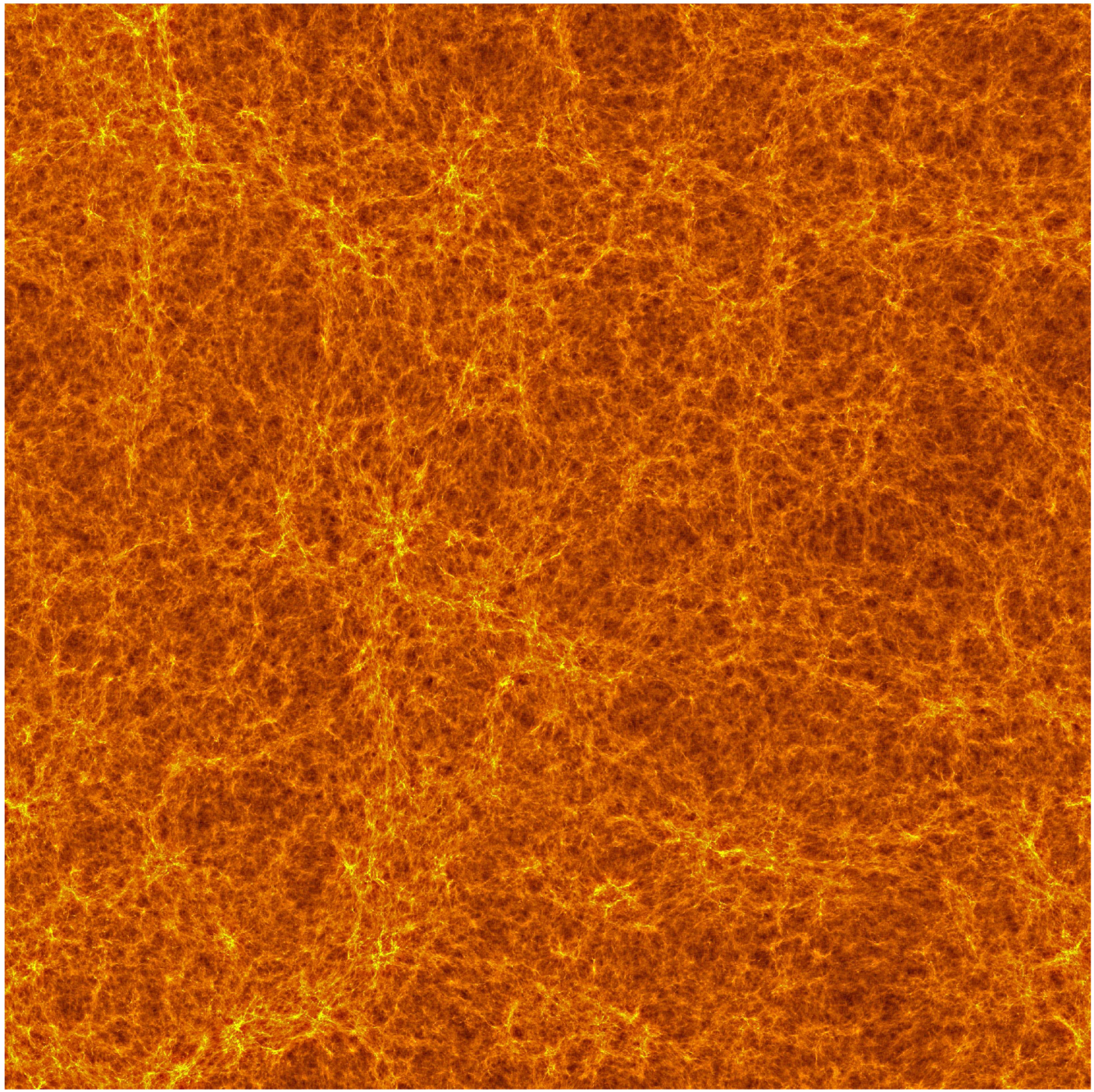

A Dwarf Galaxy Turns on at z=9

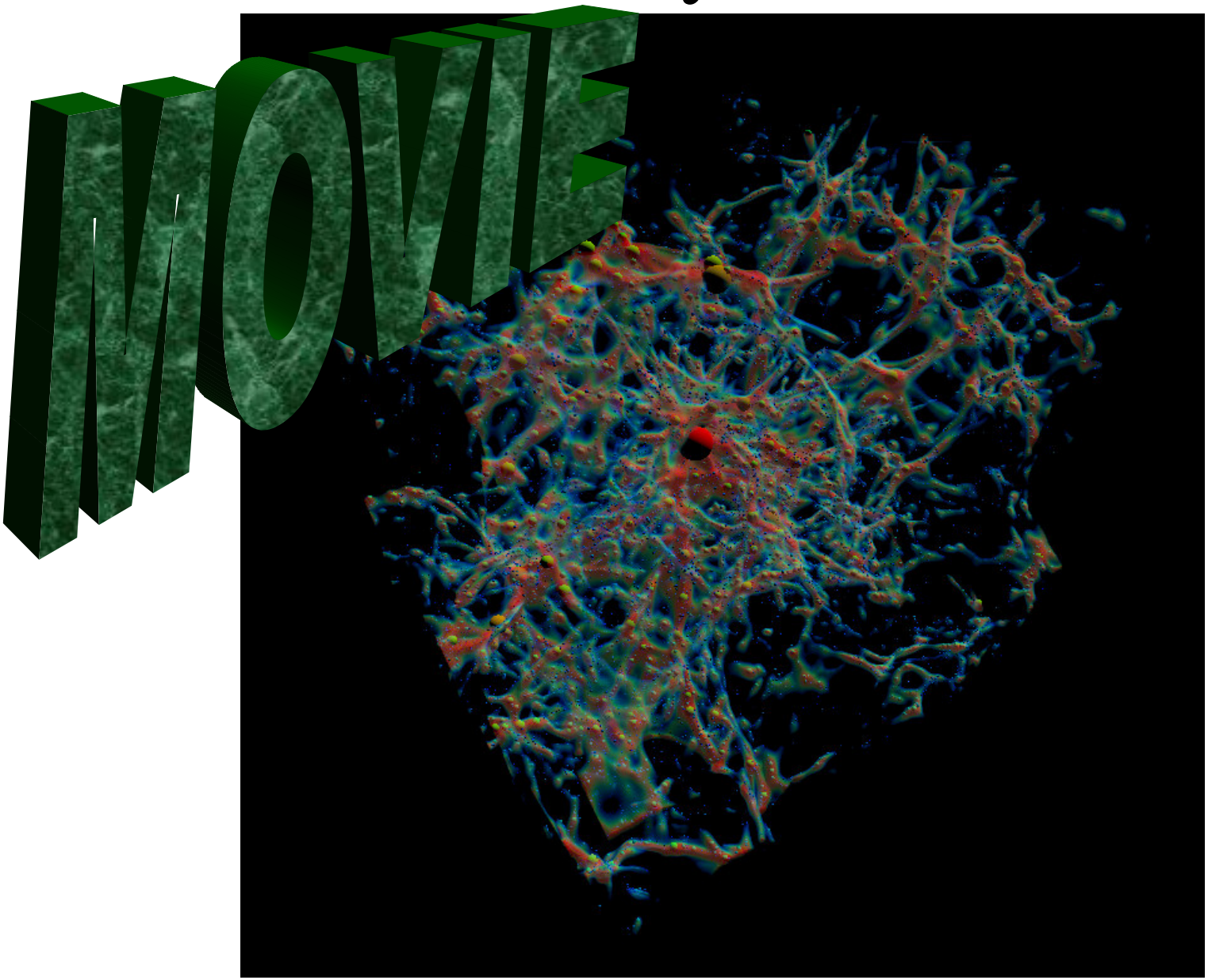

THE PHOTOEVAPORATION OF MINIHALOS OVERTAKEN BY COSMOLOGICAL I-FRONTS

(Shapiro, Iliev & Raga 2004, MNRAS, 348, 753;
Iliev, Shapiro, & Raga 2005, MNRAS, 361, 405)

- We performed radiation-hydrodynamical simulations of the photoevaporation of a cosmological minihalo overrun by a weak, R-type I-front in surrounding IGM, created by external source of radiation.
- 2D, axisymmetric, Eulerian hydro code with Adaptive Mesh Refinement and the van Leer flux-splitting algorithm, including radiative transfer (H, He bound-free opacity).
- Nonequilibrium ionization rate equations: H, He + (C, N, O, Ne, S) @ 10-3 solar abundance

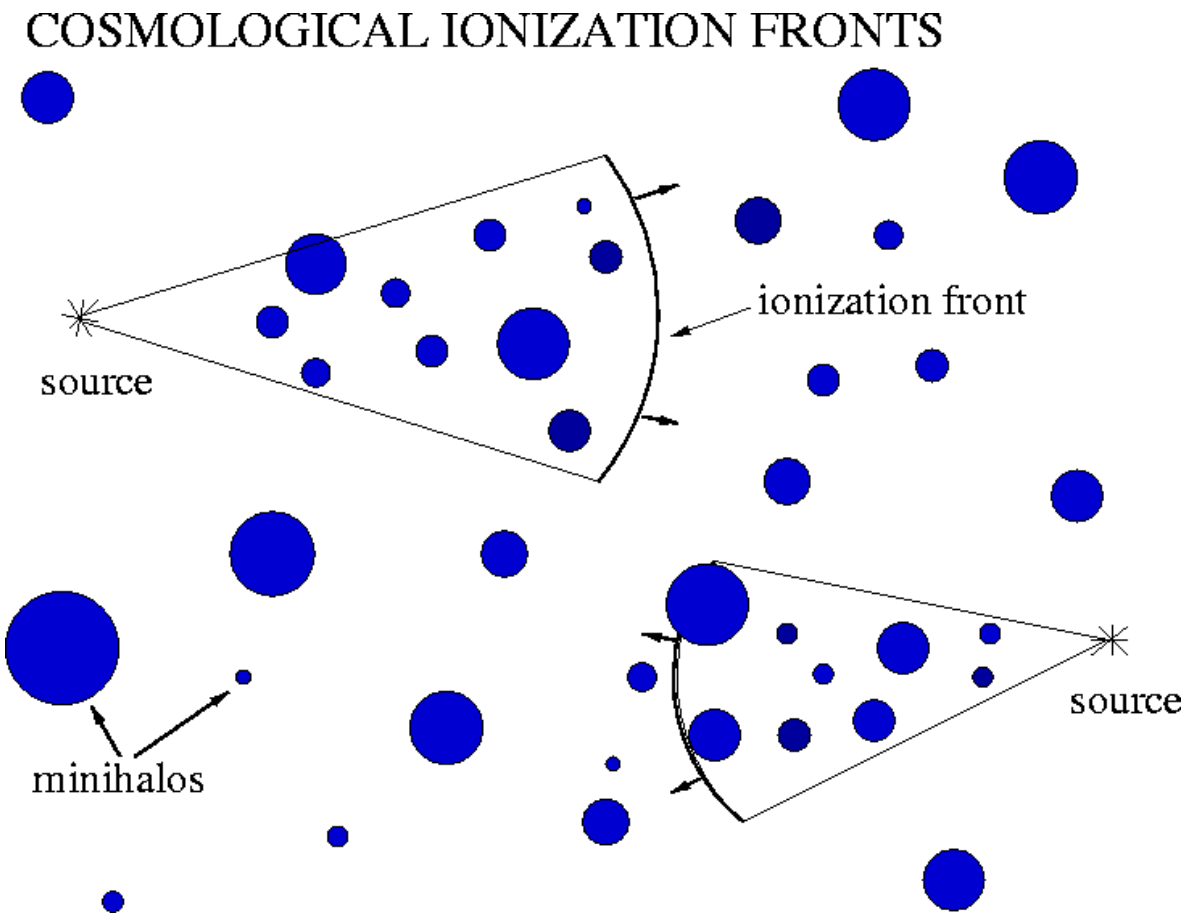

Temperature at times t = 0.0, 0.2, 2.5, 10, 60, 150 Myrs.

(M_{halo}, $z_{initial}$, F_0) = ($10^7 M_{sun}$, 9, 1).

Pop II source.

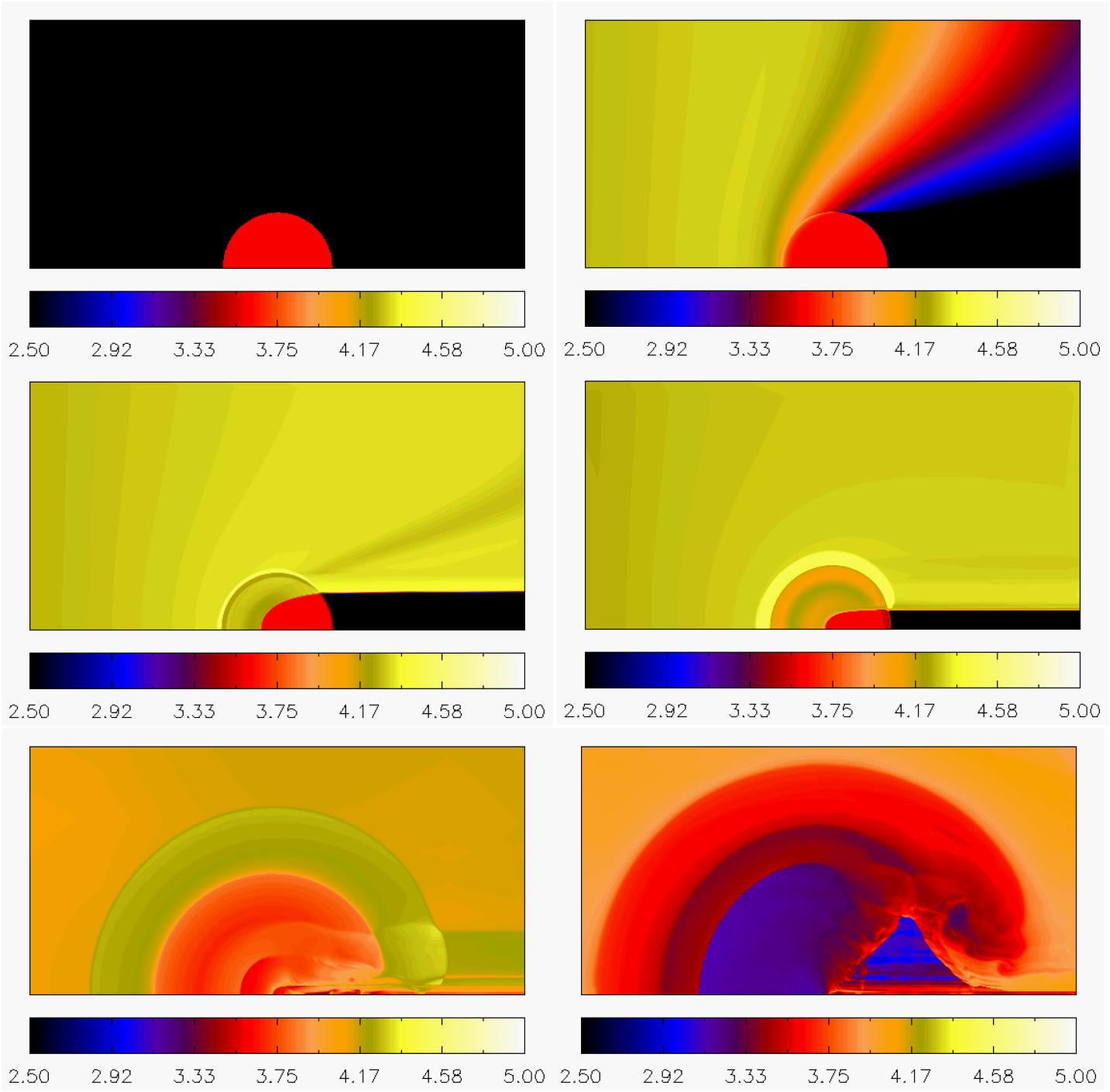

ANIMATIONS

Pop II

- **TEMPERATURE**
- **DENSITY**
- **H I**
- **He II**
- **C IV**

Pop III

- **TEMPERATURE**
- **DENSITY**
- **I**
- **e II**
- **C IV**

Simulating Cosmic Reionization at Large Scales I. : The Geometry of Reionization

Iliev, Mellema, Pen, Merz, Shapiro & Alvarez (2006)
MNRAS, 369, 1625 (astro-ph/0512187)

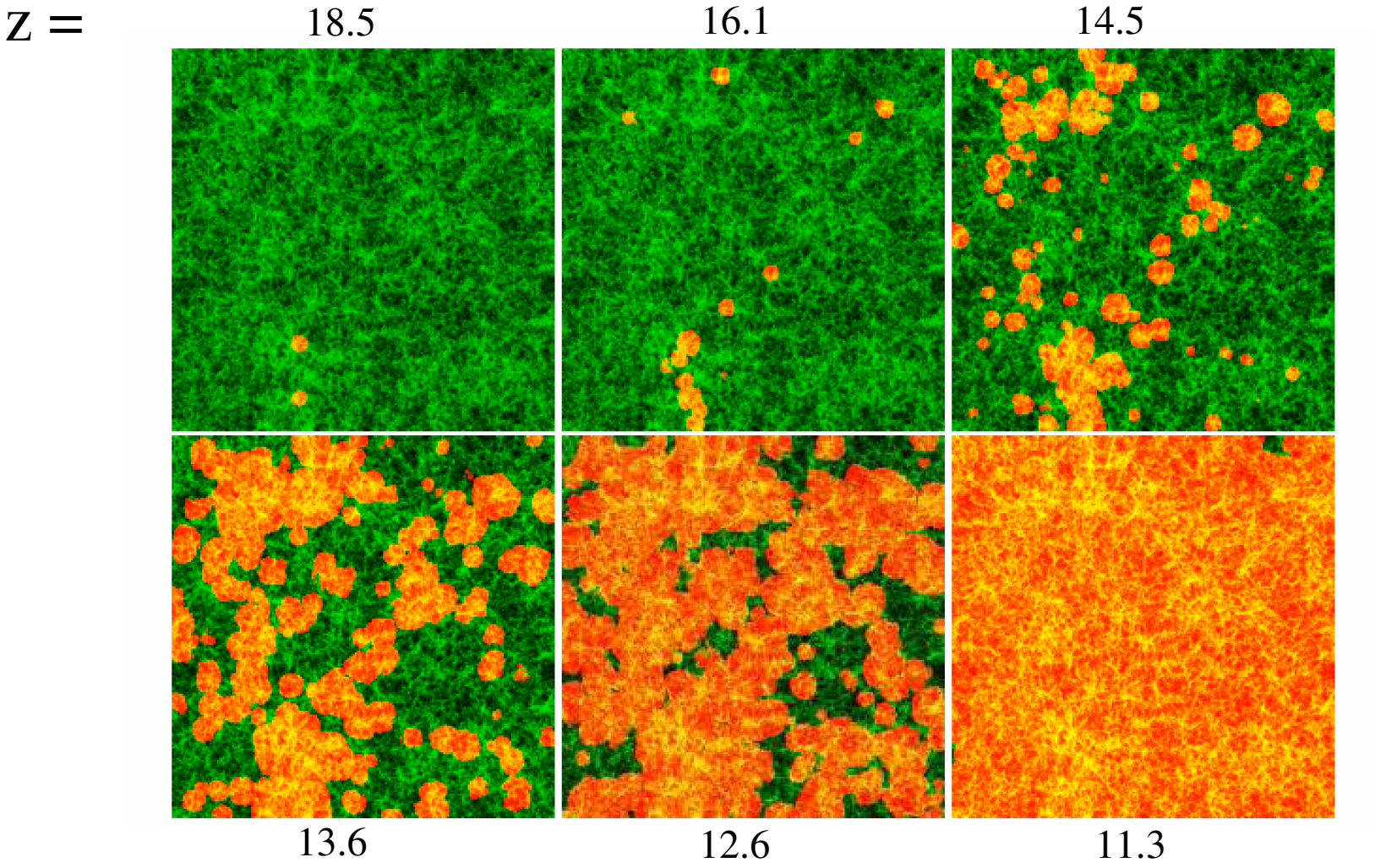

N-body + Radiative Transfer ➔ Reionization simulation

- N-body simulation yields the density field and sources of ionizing radiation
  - PMFAST code (Merz, et al. 2005) with
    1624^3 = 4.28 billion particles, 3248^3 cells,
    particle mass = $2.5 \times 10^7 M_{sun}$ (100 h^{-1}Mpc box),

  - Halo finder "on-the-fly" yields location, mass, other properties of all galaxies,
    $M \geq 2.5 \times 10^9 M_{sun}$ (100 h^{-1}Mpc box),

e.g. N_{halo} ~ 4 x 10^5 by z ~ 8 (WMAP1)
~ 3 x 10^5 by z ~ 6 (WMAP3)

N-body + Radiative Transfer ➔ Reionization simulation

- N-body simulation yields the density field and sources of ionizing radiation
  - New: 2nd generation N-body code CUBEP^{3}M,

New

a P^{3}M code, massively paralleled (MPI+Open MP),
3072^3 = 29 billion particles, 6144^3 cells,
particle mass = 5 x 10^6 M_{sun} (114 h^{-1}Mpc box),

- Halo finder "on-the-fly" yields location, mass, other properties of all galaxies,

$M \geq 10^8$ M_{sun} (114 h^{-1}Mpc box),

e.g. N_{halo} ~ 10^7 by z ~ 8 (WMAP3)

N-body + Radiative Transfer ➔ Reionization simulation

- Radiative transfer simulations evolve the radiation field and nonequilibrium ionization state of the gas

  - New, fast, efficient C^2-Ray code (Conservative, Causal Ray-Tracing) (Mellema, Iliev, Alvarez, & Shapiro 2006, *New Astronomy*, 11, 374) uses short-characteristics to propagate radiation throughout the evolving gas density field provided by the N-body results, re-gridded to $(203)^3$ and $(406)^3$ cells, for different resolution runs, from each and every galaxy halo source in the box.

e.g. N_{halo} ~ 4 x 10^5 by z ~ 8 (WMAP1) (> 2 x 10^9 M_{sun})

~ 3 x 10^5 by z ~ 6 (WMAP3) (> 2 x 10^9 M_{sun})

~ 10^7 by z ~ 8 (WMAP5) (> 10^8 M_{sun})

for simulation volumes ~ $(100\ h^{-1}\ Mpc)^3$

Every galaxy in the simulation volume emits ionizing radiation

- We assume a constant mass-to-light ratio for simplicity:

f_γ = # ionizing photons released by each galaxy per halo baryon

$= f_* \ f_{esc} \ N_i$,

where f_* = star-forming fraction of halo baryons,

f_{esc} = ionizing photon escape fraction,

N_i = # ionizing photons emitted per stellar baryon over stellar lifetime

e.g. $N_i = 50{,}000$ (top-heavy IMF), $f_* = 0.2$, $f_{esc} = 0.2$ ➔ $f_\gamma = 2000$

Every galaxy in the simulation volume emits ionizing radiation

- We assume a constant mass-to-light ratio for simplicity:

f_γ = # ionizing photons released by each galaxy per halo baryon

$= f_* \ f_{esc} \ N_i$,

where f_* = star-forming fraction of halo baryons,

f_{esc} = ionizing photon escape fraction,

N_i = # ionizing photons emitted per stellar baryon over stellar lifetime

e.g. $N_i = 50{,}000$ (top-heavy IMF), $f_* = 0.2$, $f_{esc} = 0.2$ ➔ $f_\gamma = 2000$

- This yields source luminosity: $dN_\gamma/dt = f_\gamma \, M_{bary} / (\mu \, m_H \, t_*)$,

t_* = source lifetime (e.g. 2×10^7 yrs),

M_{bary} = halo baryonic mass

C^2 - Ray : A New Method for Photon-Conserving Transport of Ionizing Radiation

Mellema, Iliev, Alvarez & Shapiro (2006) *New Astronomy*, 11, 374

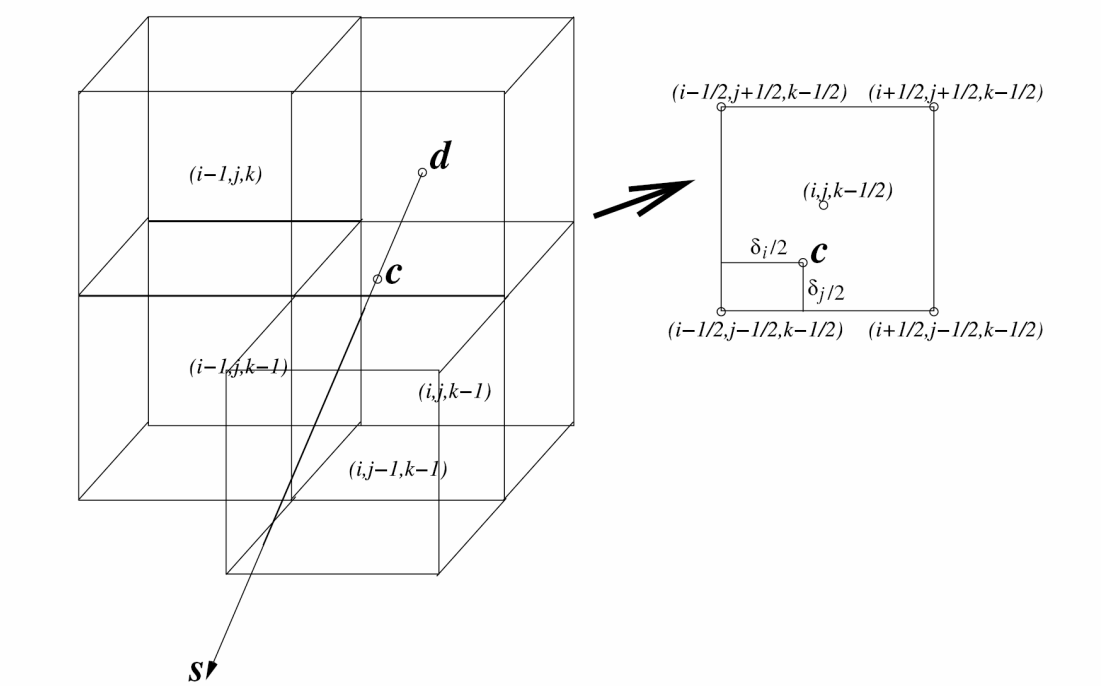

Fig. A.1. Short-characteristics ray tracing.

Cosmological Radiative Transfer Codes Comparison Project I. : The Static Density Field Tests

Iliev, Ciardi, …, Shapiro, … (2006) MNRAS, 371, 1057

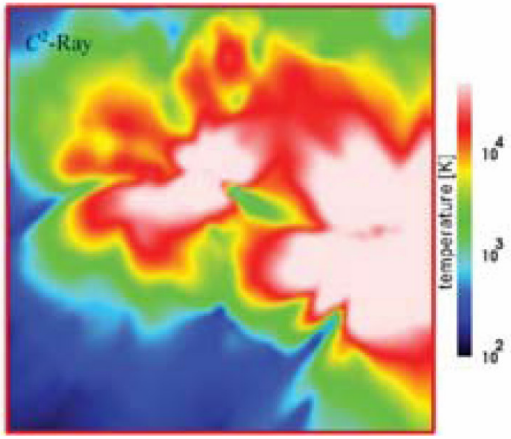

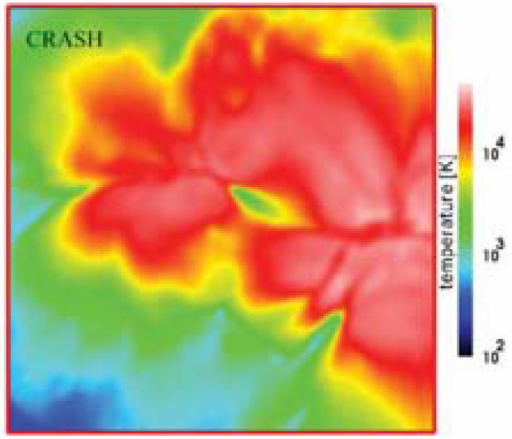

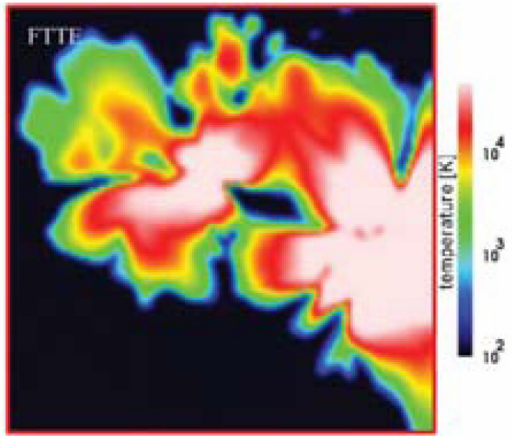

Cosmological Radiative Transfer Comparison Project II. : The Radiation-HydrodynamicTests

Iliev, Whalen, …, Shapiro, … (2009) MNRAS, submitted (astro-ph/0905.2920)

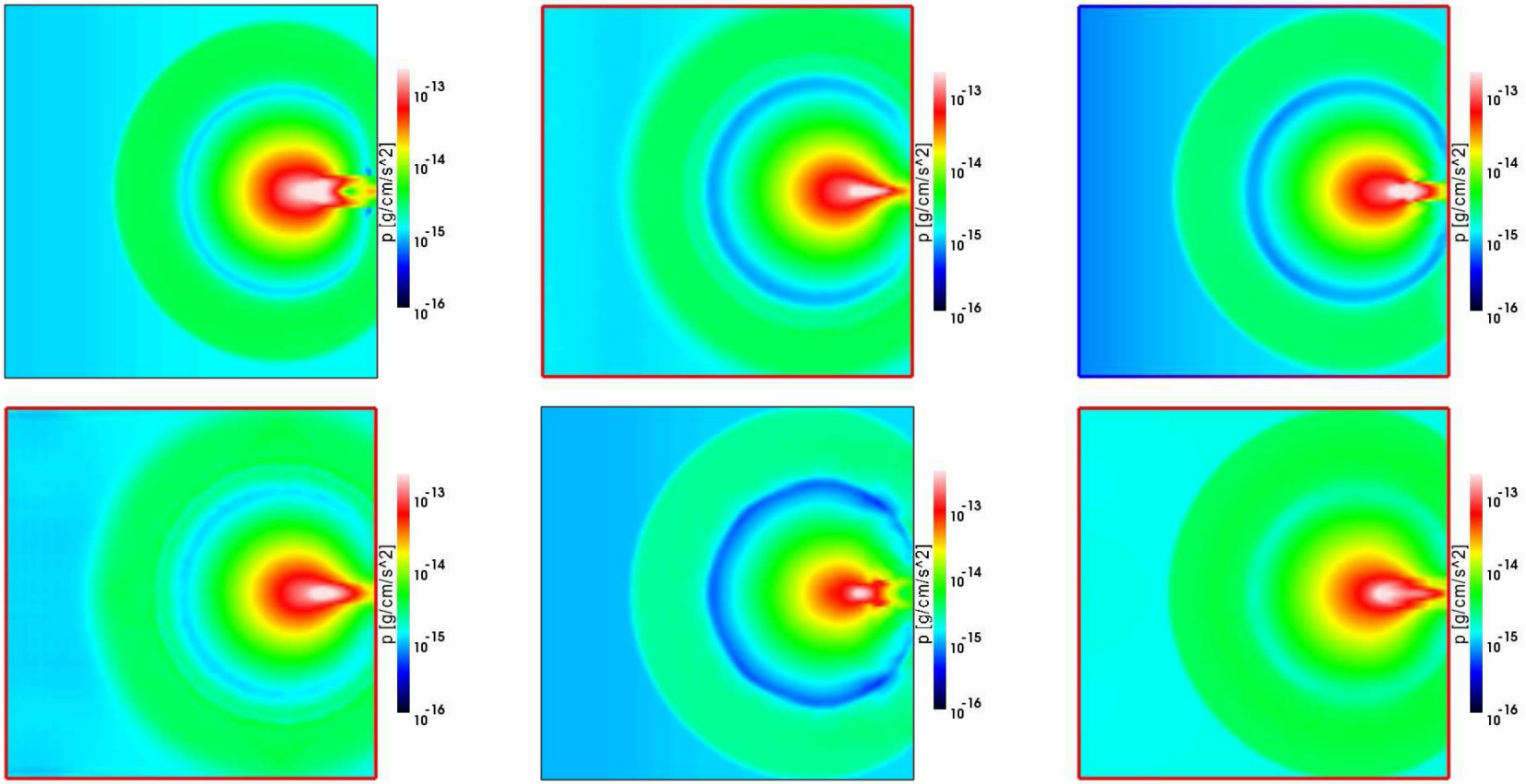

Dynamical H II Region Evolution in Turbulent Molecular Clouds

Mellema, Arthur, Henney, Iliev & Shapiro (2006) ApJ, 647, 397 (astro-ph/0512187)

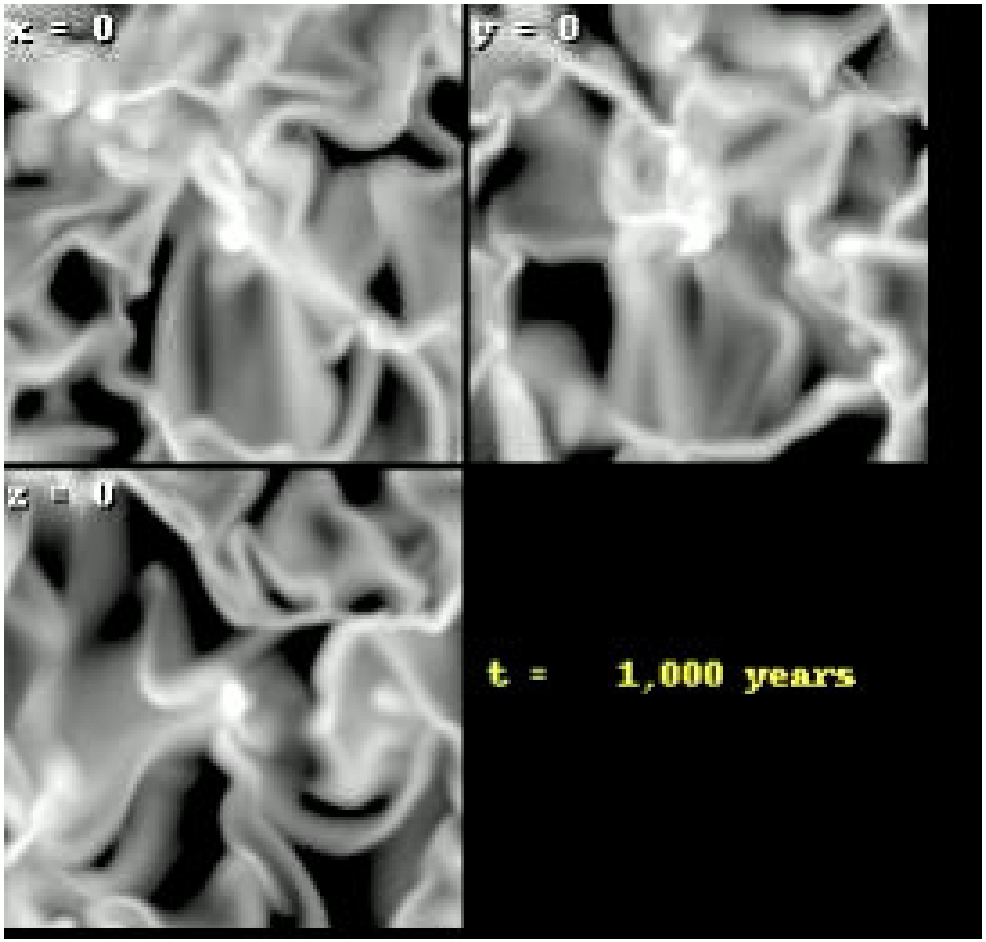

Dynamical H II Region Evolution in Turbulent Molecular Cl

Mellema, Arthur, Her 06) ApJ, 647, 397

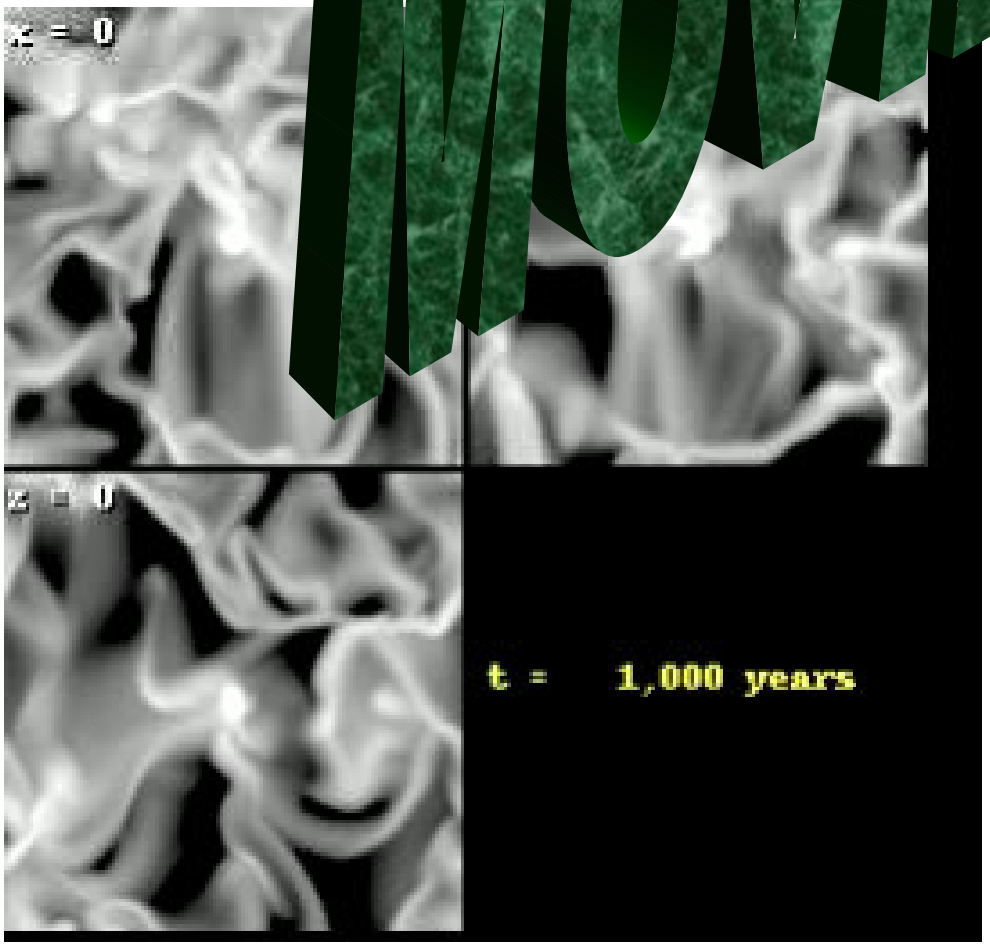

MOVIE

Dynamical H II Region Evolution in Turbulent Molecular Clouds

Mellema, Arthur, Henney, Iliev & Shapiro (2006) ApJ, 647, 397 (astro-ph/0512187)

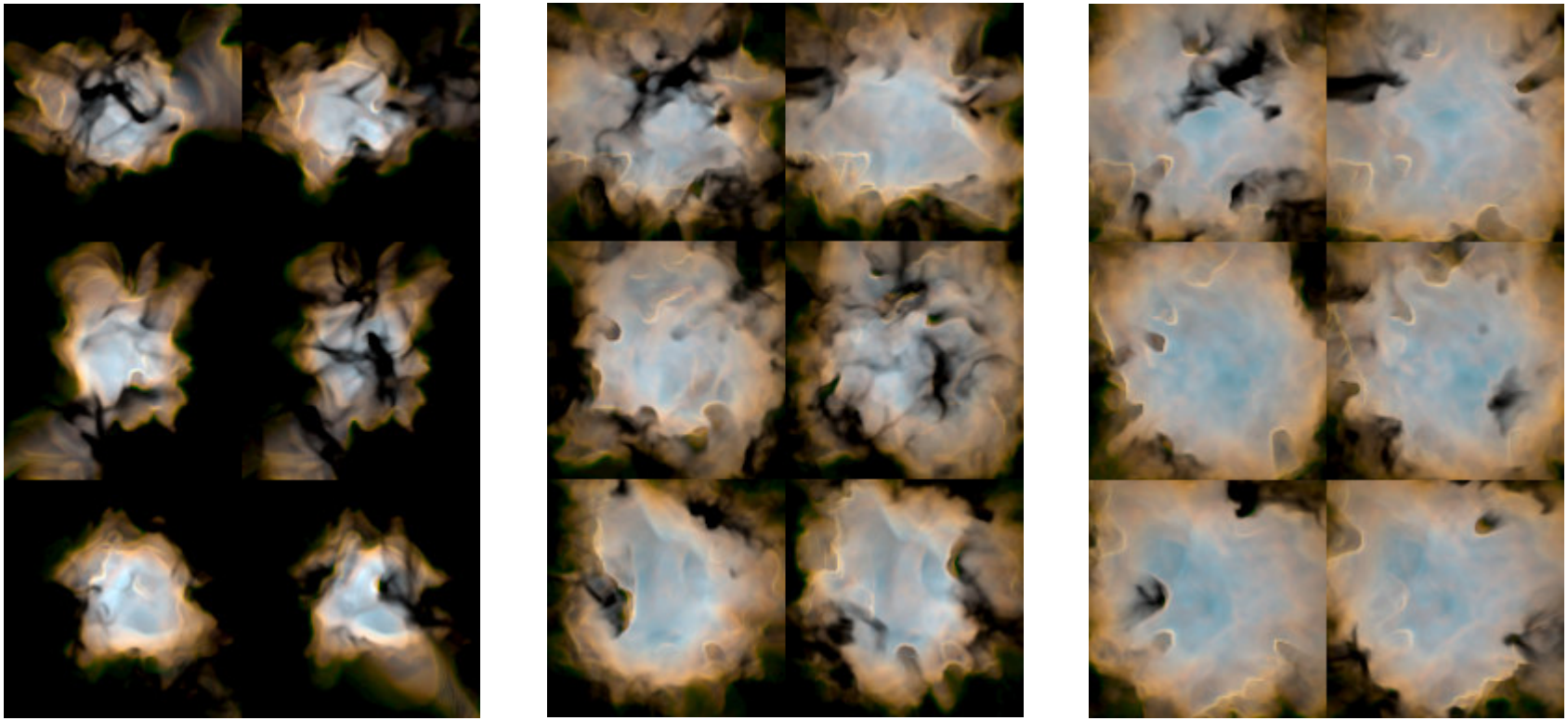

Simulating Reionization at Large Scales II : The 21-cm Emission Features and Statistical Signals

Mellema, Iliev, Pen, & Shapiro (2006), MNRAS, 372,679 (astro-ph/0603518)

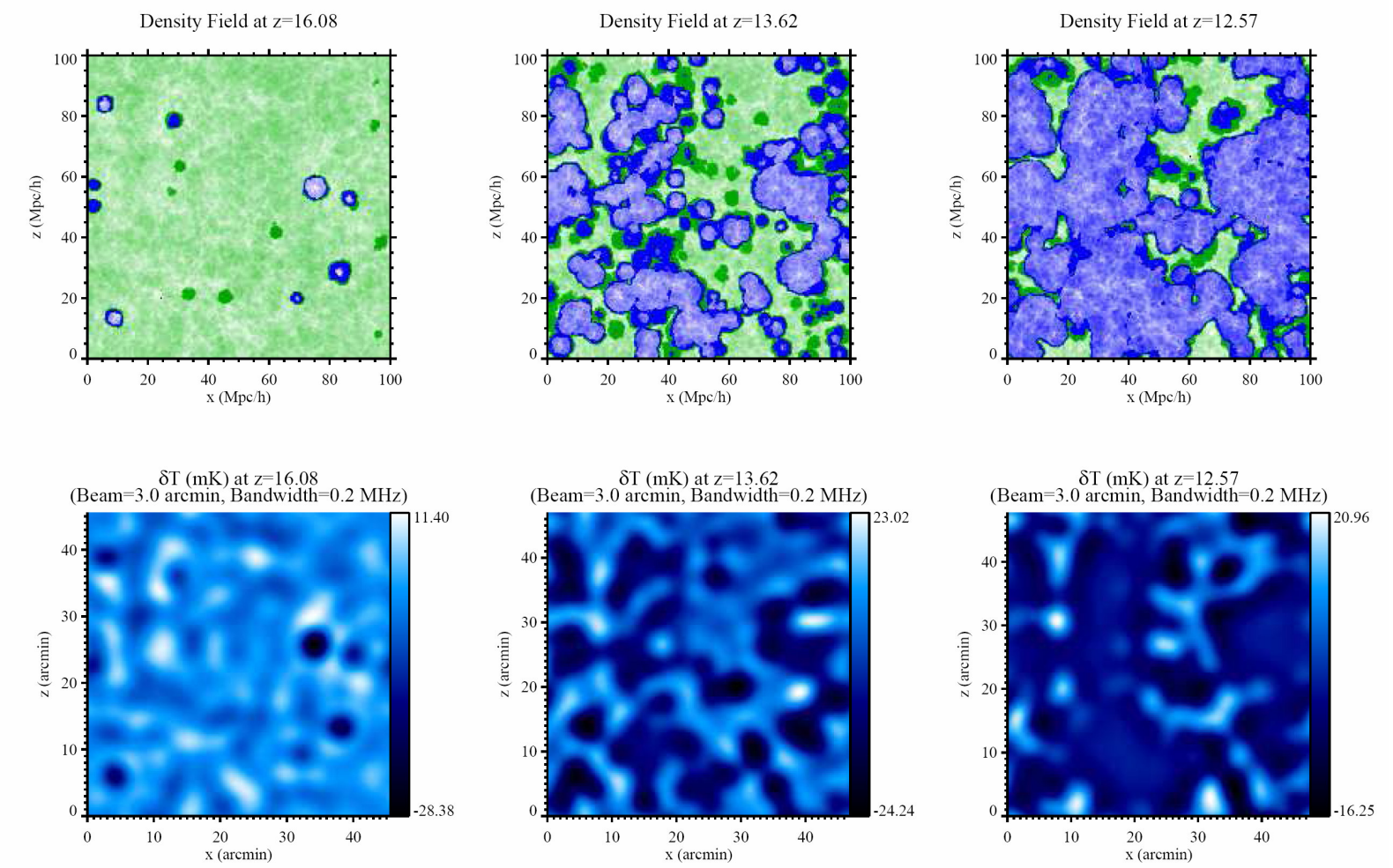

Low Frequency Array (LOFAR)

Murchison Widefield Array (MWA)

PrimevAl Structure Telescope (PAST/21CMA)

Prototype Tests, Ulastai, Xin Jiang, China

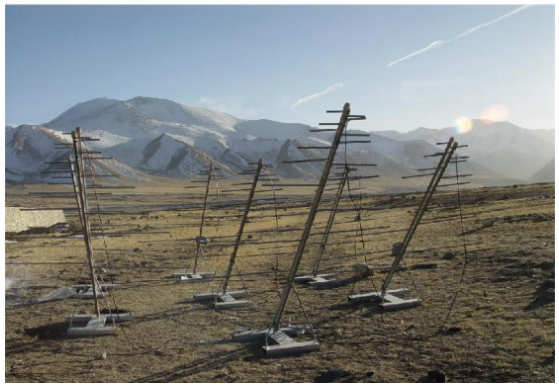

Giant Meterwave Radio Telescope (GMRT)

Square Kilometer Array (SKA)

Q: How large must a reionization simulation volume be to predict 21-cm background fluctuations?

- Simulation volumes must exceed the beamsize and bandwidth of future radio arrays by a large enough factor to make 21-cm predictions meaningful.

e.g. for GMRT, MWA, LOFAR,

$\Delta\theta_{beam} \geq 3'$

$\Delta\nu_{bandwidth} > 0.1$ Mhz

- Our $(143\ \mathrm{Mpc})^3$ comoving volume simulation was the first to be large enough to predict 21-cm fluctuations.

$L_{box} = 100\ h^{-1}$ Mpc (comoving)

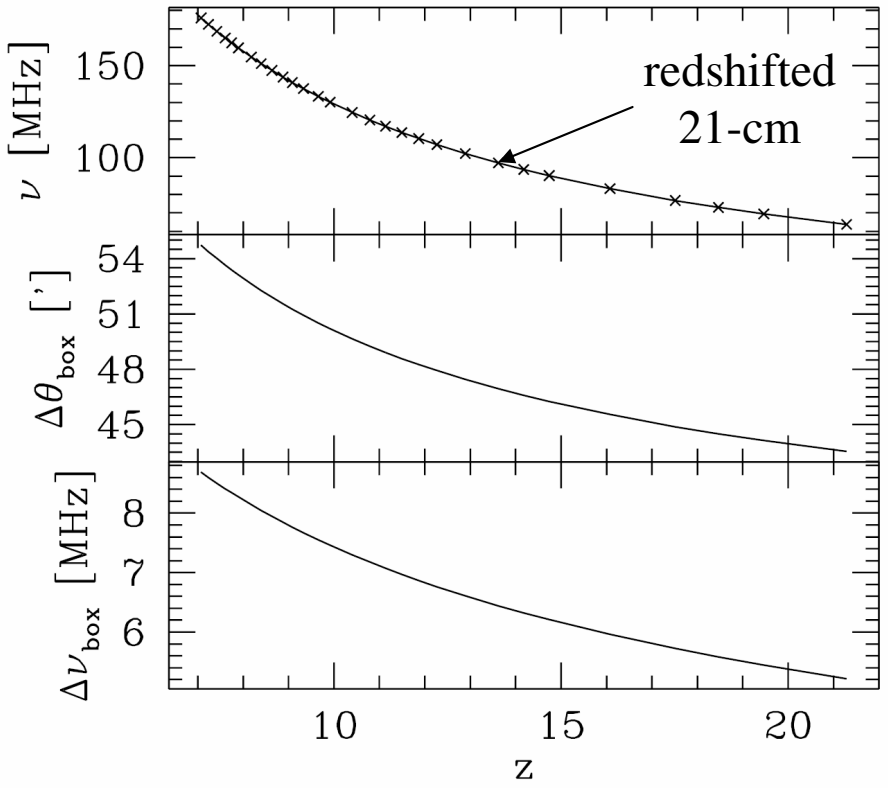

Reionization topology revealed by fluctuations in 21-cm brightness temperature, δT_b , along the line of sight

Iliev, Mellema, Pen, Bond, & Shapiro (2008), MNRAS, 384, 863 (astro-ph/0702099)

- mapping the sky along the LOS: high-resolution cuts in position-redshift space

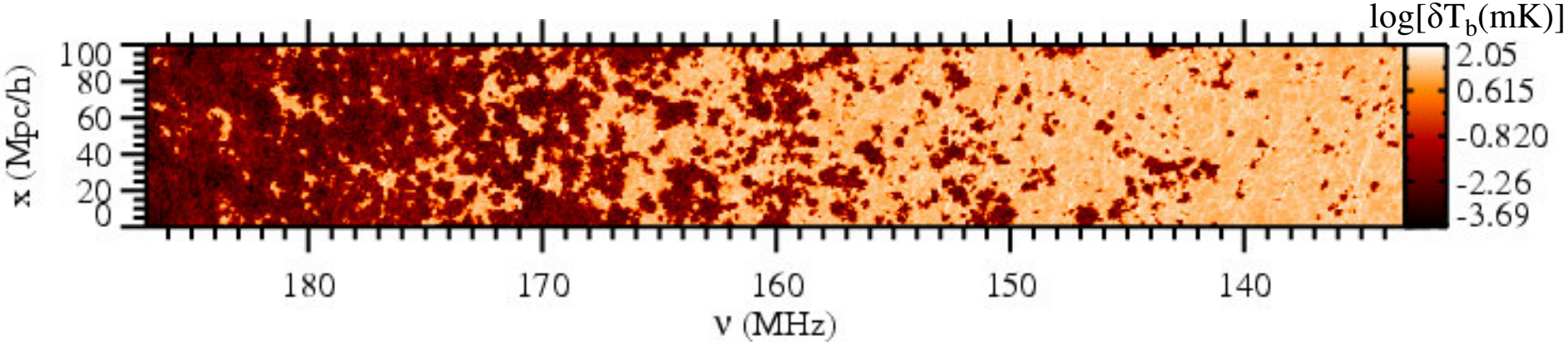

- beam- and bandwidth-smoothed : 3 arcmin, 0.2 MHz (e.g. LOFAR)

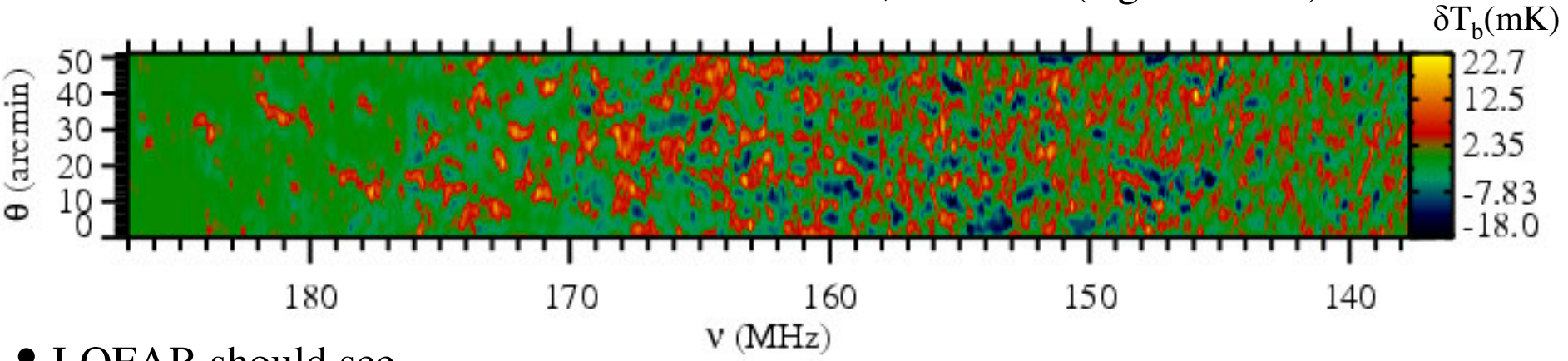

- LOFAR should see large ionized bubbles!

Case: $f_\gamma = 250$, subgrid clumping factor C(z), WMAP3

The Geometry of Reionization

for source efficiency
$f_\gamma = 2000$

from z = 20 to z = 12

a cut through the simulation volume, one cell deep

gas density (green in neutral regions, yellow in ionized regions), H II regions (red) and sources (dots)

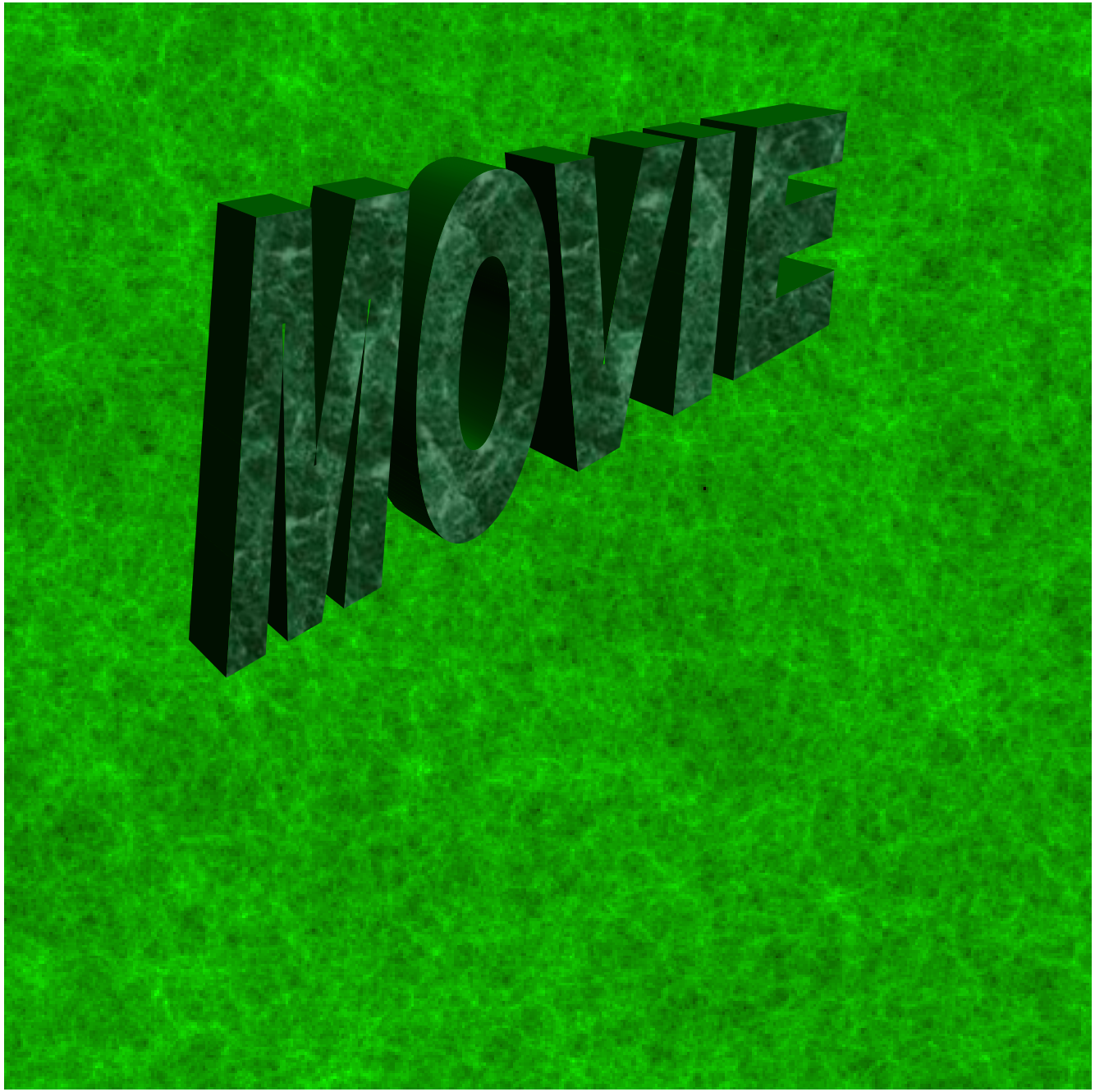

Kinetic Sunyaev-Zel'dovich Effect from Patchy Reionization

- kSZ effect is the CMB temperature anisotropy induced by electron scattering by free electrons moving along the line-of-sight:

$$\frac{\Delta T}{T_{\rm CMB}} = \int d\eta e^{-\tau_{\rm es}(\eta)} a n_e \sigma_T \mathbf{n}\cdot\mathbf{v},$$

where η is conformal time,

$$\eta = \int_0^t dt'/a(t')$$

($\delta T/T_{CMB}$) Maps of the Kinetic Sunyaev-Zel'dovich Effect from Radiative Transfer Simulations of Patchy Reionization

Iliev, Pen, Bond, Mellema & Shapiro (2007), ApJ, 660, 933; (astro-ph/0609592)
Iliev, Mellema, Pen, Bond, & Shapiro (2008), MNRAS, 384, 863; (astro-ph/0702099)

- Box size 100/h Mpc comoving
  ➔ 50' x 50'

- Even so large a box is missing large-scale power in velocity field perturbations

➔ must correct for missing large-scale velocity perturbations

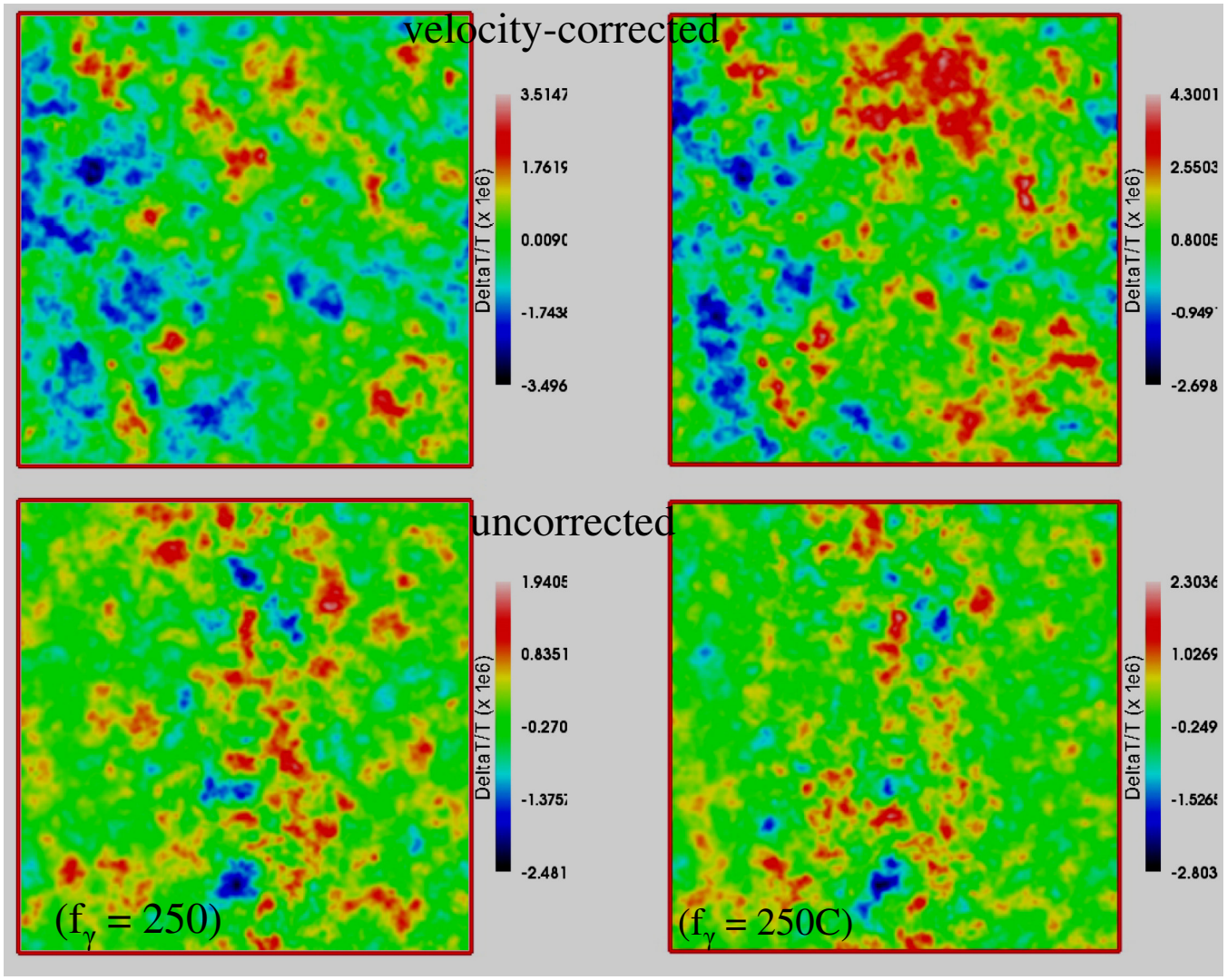

kSZ CMB Anisotropy Signal: Sky Power Spectra of $\delta T_{kSZ} / T_{CMB}$

- kSZ anisotropy from inhomogeneous reionization dominates primary CMB anisotropy for $\ell > 4000$, peaking at $\ell = 3000 - 4000$, determined by typical sizes of H II regions, 5 – 20 Mpc.

- Patchy reionization doubles *total* kSZ for $\ell = 3000 - 10{,}000$ compared to homogeneous reionization with the same total τ_{es}.

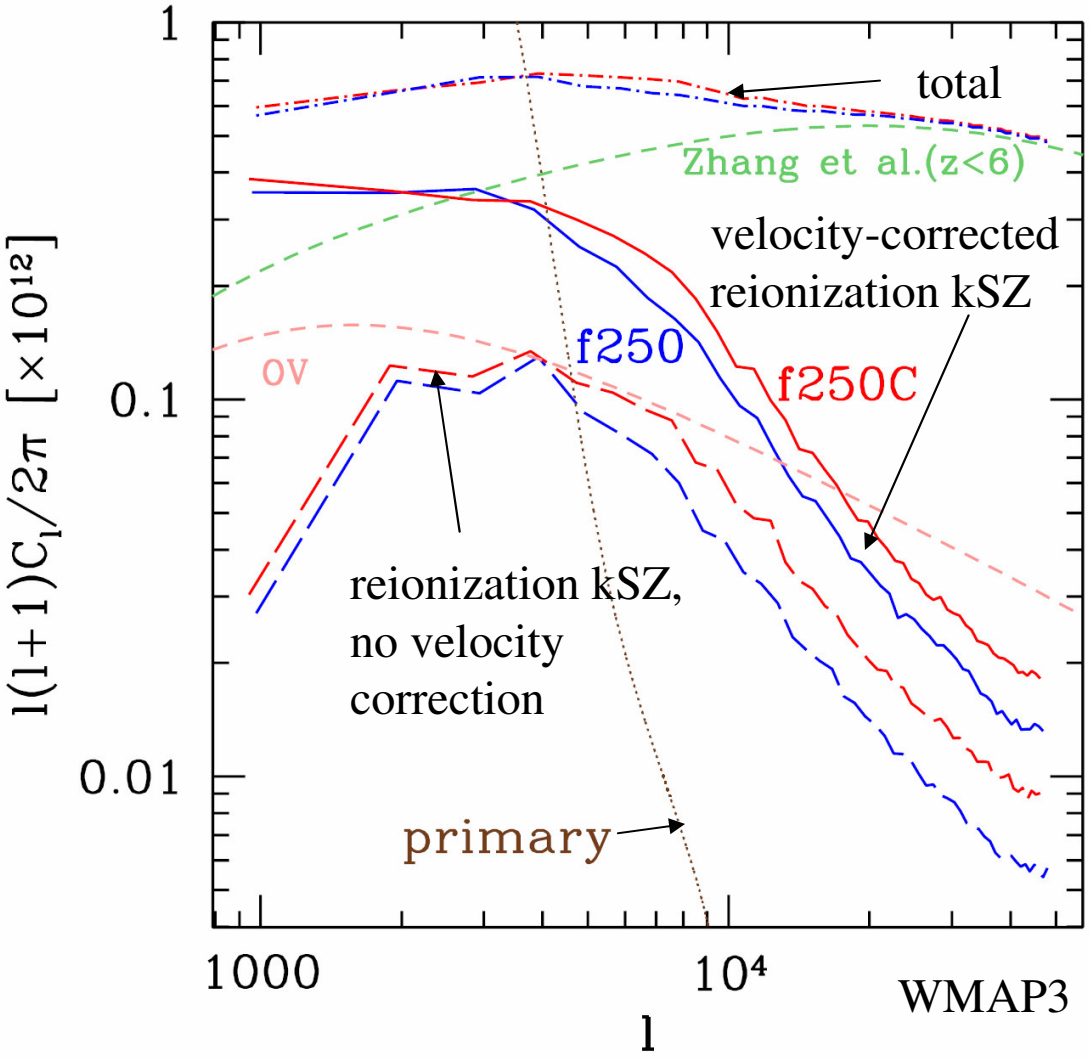

- This predicted kSZ signal at arcminute scales should be detectable by upcoming experiments. e.g. Atacama Cosmology Telescope, South Pole Telescope, (~ 1' resolution, ~ μK sensitivity)

Observability of the kSZ from reionization: sky power spectrum

- Predicted kSZ from reionization simulations and *Atacama Cosmology Telescope* (ACT) expected sensitivity;
- primary CMB and post-reionization kSZ added to noise error bars for reionization signal;
- reionization kSZ signal is comparable to that from post-reionization, so necessary to separate them to extract info on reionization, alone.
- In principle, results show that reionization signal should be observable.

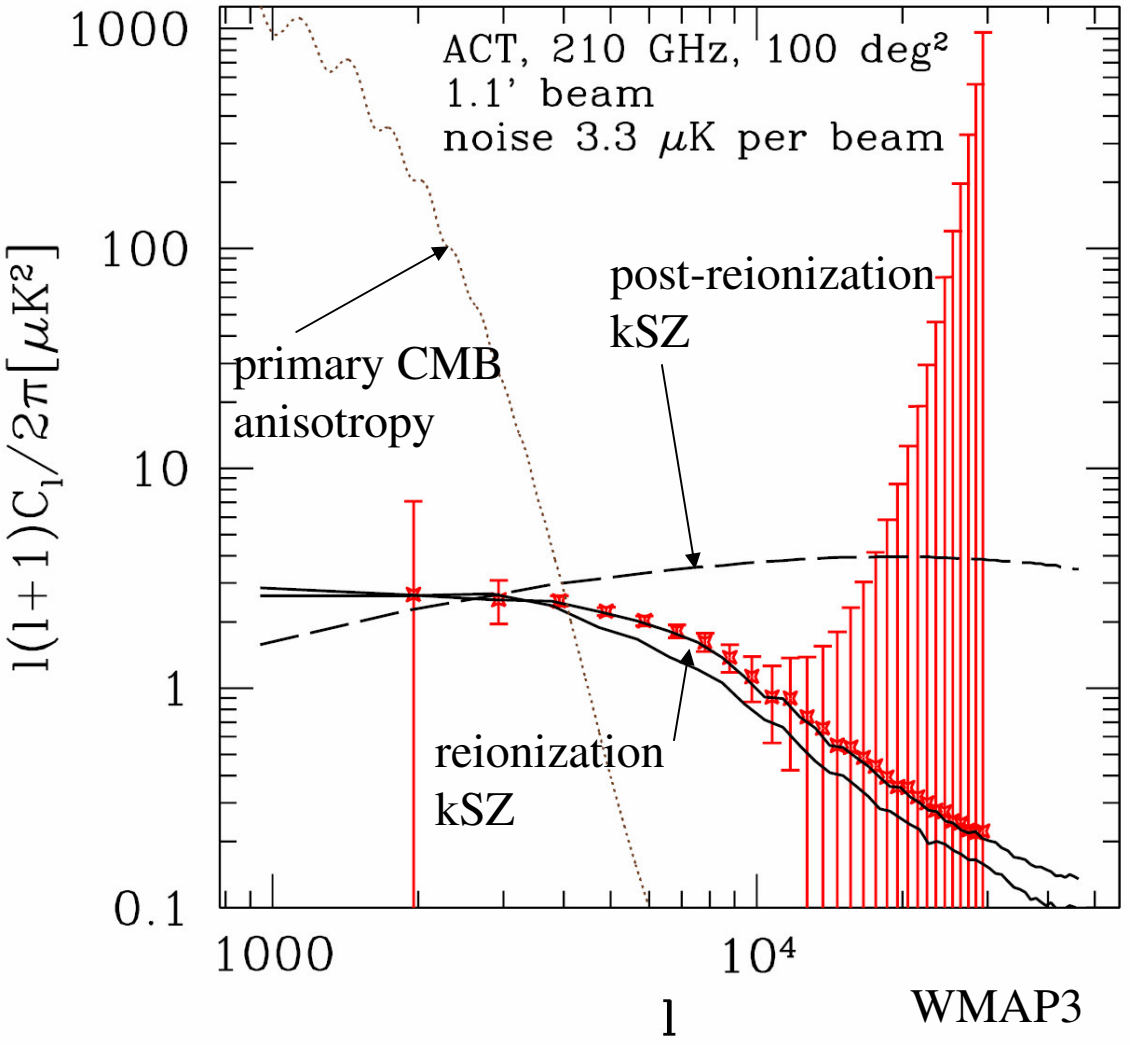

f250, f250C

Observability of the kSZ from reionization: sky power spectrum

- Predicted kSZ from reionization simulations and *South Pole Telescope* (SPT) expected sensitivity;
- primary CMB and post-reionization kSZ added to noise error bars for reionization signal;
- reionization kSZ signal is comparable to that from post-reionization, so necessary to separate them to extract info on reionization, alone.
- In principle, results show that reionization signal should be observable.

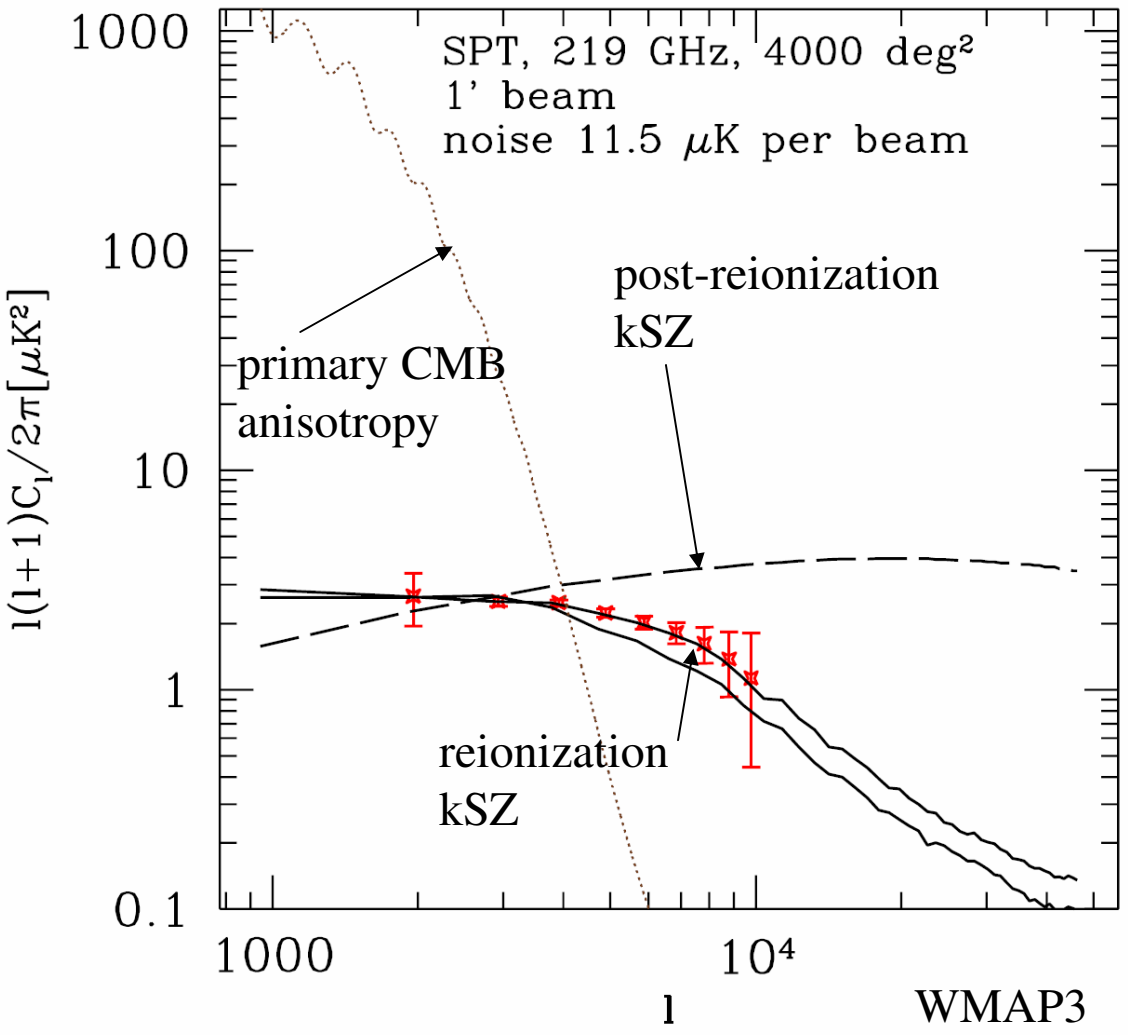

f250, f250C

Effect of IGM on Observability of Ly-α Sources During Reionization

(Iliev, Shapiro, McDonald, Mellema, Pen 2008, MNRAS, 391, 63)

•reionization, centered on most massive halo in $(100h^{-1}\ \mathrm{Mpc})^3$:

$M\ (z = 6) = 1.5 \times 10^{12}\ M_{solar}$ ➔

rare (~ 5-σ) density peak ➔

bright Ly-α emitter ;

•H II regions form first around such density peaks and grow continuously, as halos form inside, clustered around peak ➔

Ly-α emitters will be centered on large HII regions ;

(blue dots = source cells)

•Fluctuating GP optical depth inside H II regions can still affect Ly-α source detection, though;

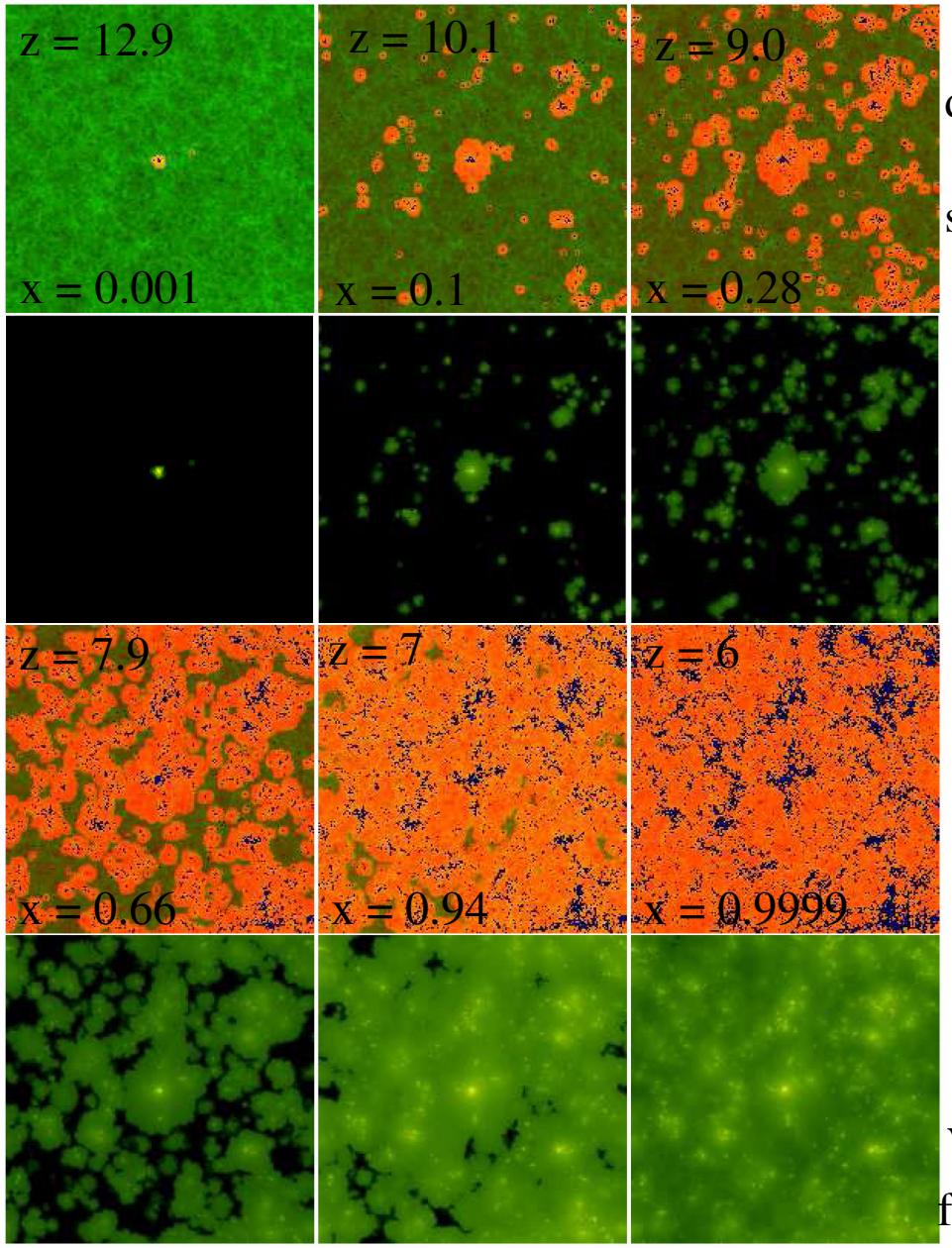

densities + sources

ioniz'n rates

WMAP3 $f_\gamma = 250C$

Discovery of a Giant Lyman Alpha Emitter Near the Epoch of Reionization
(Ouchi et al. 2009, ApJ, 696, 1164)

- Optical and IR images of *Himiko* by *Subaru*, UKIDSS-Ultra Deep Survey, and *Spitzer*/IRAC ➔ Ly α emitter (LAE) at z = 6.595

- High luminosity:
  L (Ly α) = 3.9 x 10^{43} erg s^{-1}

- Highest luminosity LAE in survey volume 10^6 Mpc^3

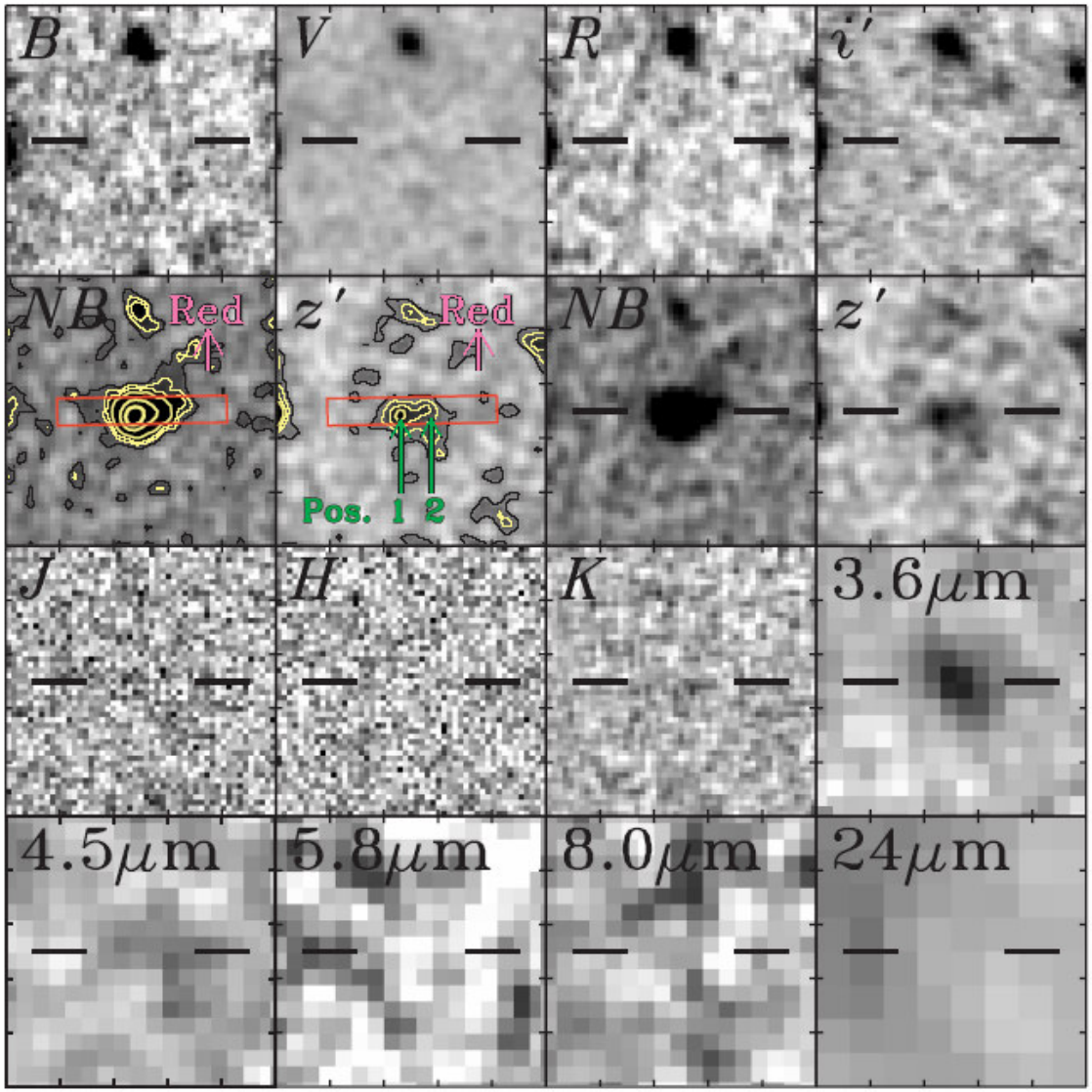

Discovery of a Giant Lyman Alpha Emitter Near the Epoch of Reionization
(Ouchi et al. 2009, ApJ, 696, 1164)

- Composite image shows extended emission 3" (or 17 kpc) across

- Keck and Megellan Telescopes confirm Ly α line spectroscopically

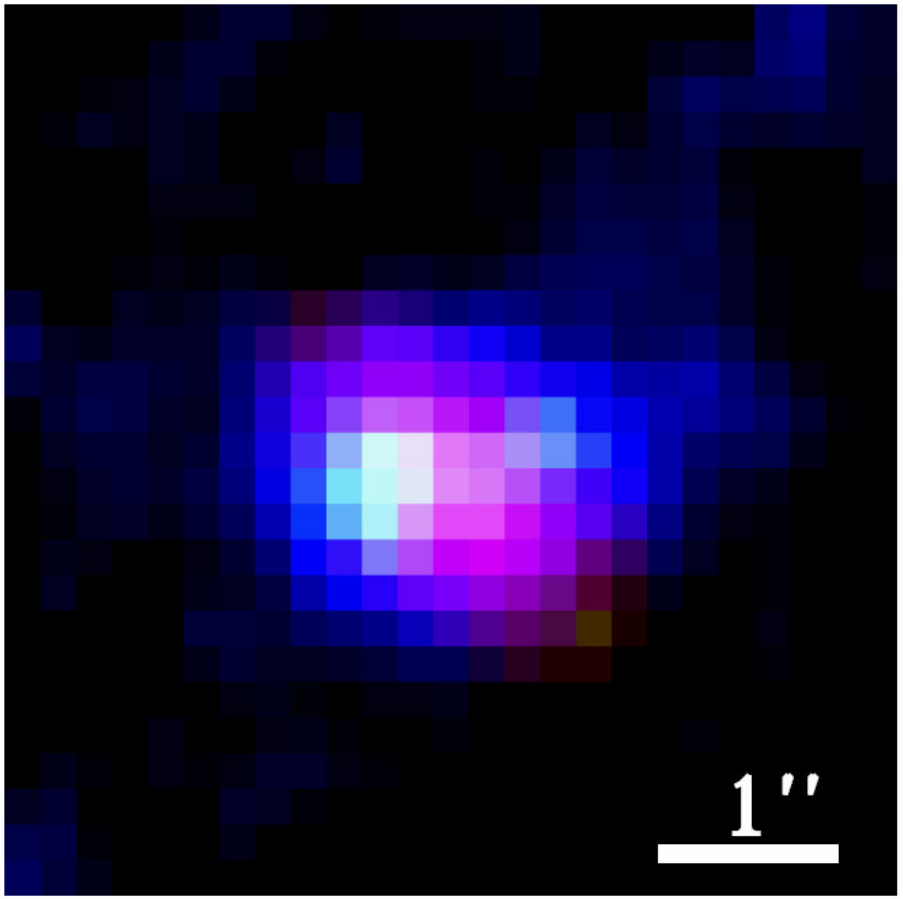

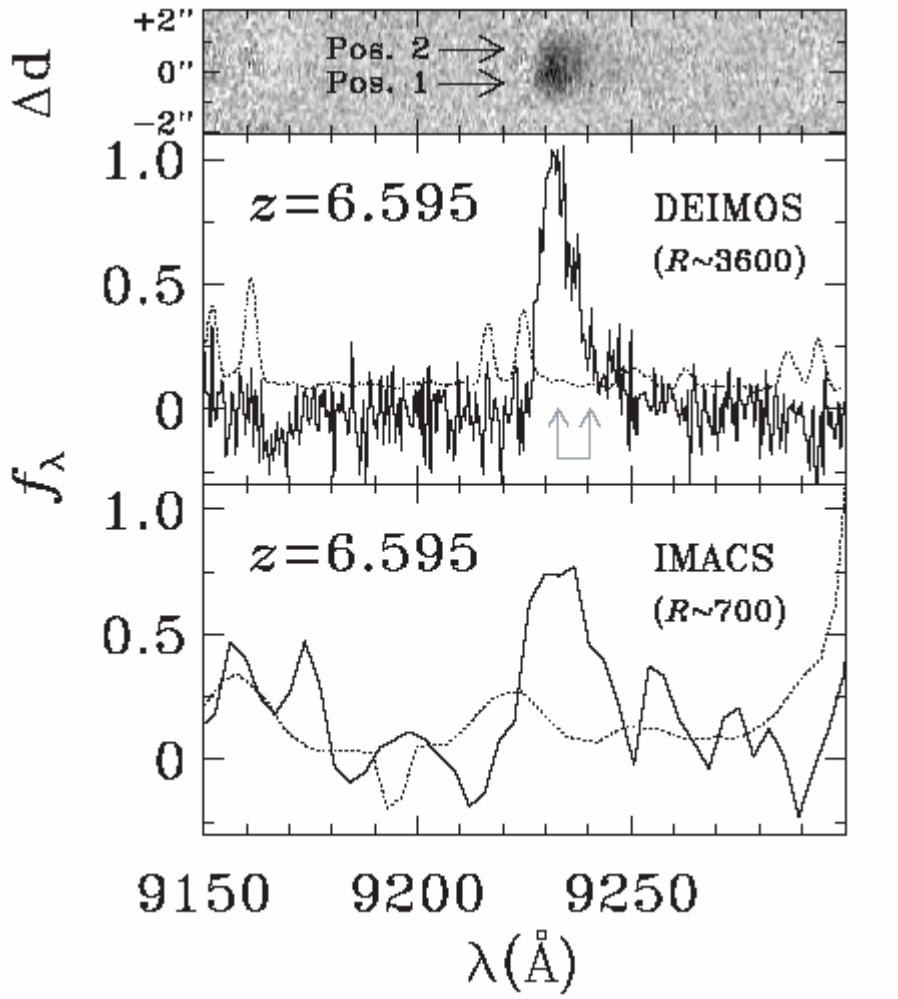

Effect of IGM on Observability of Ly-α Sources During Reionization

(Iliev, Shapiro, McDonald, Mellema, Pen 2008, MNRAS, 391, 63)

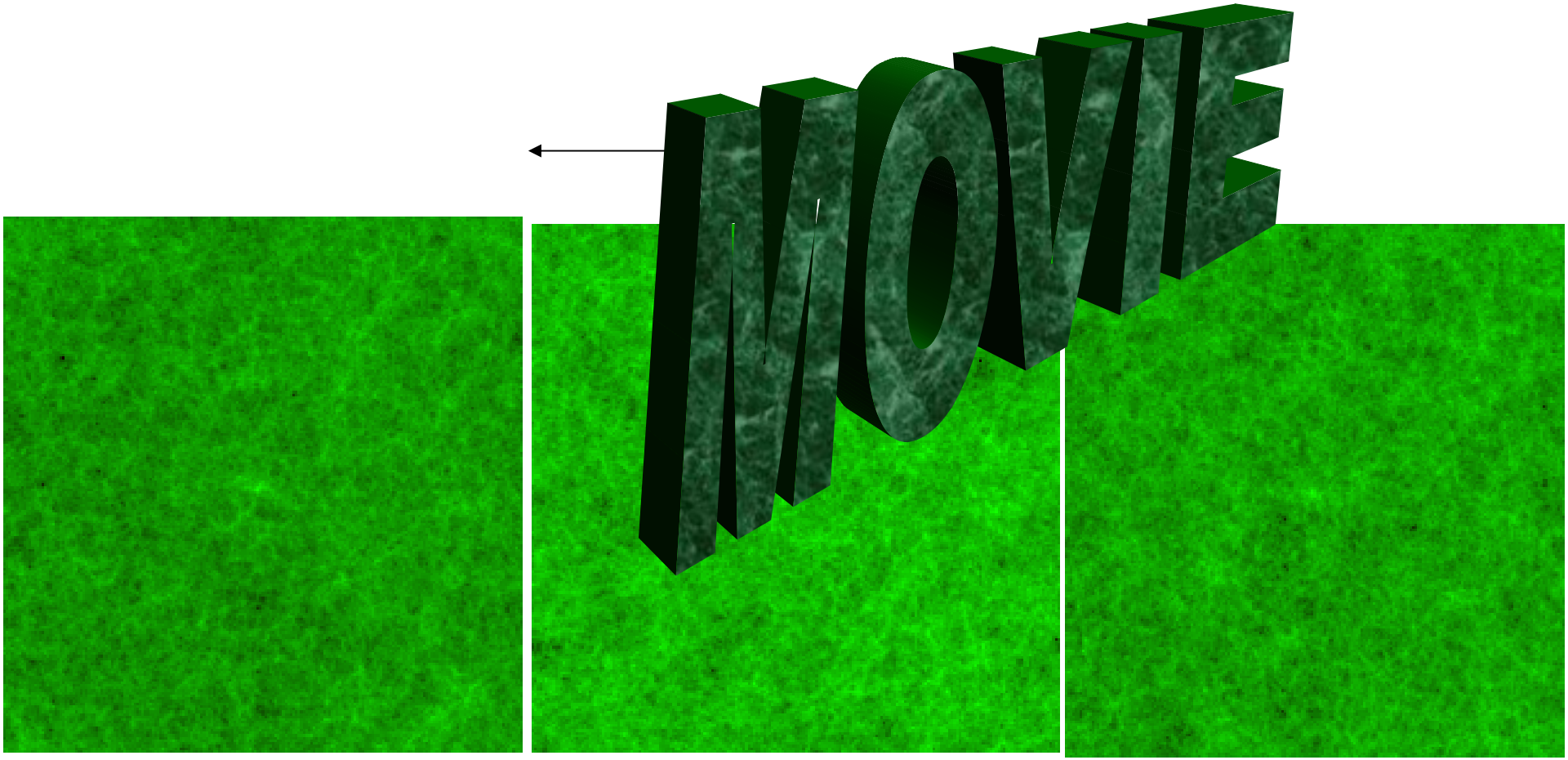

xz xy yz

Q: Do luminous Lyman alpha emitters observed during the EOR dominate the ionization of their own H II regions?

- **A**: not really ("they get by with a little help from their friends…")
  - LAE forms at high-σ density peak, surrounded by a cluster of smaller mass halos ➔ smaller halos dominate ionization
  - e.g. most massive source contributed only

    ~50% by z = 12.9

    ~10% by z = 7

    ~1% by z = 6.25!

ionizing photons released over time by halos within a sphere of distance R from most massive object

H II region sizes @ z = 12.9, 9, 8, 7, 6.25

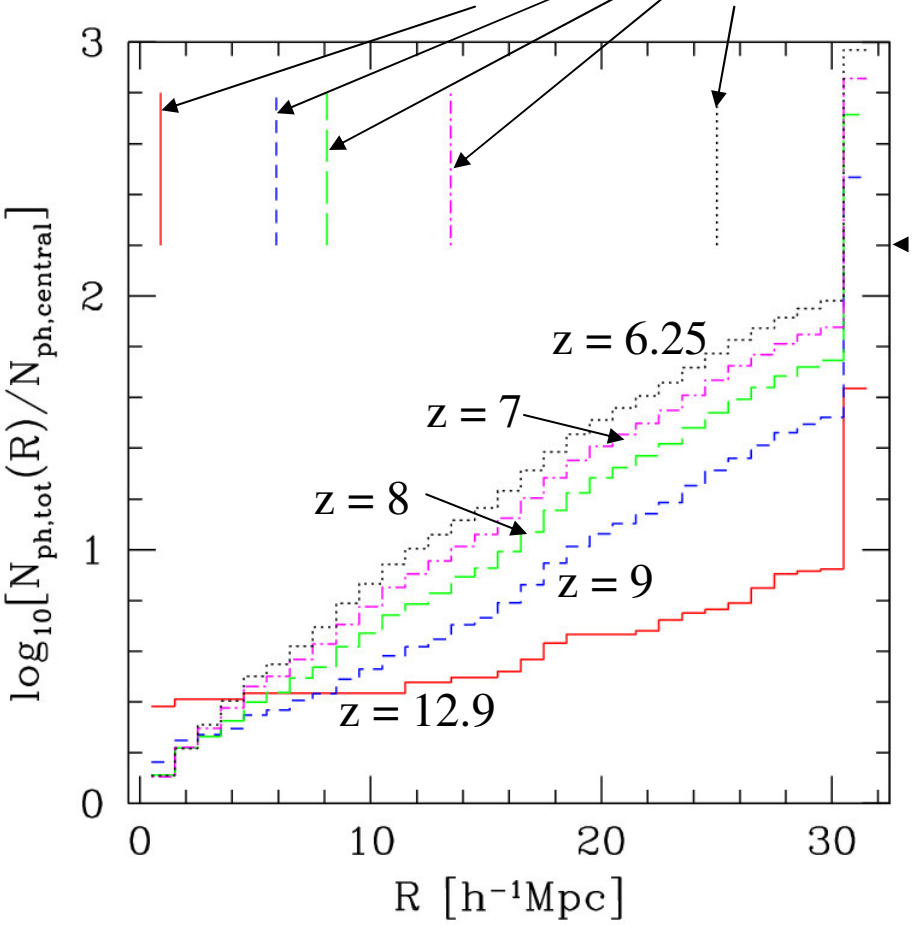

Mean Ly-α transmission vs. redshift

- Strong damping wings at z>10, only minor differences between average and luminous source.
- Some transmission on blue side of line, as IGM slowly becomes transparent; large proximity transmission region for luminous sources.

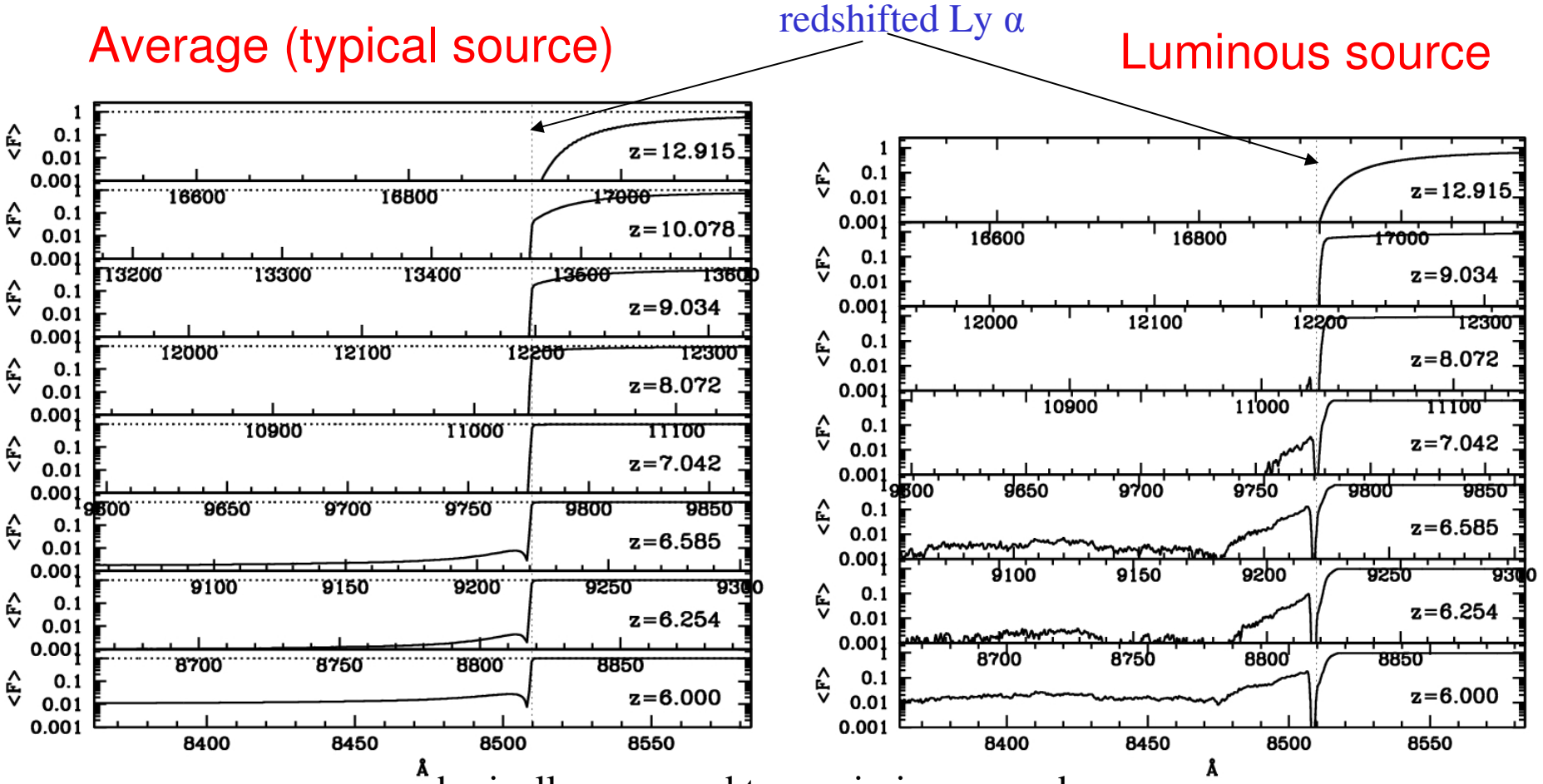

spherically-averaged transmission around sources

Mean transmitted Ly-α line profile vs. redshift

- Mostly, the red wing comes through (but damped at z>10).
- Infall more important for luminous sources, changes the line shape.

Average (typical source)

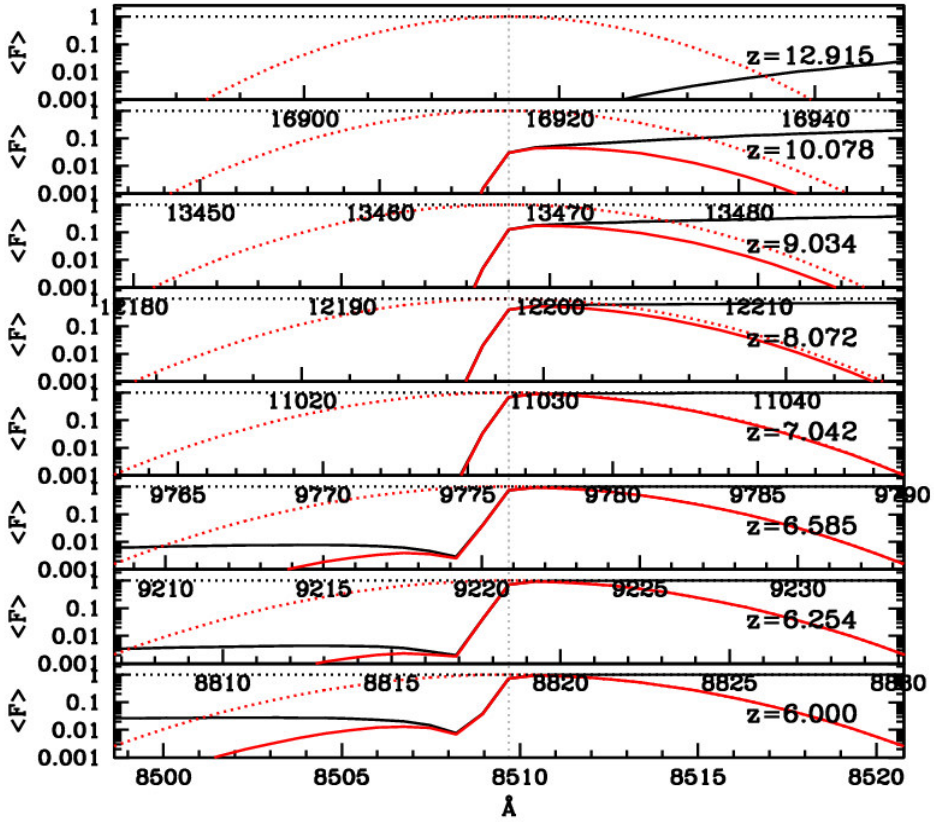

Luminous source

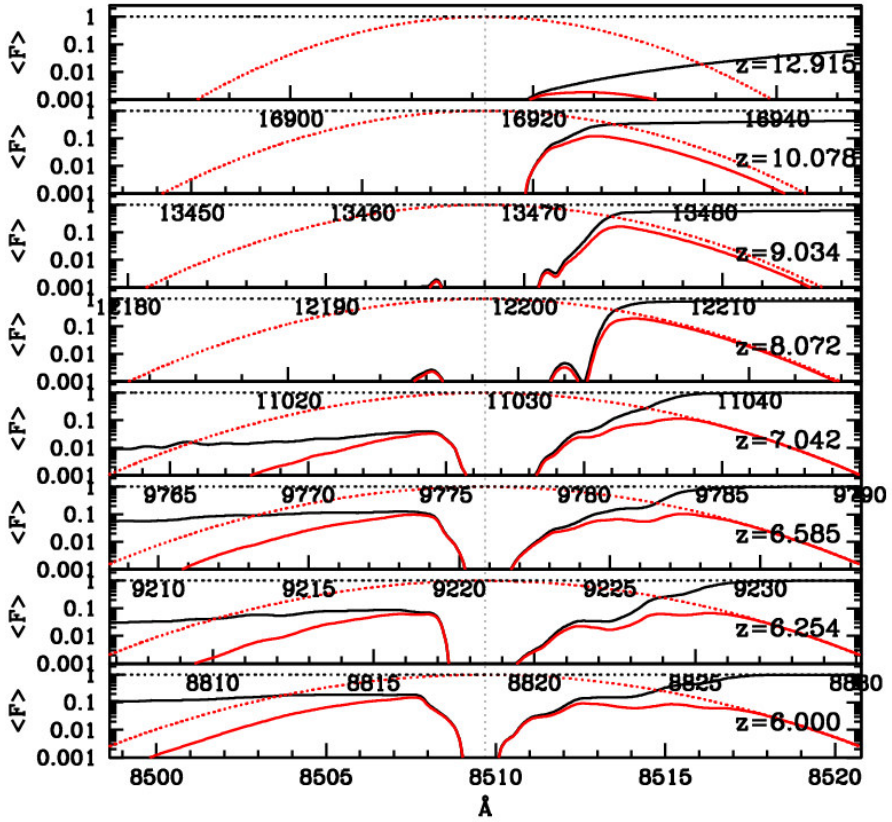

spherically-averaged transmitted line profiles

The Intergalactic Medium Surrounding the Most Massive Galaxy at the End of Reionization : $\langle x_{H\,II} \rangle = 99\%$

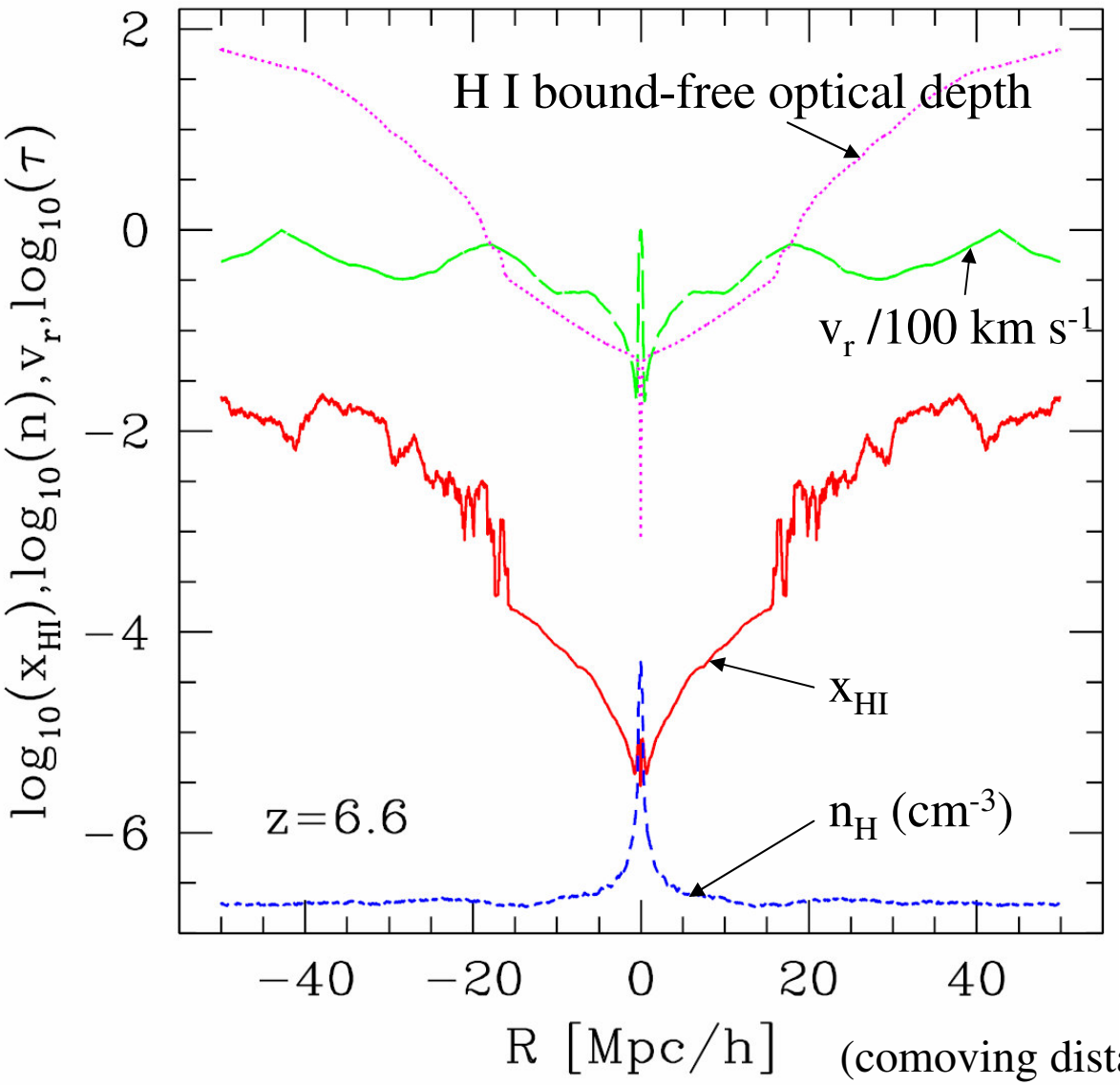

spherically-averaged profiles

(comoving distance from galaxy)

Luminosity Function of High-Redshift Ly-α Sources is Filtered By the Partially Ionized IGM

- Assuming all halos are Ly-α emitters with M/L = constant and 160 km/s Gaussian line profile;
- At z = 9, observed luminosity function is reduced by 0.01 -0.1 from intrinsic luminosity function;
- Attenuation exceeds 50% (i.e. blue-half absorbed, red-half not), since damping wings reduce the red-half, as well..

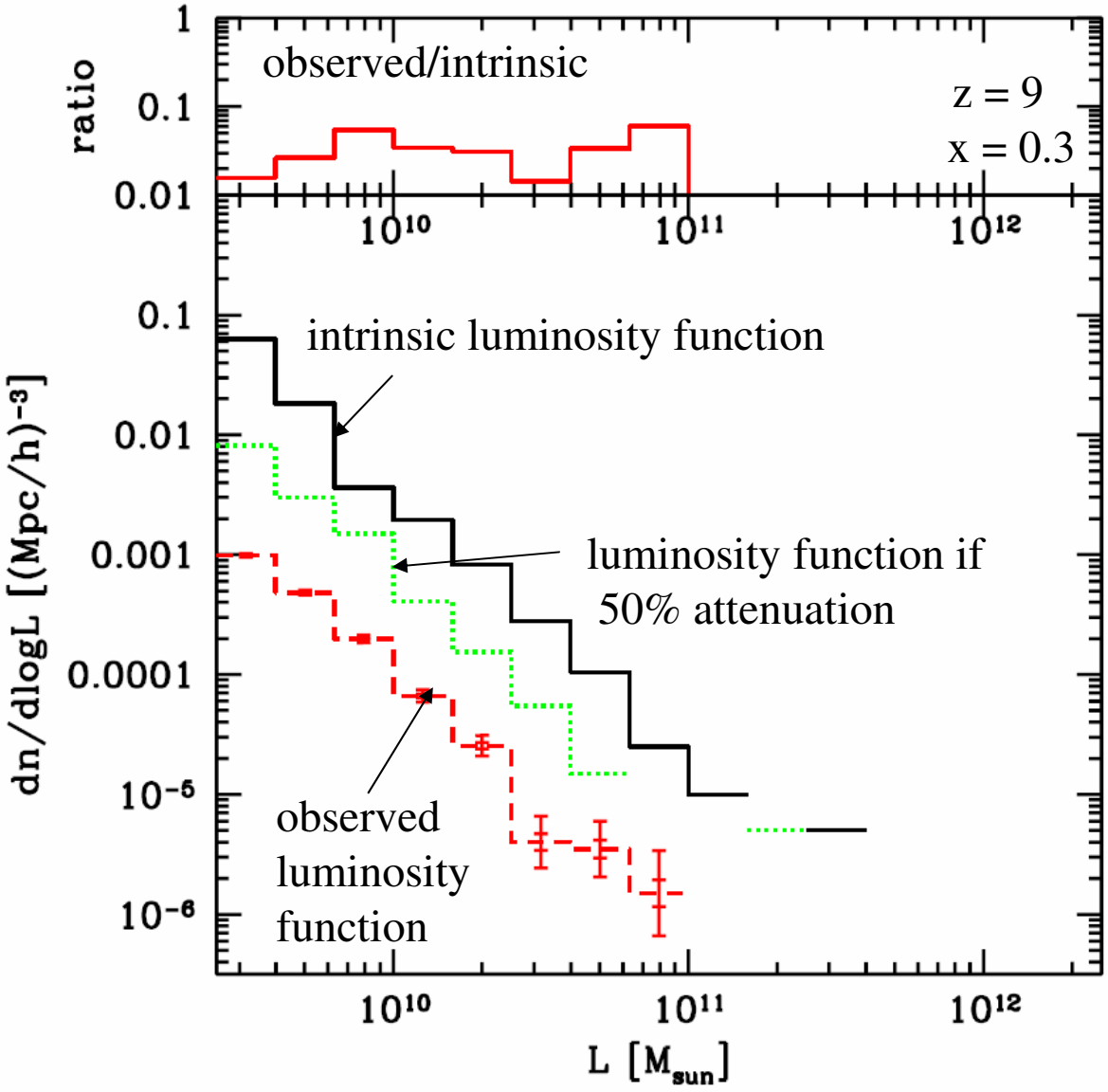

Luminosity Function of High-Redshift Ly-α Sources is Filtered By the Partially Ionized IGM

- Assuming all halos are Ly-α emitters with M/L = constant and 160 km/s Gaussian line profile;
- At z = 7, observed luminosity function is reduced by 0.5 from intrinsic luminosity function, except at bright end where factor is 0.1 or below;
- Attenuation exceeds 50% (i.e. blue-half absorbed, red-half not), now, only at bright end.

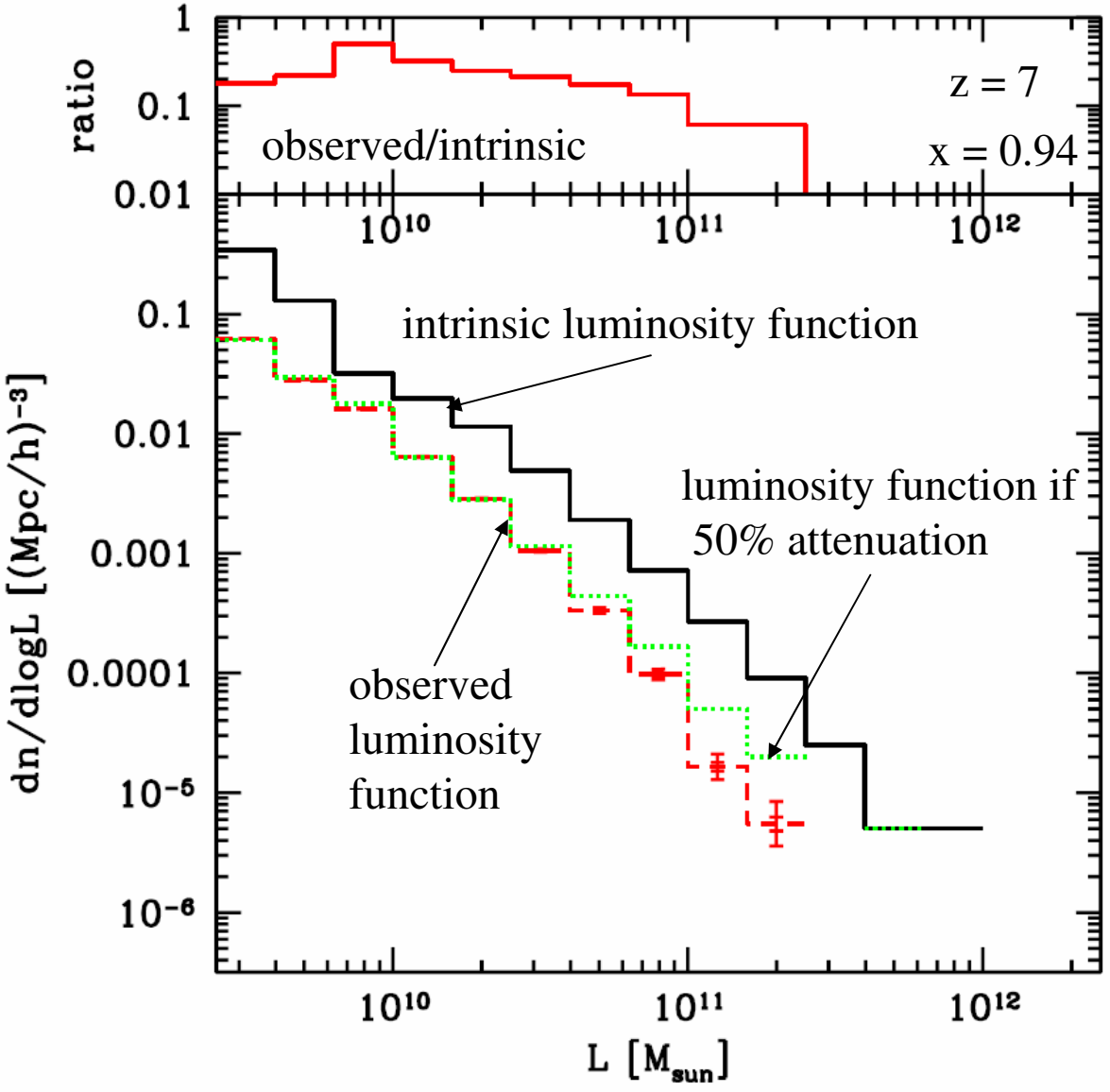

Luminosity Function of High-Redshift Ly-α Sources is Filtered By the Partially Ionized IGM

- Assuming all halos are Ly-α emitters with M/L = constant and 160 km/s Gaussian line profile;
- Even at z = 6, observed luminosity function is reduced by 0.5 from intrinsic luminosity function, except at bright end where factor is 0.1 or below;
- Attenuation exceeds 50% (i.e. blue-half absorbed, red-half not), now, but only at bright end.

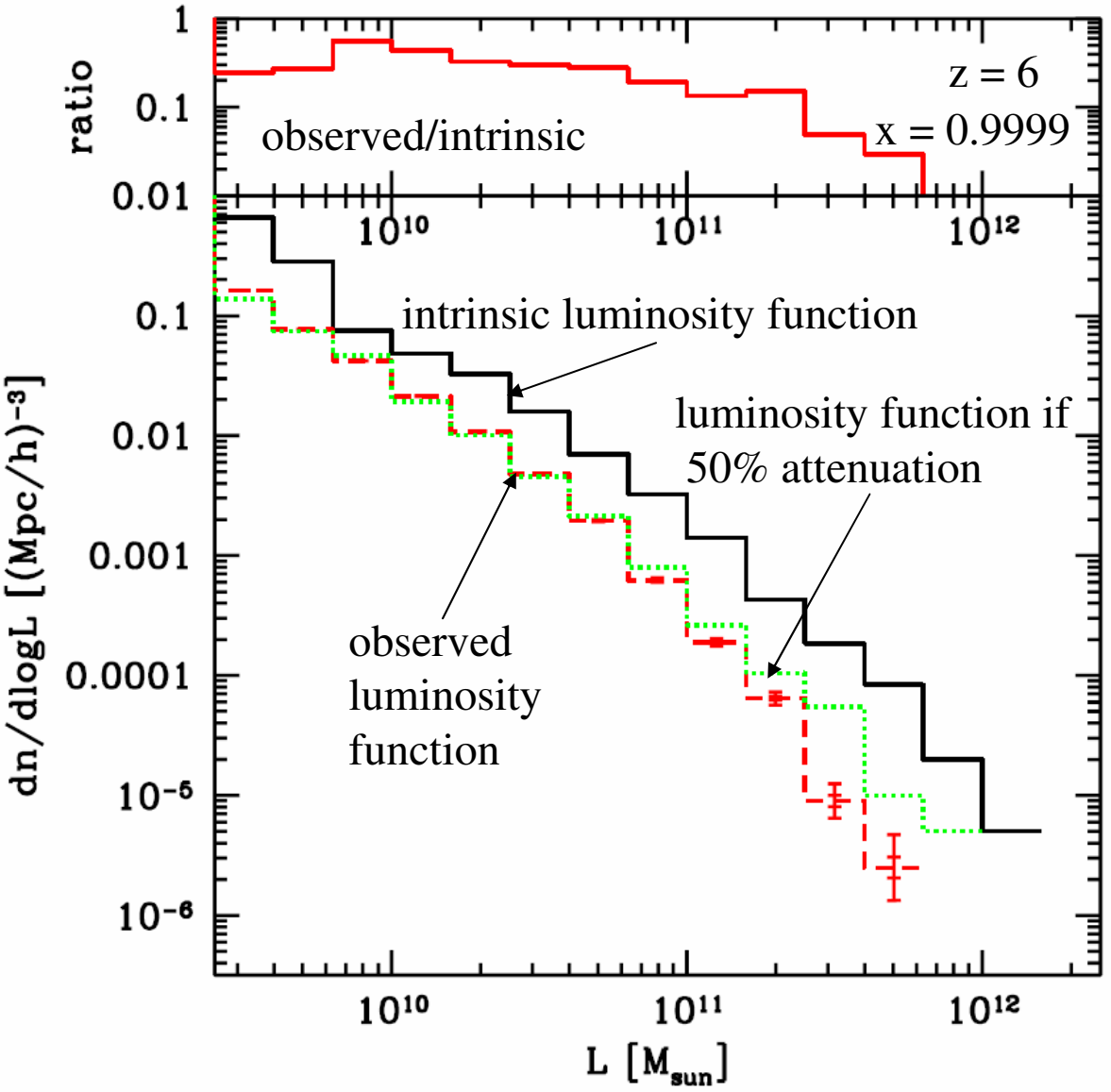

Predicting the observed luminosity function of Ly-α sources at the end of the EOR : simulations vs. observations

- To use our simulations to predict the observed LF, we "tune" the assumed M/L per halo to match the number density of sources in our simulations to the observed one reported by Kashikawa et al. (2006)
- ➔ simulated LF is an excellent match of the shape, for an assumed faint-end slope of -1.5 for the fit to the observations.
- ➔ the majority of sources responsible for reionization are too faint to be observed at present.

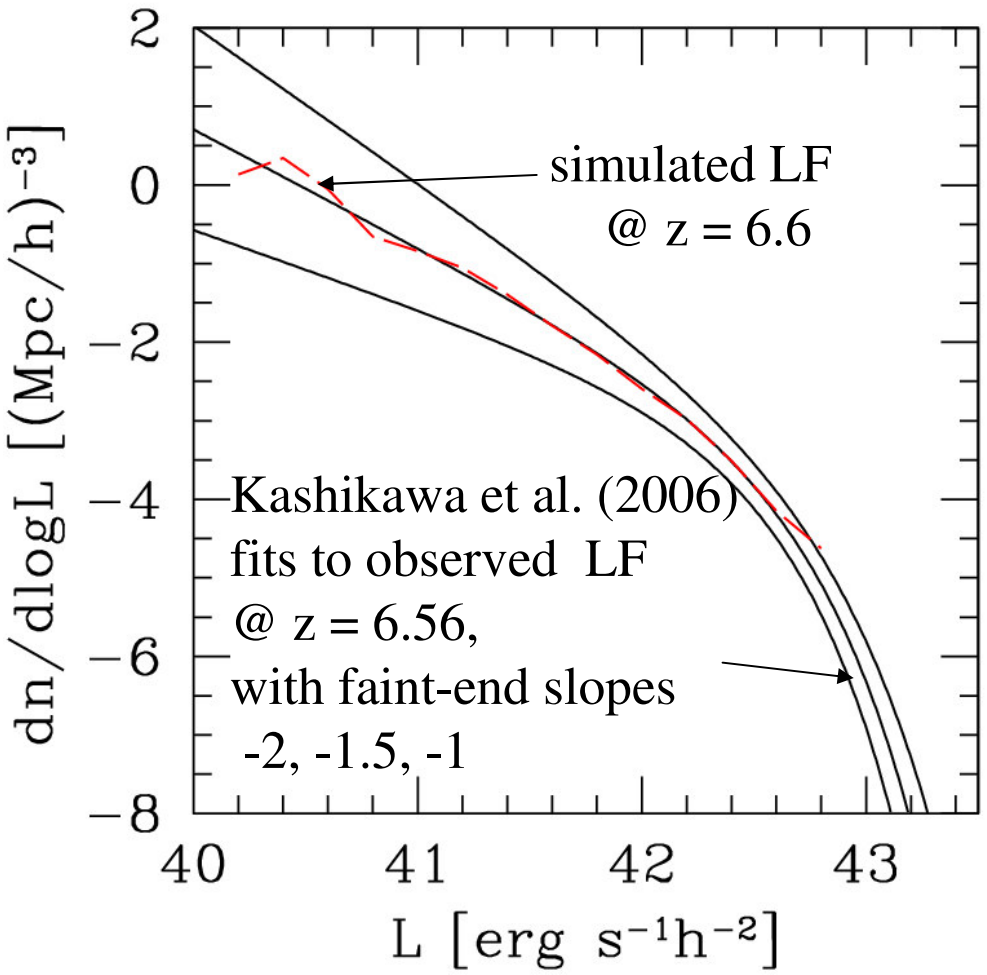

Mean IGM transmission due to Lyman-line resonance scattering at the end of the EOR : the Gunn-Peterson Effect at z > 6

- Simulations predict the Ly-α, Ly-β, and Ly-γ opacity of the IGM and its evolution during the EOR ➔ compare with the absorption spectra of observed high-redshift quasars to test the theory and the efficiencies assumed for the release of ionizing photons by early galaxies.

- e.g. for this illustrative simulation, EOR ended a bit too early to match the data from Fan et al. (2006) ➔ predicts somewhat higher transmission than observed, but captures the observed trend with redshift well ➔ lower source efficiencies are required for a better fit.

- Higher-z data can constrain reionization parameters better.

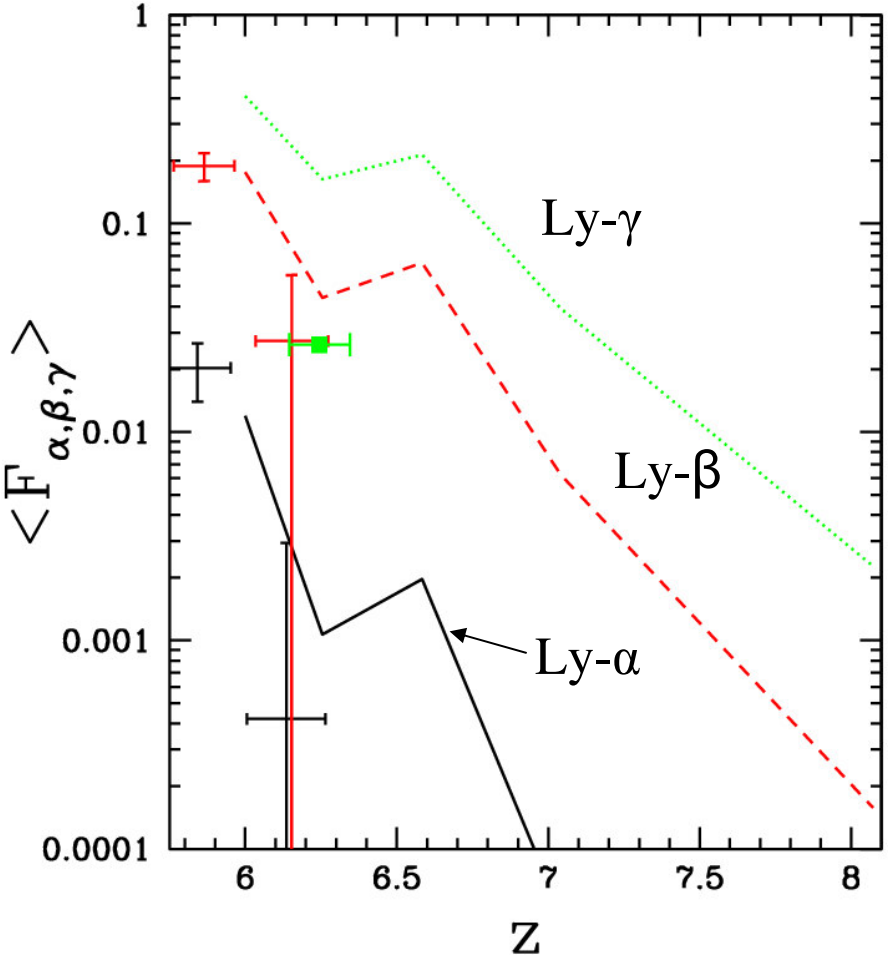

The Cosmic Near-Infrared Background: Fluctuations from the Epoch of Reionization

Fernandez, E., Komatsu, E., Iliev, I. T. & Shapiro, P. R. 2009, ApJ, submitted (astro-ph/0906.4552)

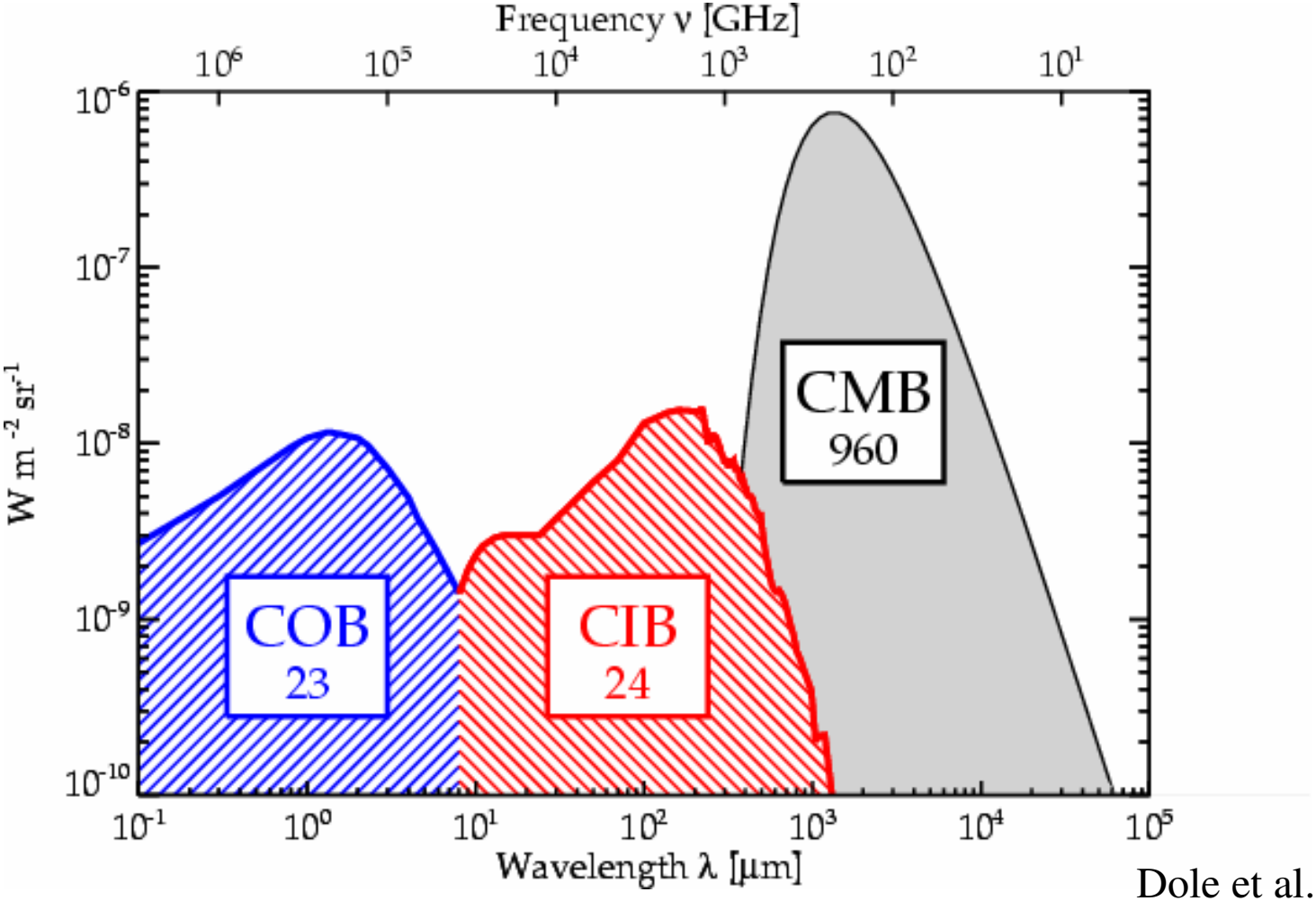

Dole et al. (2006)

The Cosmic Near-Infrared Background: Fluctuations from the Epoch of Reionization

Fernandez, E., Komatsu, E., Iliev, I. T. & Shapiro, P. R. 2009, ApJ, submitted (astro-ph/0906.4552)

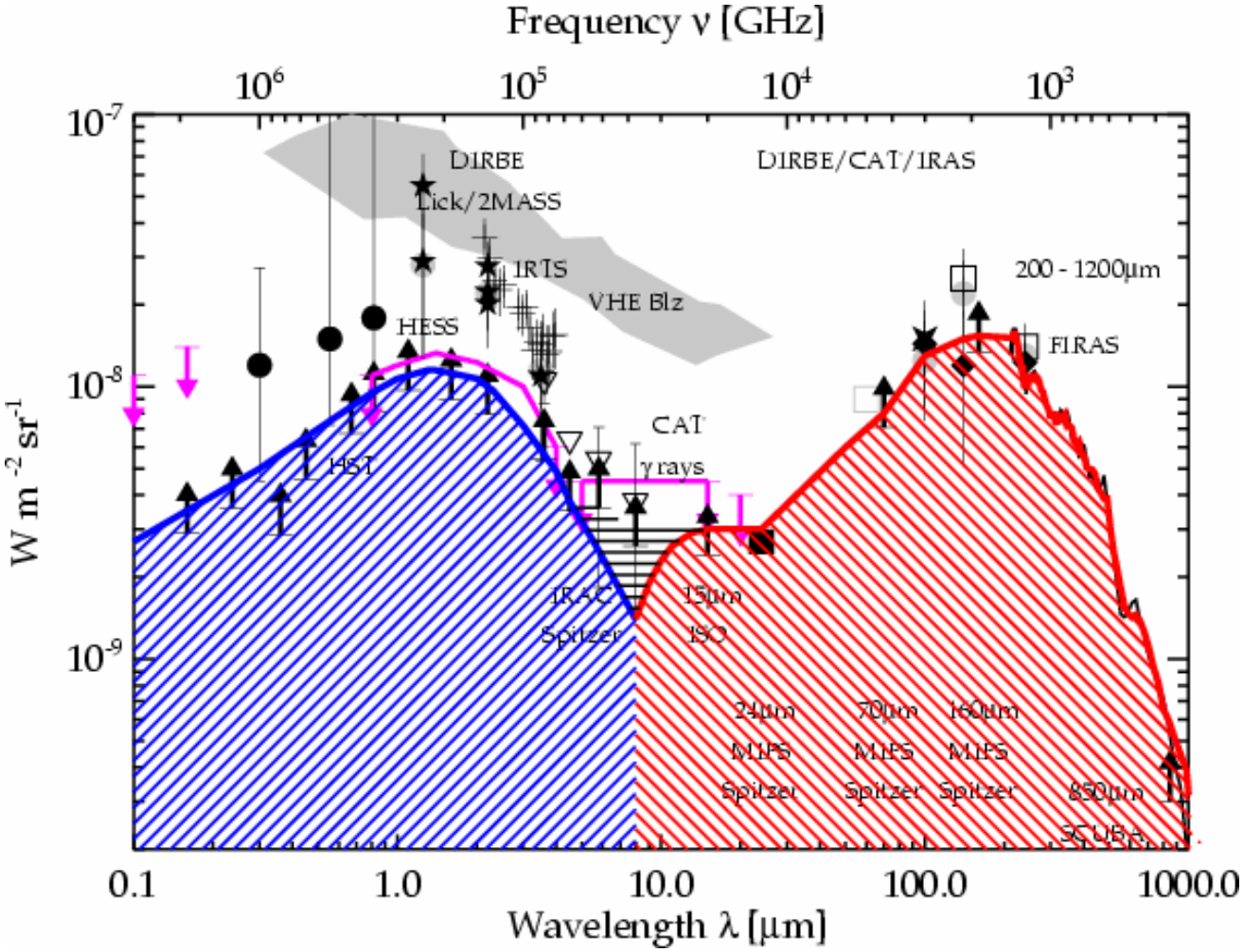

Dole et al. (2006)

The Cosmic Near-Infrared Background: Fluctuations from the Epoch of Reionization

Fernandez, E., Komatsu, E., Iliev, I. T. & Shapiro, P. R. 2009, ApJ, submitted (astro-ph/0906.4552)

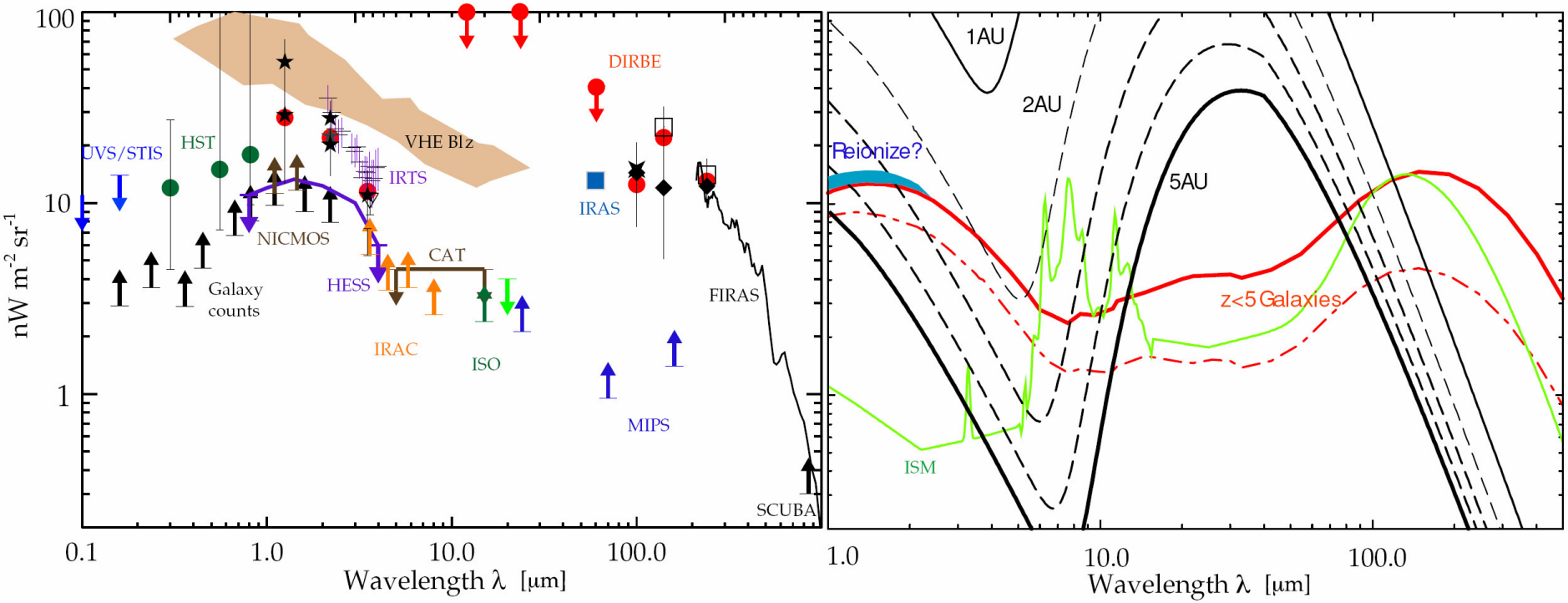

Cooray etal. (2009)

The Cosmic Near-Infrared Background: Fluctuations from the Epoch of Reionization

Fernandez, E., Komatsu, E., Iliev, I. T. & Shapiro, P. R. 2009, ApJ, submitted (astro-ph/0906.4552)

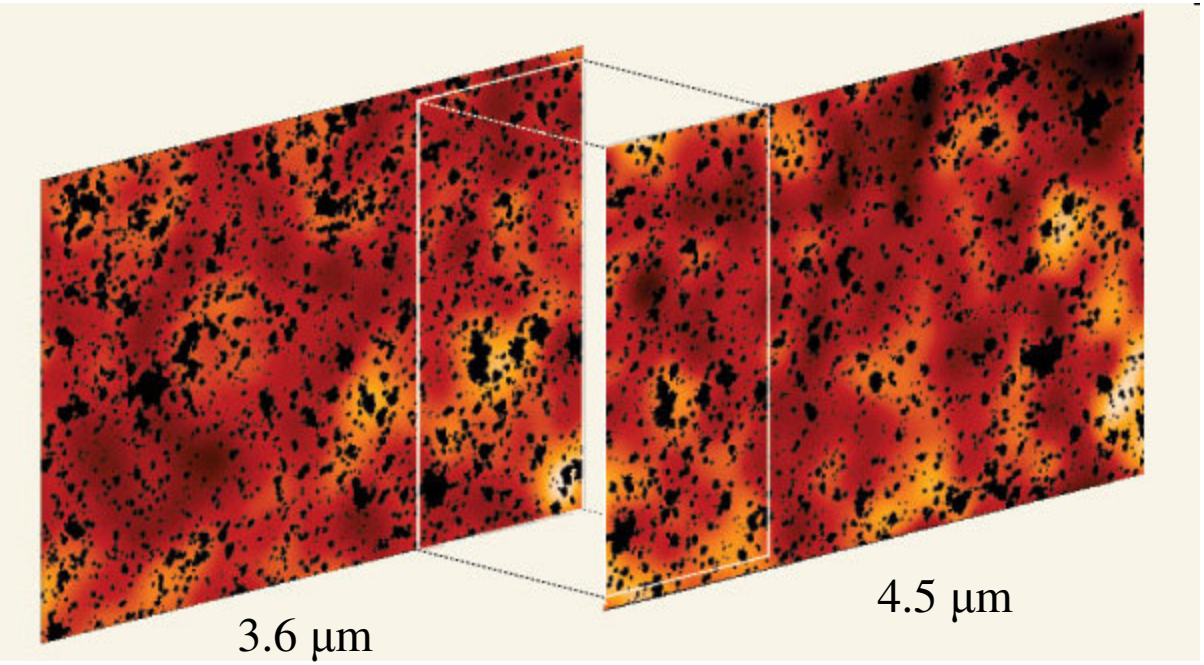

Near-Infrared Images of the sky in Hubble Deep Field North, by NASA's *Spitzer* Satellite, in two, partially-overlapping fields of view, with point sources removed and regions near bright sources masked

Kashlinsky et al. (2006)

The Cosmic Near-Infrared Background: Fluctuations from the Epoch of Reionization

Fernandez, E., Komatsu, E., Iliev, I. T. & Shapiro, P. R. 2009, ApJ, submitted (astro-ph/0906.4552)

- For a given reionization history, the product of f_* and f_{esc} are fixed.
- NIRB fluctuations are maximized by high f_* and low f_{esc}

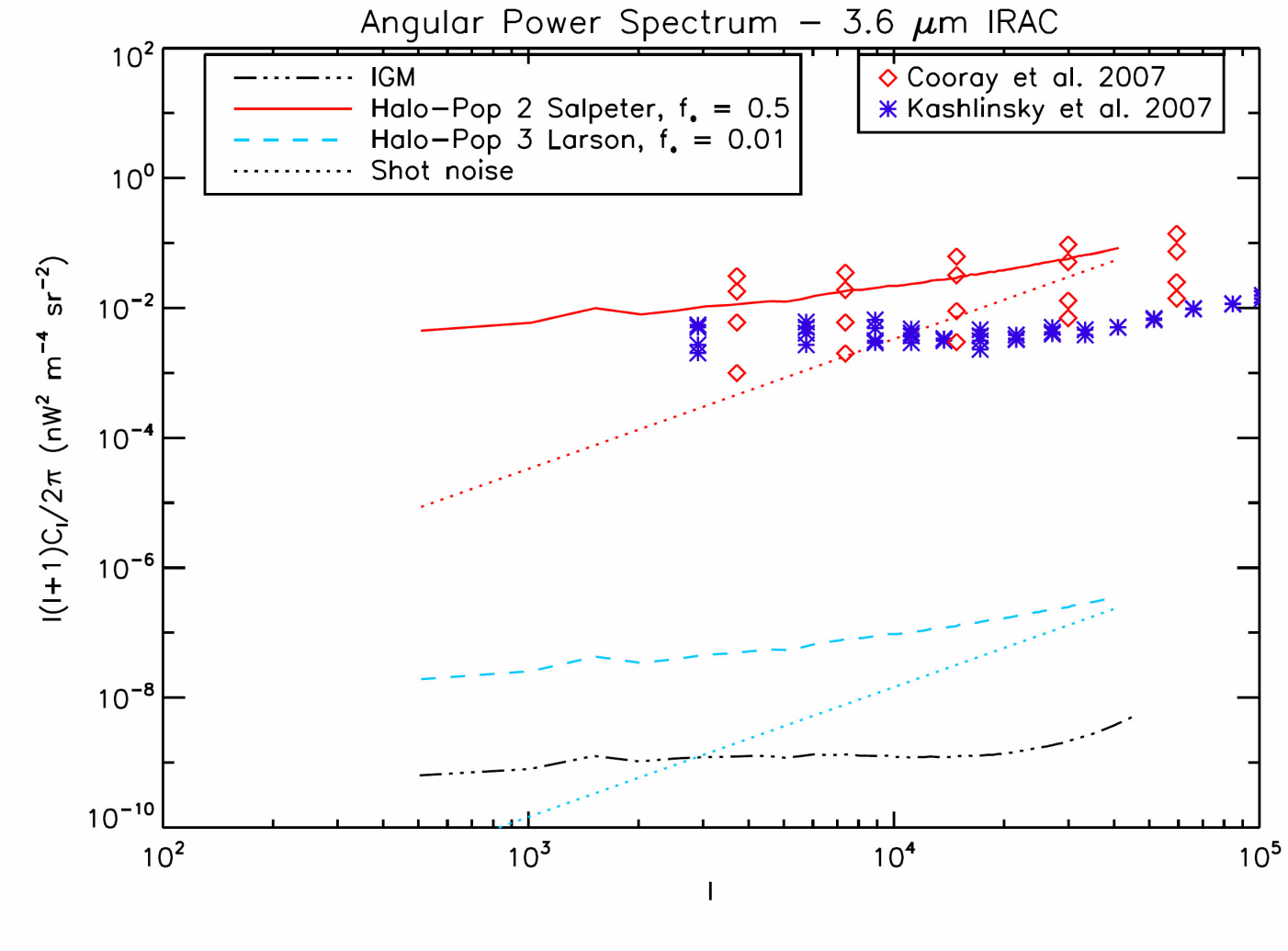

The Cosmic Near-Infrared Background: Fluctuations from the Epoch of Reionization

Fernandez, E., Komatsu, E., Iliev, I. T. & Shapiro, P. R. 2009, ApJ, submitted (astro-ph/0906.4552)

- For a given reionization history, the product of f_* and f_{esc} are fixed.
- NIRB fluctuations are maximized by high f_* and low f_{esc}

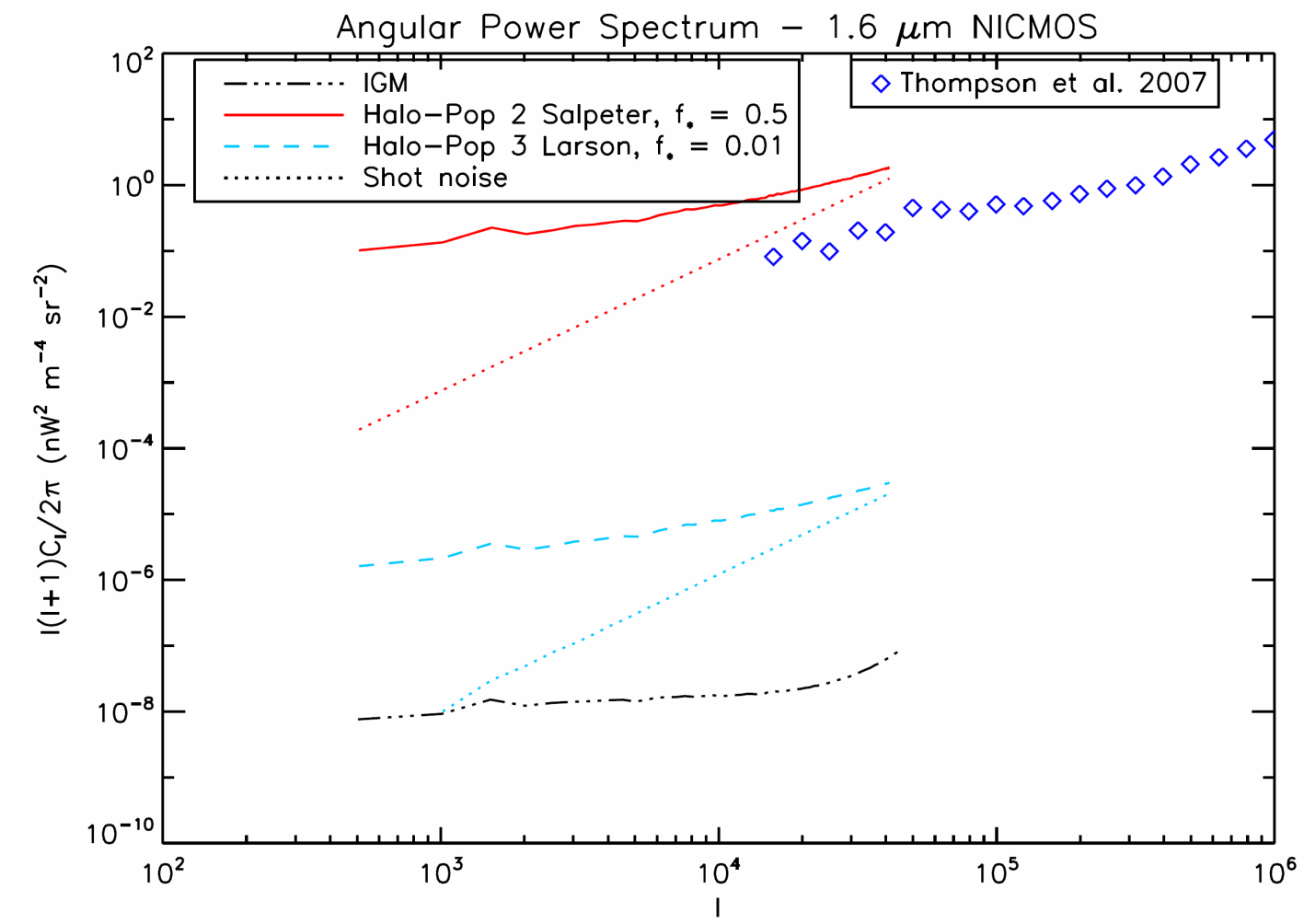

The Cosmic Near-Infrared Background: Fluctuations from the Epoch of Reionization

Fernandez, E., Komatsu, E., Iliev, I. T. & Shapiro, P. R. 2009, ApJ, submitted (astro-ph/0906.4552)

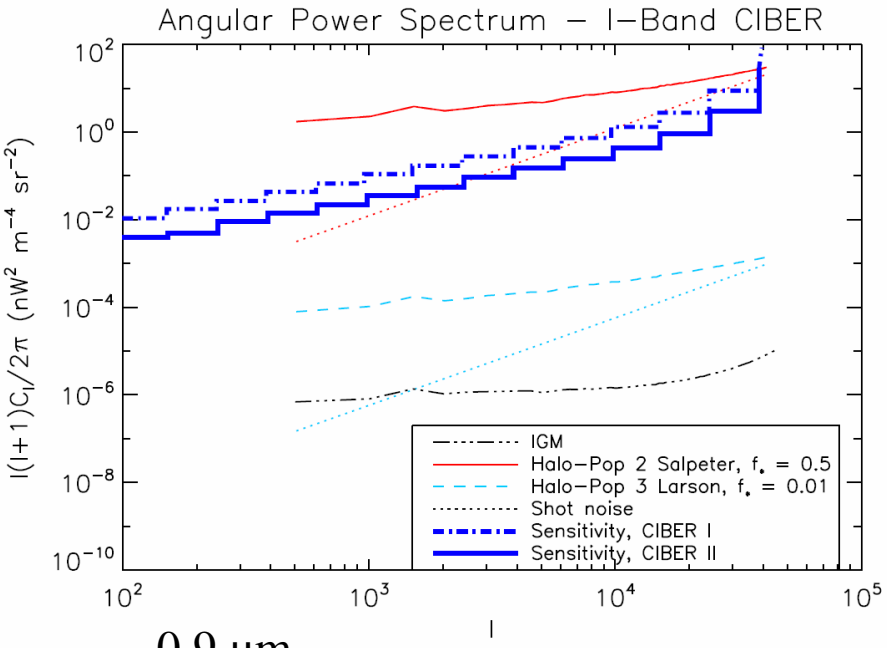

0.9 μm

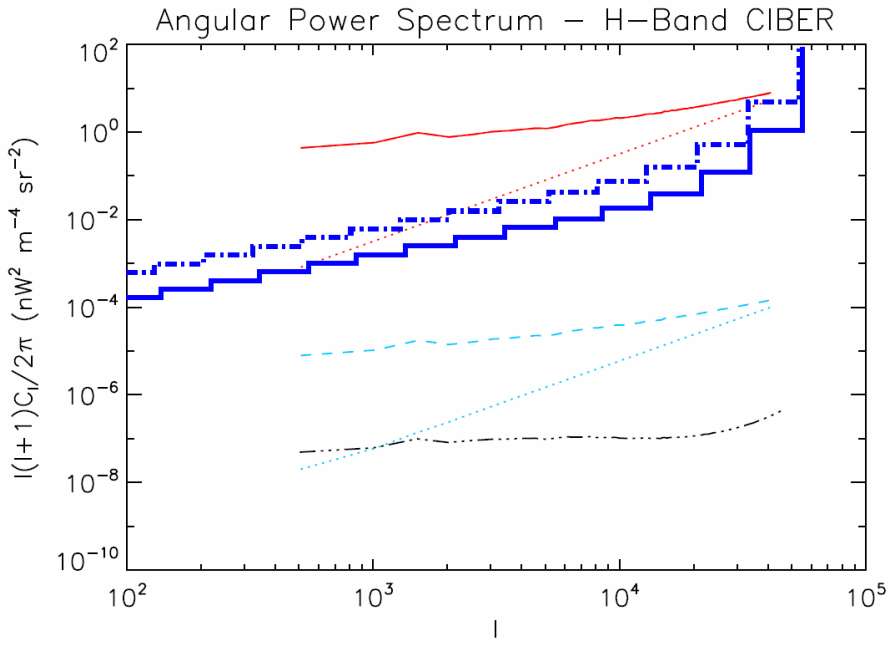

1.6 μm

CIBER sensitivity from Cooray et al. (2009)

- a range of possible reionization efficiencies makes the NIRB background fluctuations detectable by future experiments like CIBER

The Cosmic Near-Infrared Background: Fluctuations from the Epoch of Reionization

Fernandez, E., Komatsu, E., Iliev, I. T. & Shapiro, P. R. 2009, ApJ, submitted (astro-ph/0906.4552)

if mean NIRB intensity
< 3 nW m^{-2} str^{-1}
(Thompson et al. 2007)

===> high star formation efficiency (e.g. $f_* > 0.2$) makes mean NIRB too high, *regardless* of NIRB fluctuation constraints

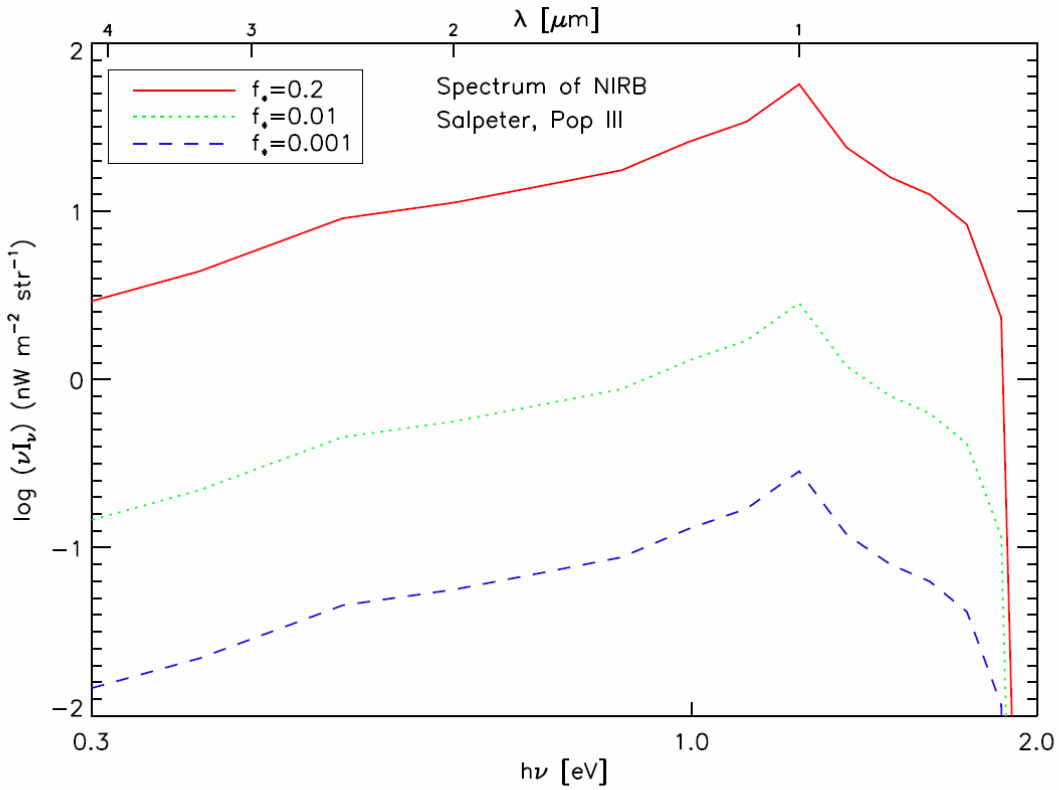

Self-Regulated Reionization

Iliev, Mellema, Shapiro, & Pen (2007), MNRAS, 376, 534; (astro-ph/0607517)

•Jeans-mass filtering ➔ low-mass source halos ($M < 10^9 M_{solar}$) cannot form inside H II regions ;

•35/h Mpc box, 406^3 radiative transfer simulation, WMAP3, $f_\gamma = 250$;

•resolved all halos with $M > 10^8 M_{solar}$ (i.e. all atomically-cooling halos), (blue dots = source cells);

• Evolution: z=21 to $z_{ov} = 7.5$.

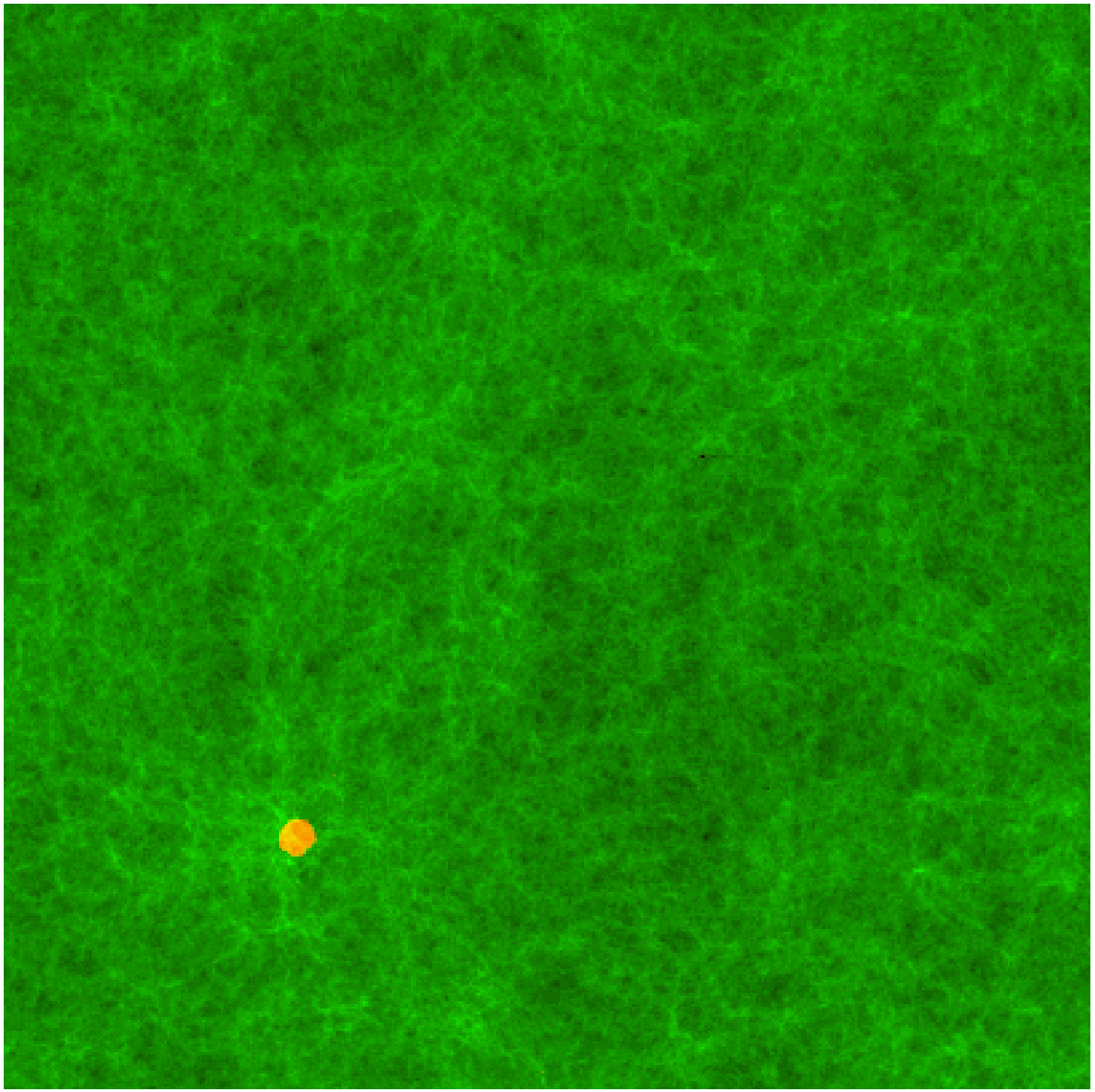

Self-Regulated Reionization

Iliev, Mellema, Shapiro, & Pen (2007), MNRAS, 376, 534; (astro-ph/0607517)

•Jeans-mass filtering ➔ low-mass source halos ($M < 10^9 M_{solar}$) cannot form inside H II regions ;

•35/h Mpc box, 406^3 radiative transfer simulation, WMAP3, $f_\gamma = 250$;

•resolved all halos with $M > 10^8 M_{solar}$ (i.e. all atomically-cooling halos), (blue dots = source cells);

• Evolution: z=21 to $z_{ov} = 7.5$.

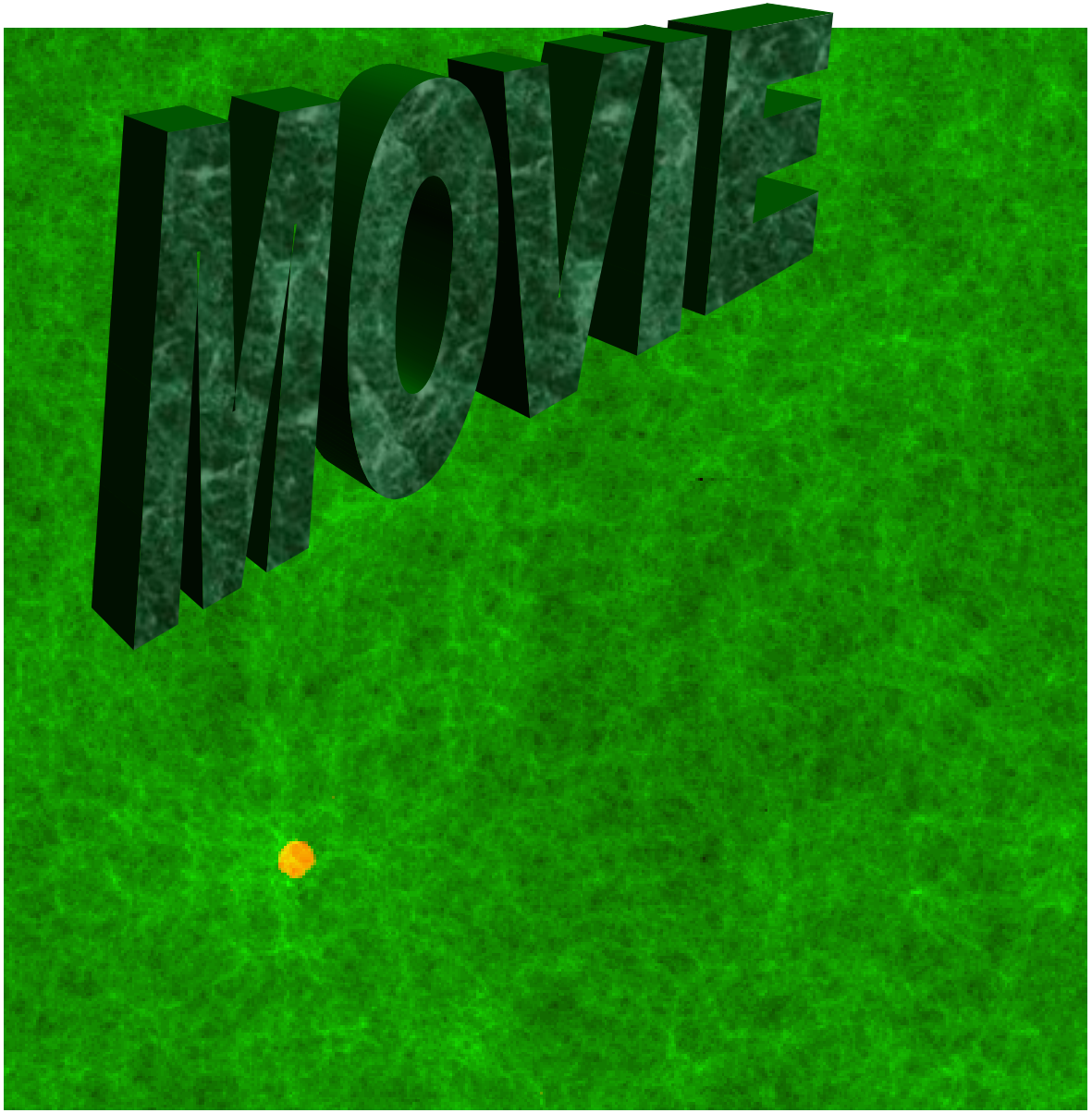

Extended reionization: Jeans-mass filtering, halo-mass-dependent emissivity

Cases

1. Halo masses $M_{solar} > 10^9$
   $f_\gamma = 2000$ (e.g. Pop III);

2. Halo masses $M_{solar} > 10^9$
   $f_\gamma = 250$ (e.g. Pop II);

3. Halo masses $M_{solar} > 10^8$
   $f_\gamma = 250$ (e.g. Pop II),
   lower-mass halos
suppressed inside H II regions
(Jeans-mass filtering) ;

4. Same as 3., but
   $f_\gamma = 2000$ ($M_{solar} < 10^9$)
   $f_\gamma = 250$ ($M_{solar} > 10^9$)

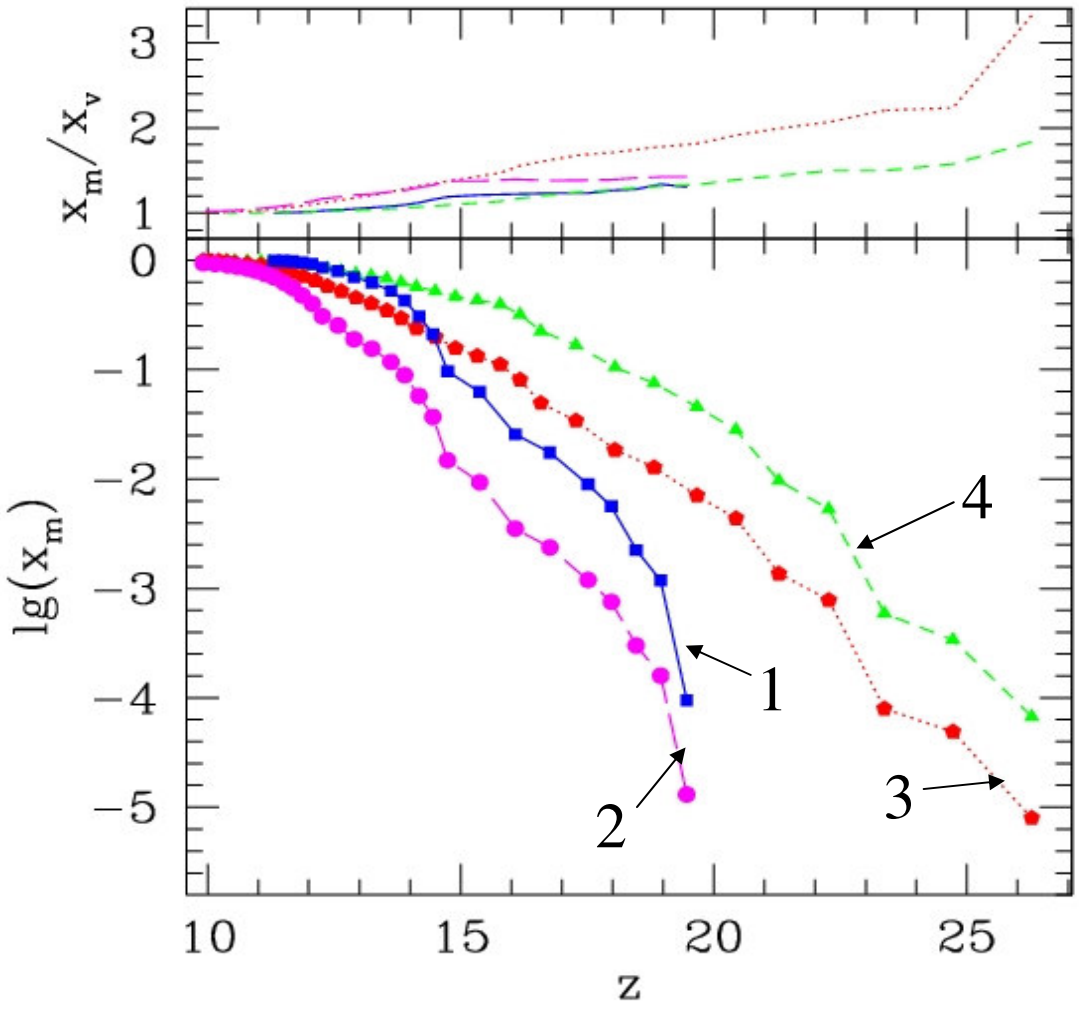

New, Large-Scale Simulations of Self-Regulated Reionization

Iliev, Mellema, Pen, Shapiro, and Merz (2008), in press (astro-ph/0806.2887); Shapiro, Iliev, Mellema, Pen, & Merz (2008), AIP 1035, 68 (astro-ph/0806.3091)

CubeP^{3}M N-body ΛCDM sim with
3072^3 (29 billion) particles,
6144^3 cells,
box size = 160 Mpc;
particle mass =
5 million solar masses

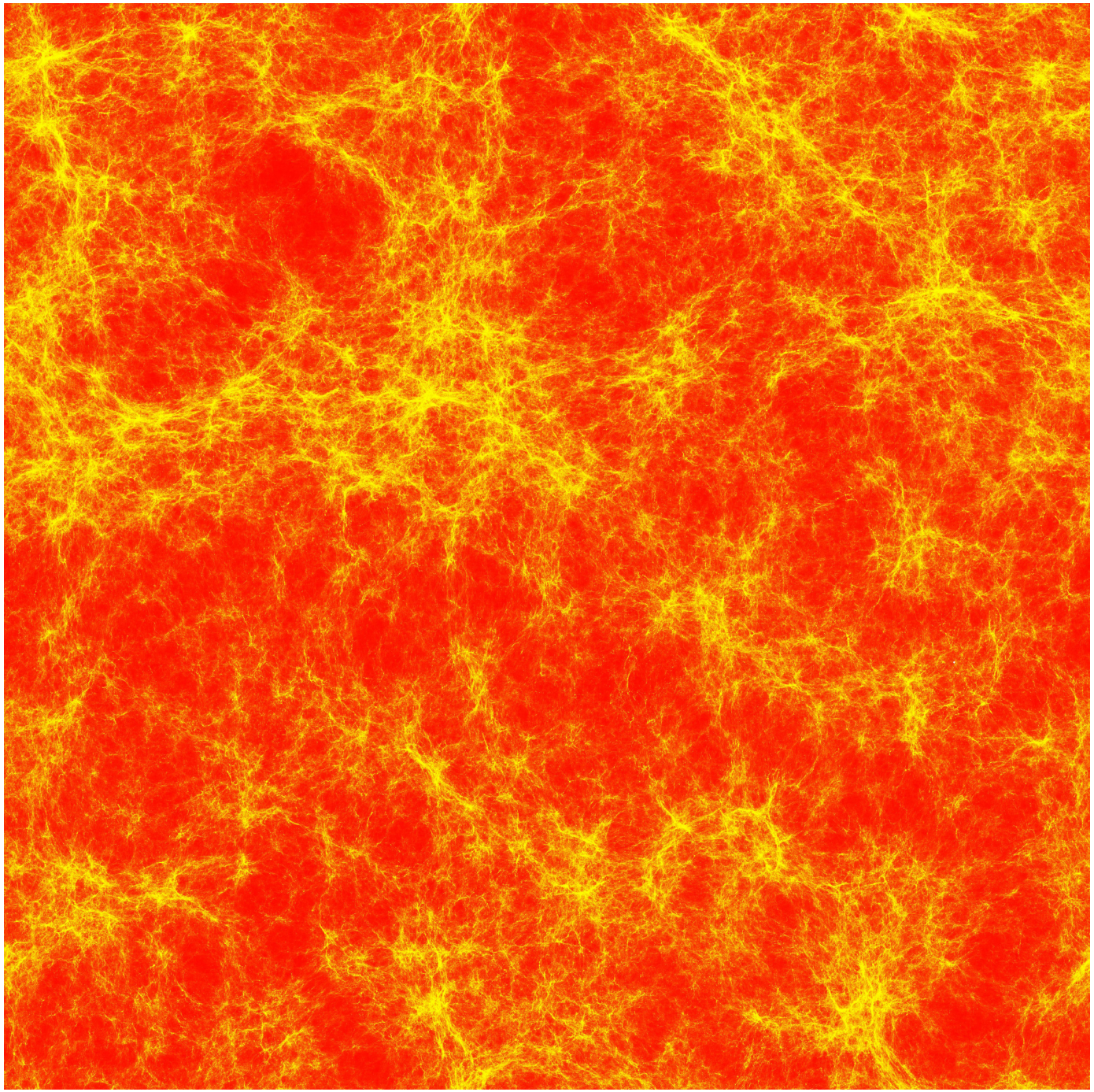

New, Large-Scale Simulations of Self-Regulated Reionization

Iliev, Mellema, Pen, Shapiro, and Merz (2008), in press (astro-ph/0806.2887); Shapiro, Iliev, Mellema, Pen, & Merz (2008), AIP 1035, 68 (astro-ph/0806.3091)

CubeP^{3}M N-body

ΛCDM sim with

3072^3 (29 billion) particles,

resolves halos above 10^8 solar masses

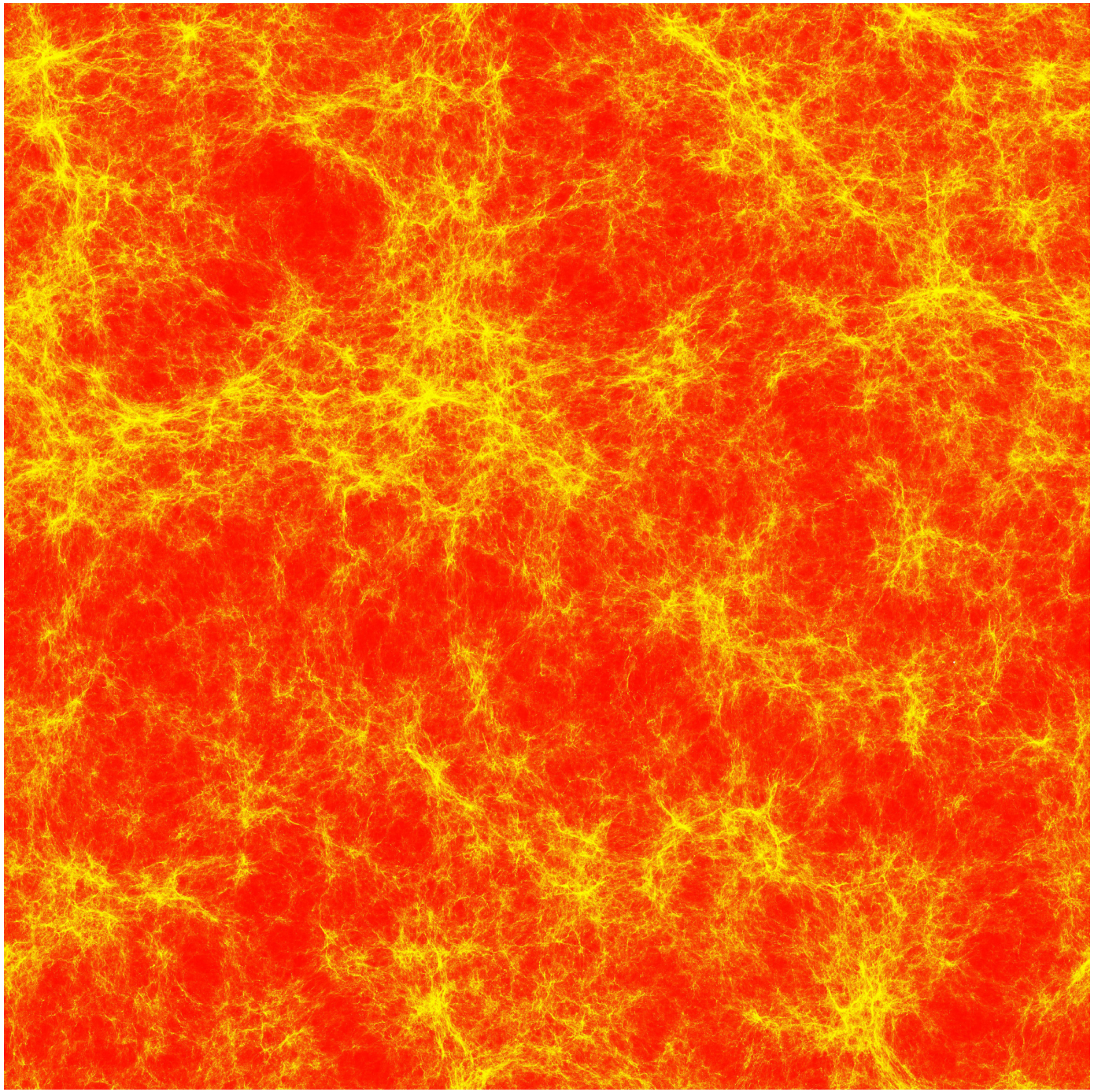

New, Large-Scale Simulations of Self-Regulated Reionization

Iliev, Mellema, Pen, Shapiro, and Merz (2008), in press (astro-ph/0806.2887); Shapiro, Iliev, Mellema, Pen, & Merz (2008), AIP 1035, 68 (astro-ph/0806.3091)

CubeP^{3}M N-body

- new Texas Sun Constellation Linux Cluster, *Ranger*, 2048 cores, 159,000 SUs (cores x hours)

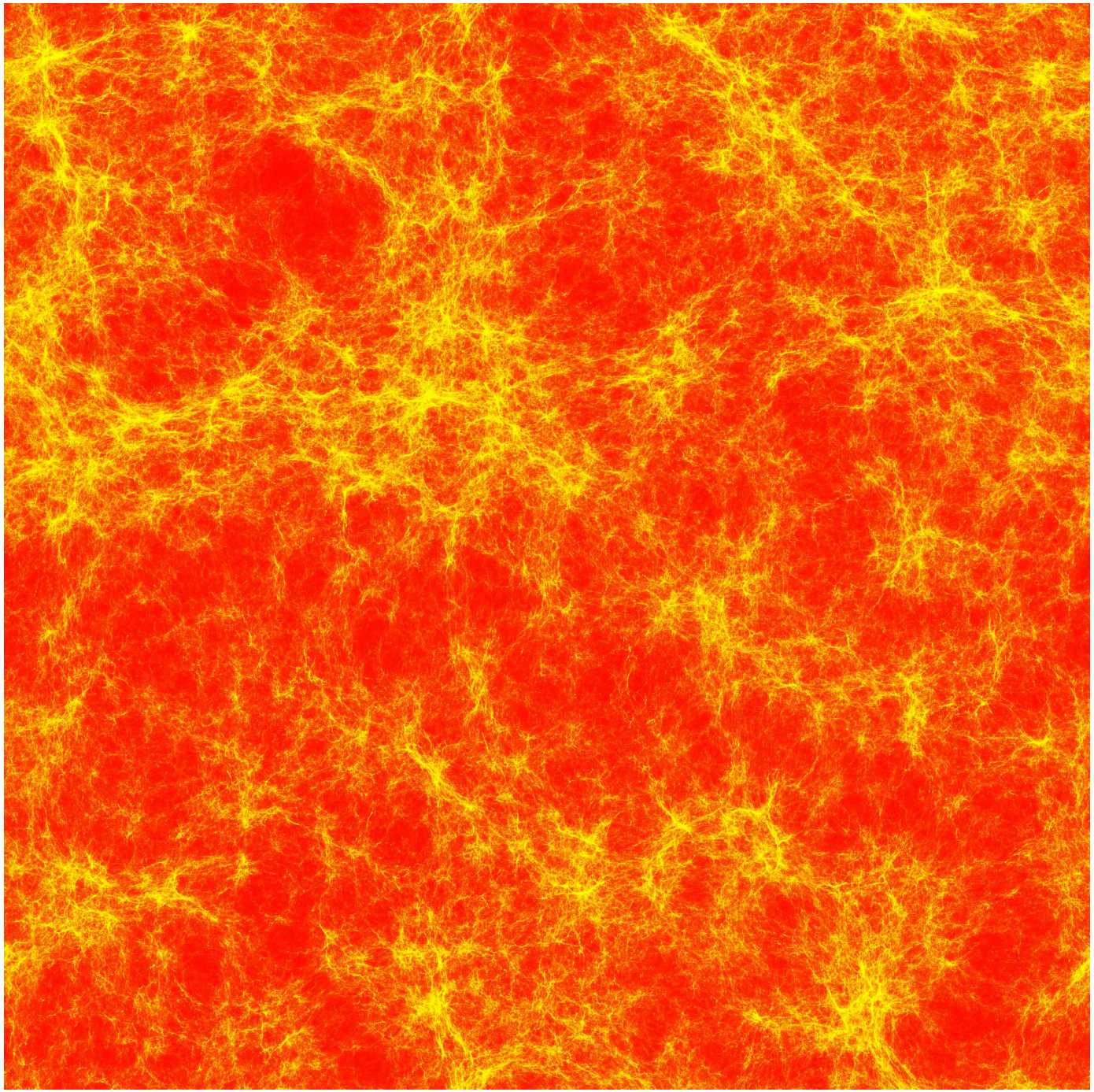

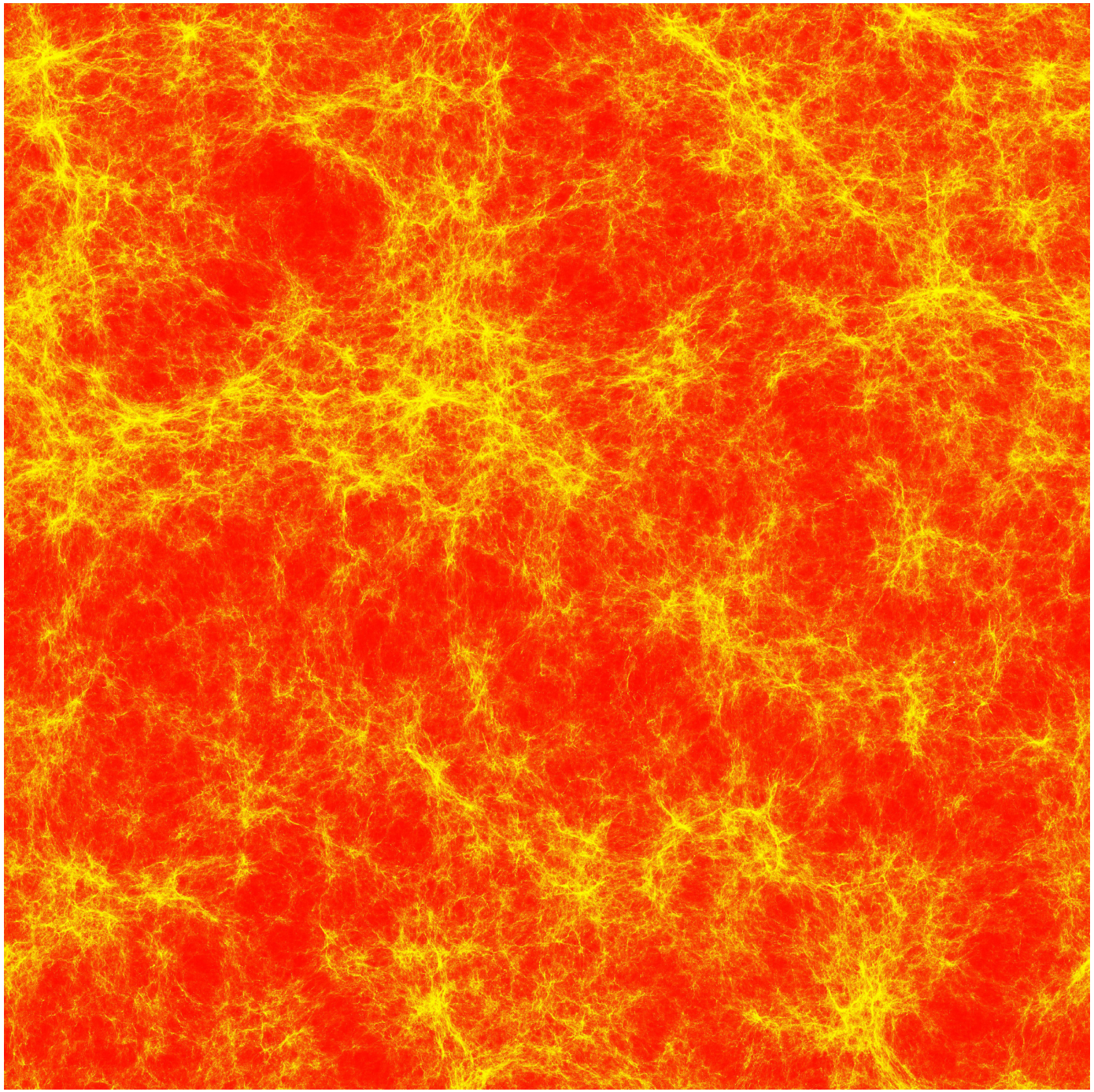

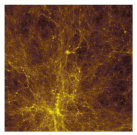

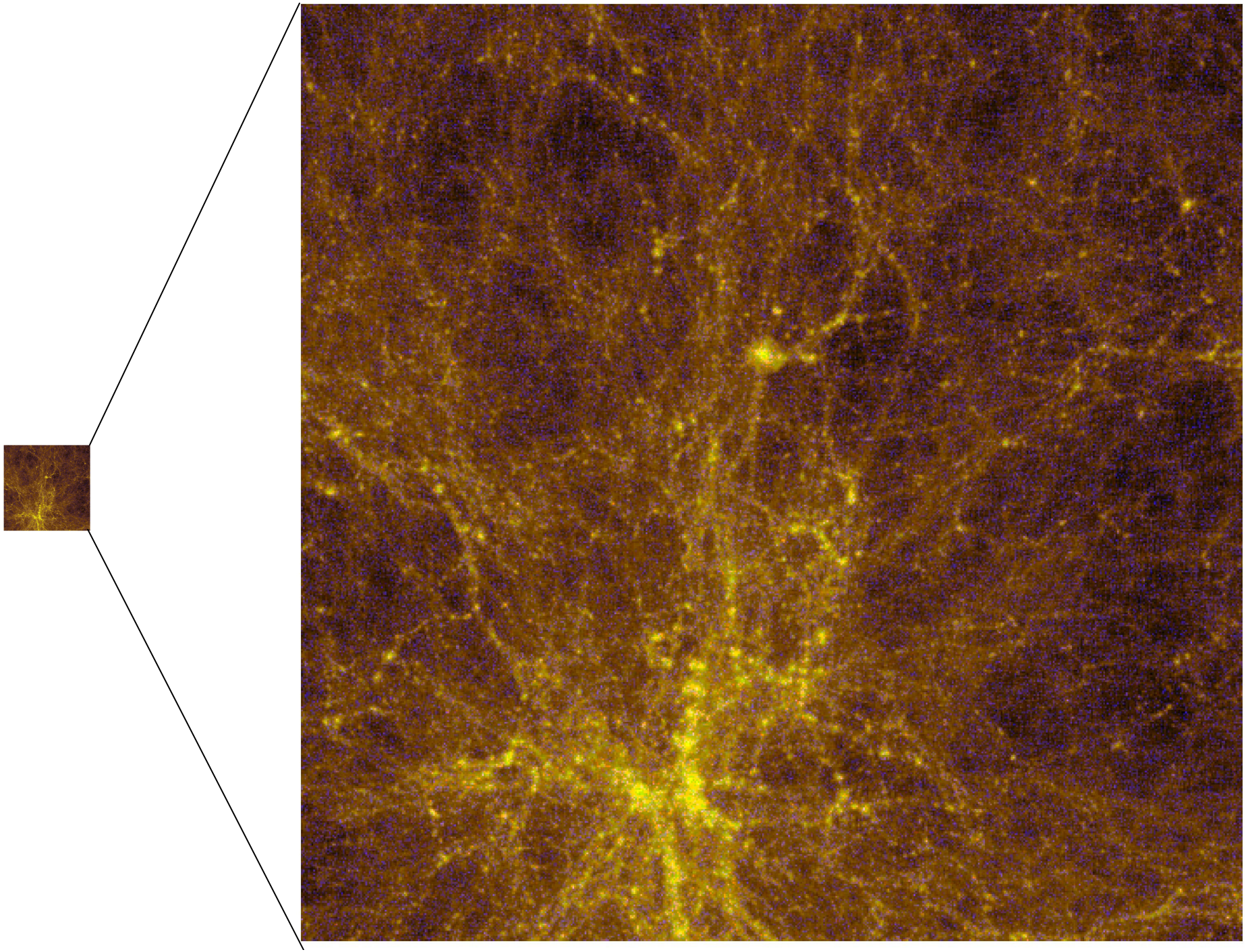

ΛCDM Halo Mass Function ($M > 10^8$ Solar Masses)

from CubeP^{3}M N-body Simulations

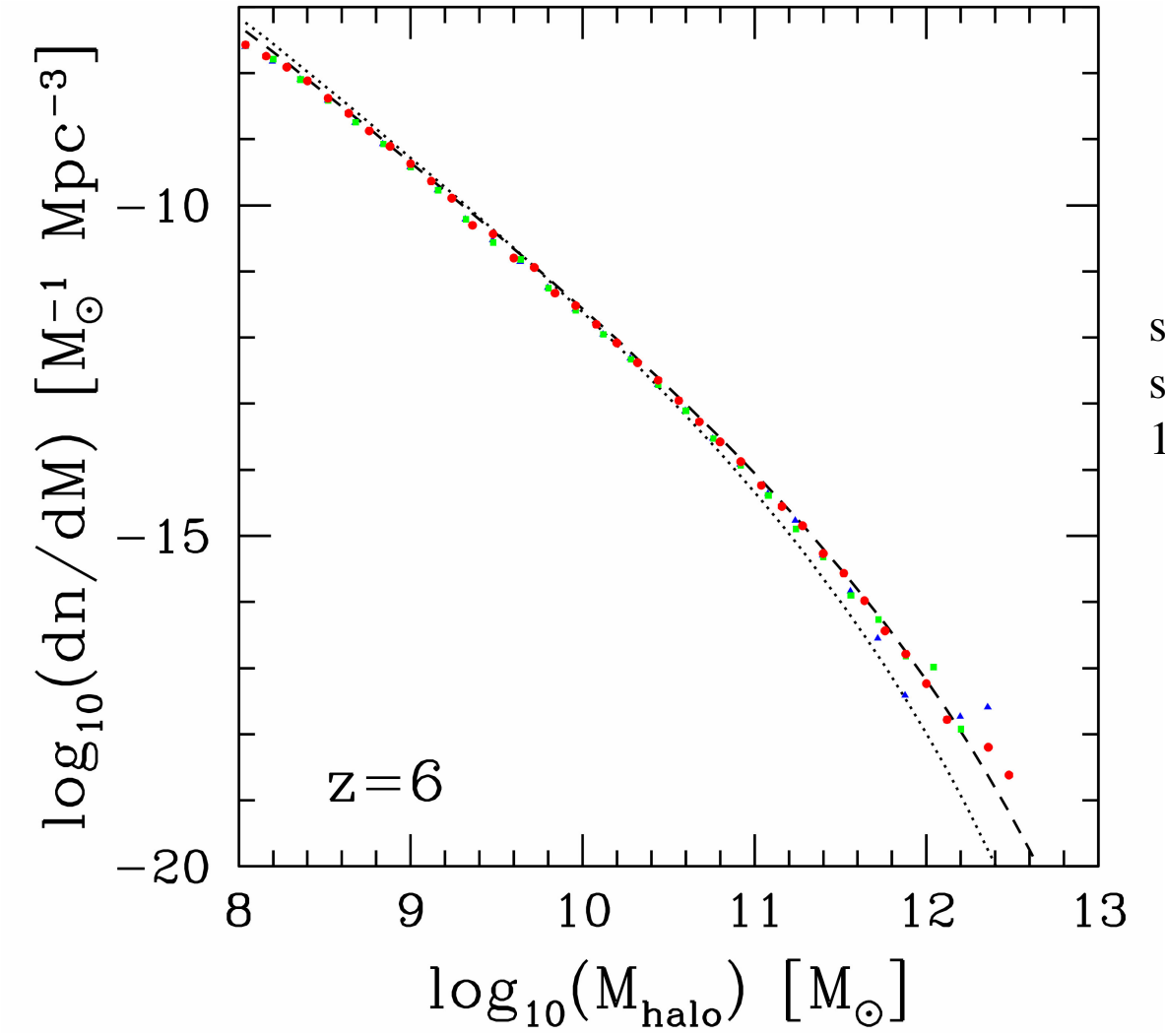

simulation box sizes 91 Mpc, 103 Mpc, 163 Mpc

C^2Ray radiative transfer

- RT grid 432^3 cells
- box size = 90 Mpc

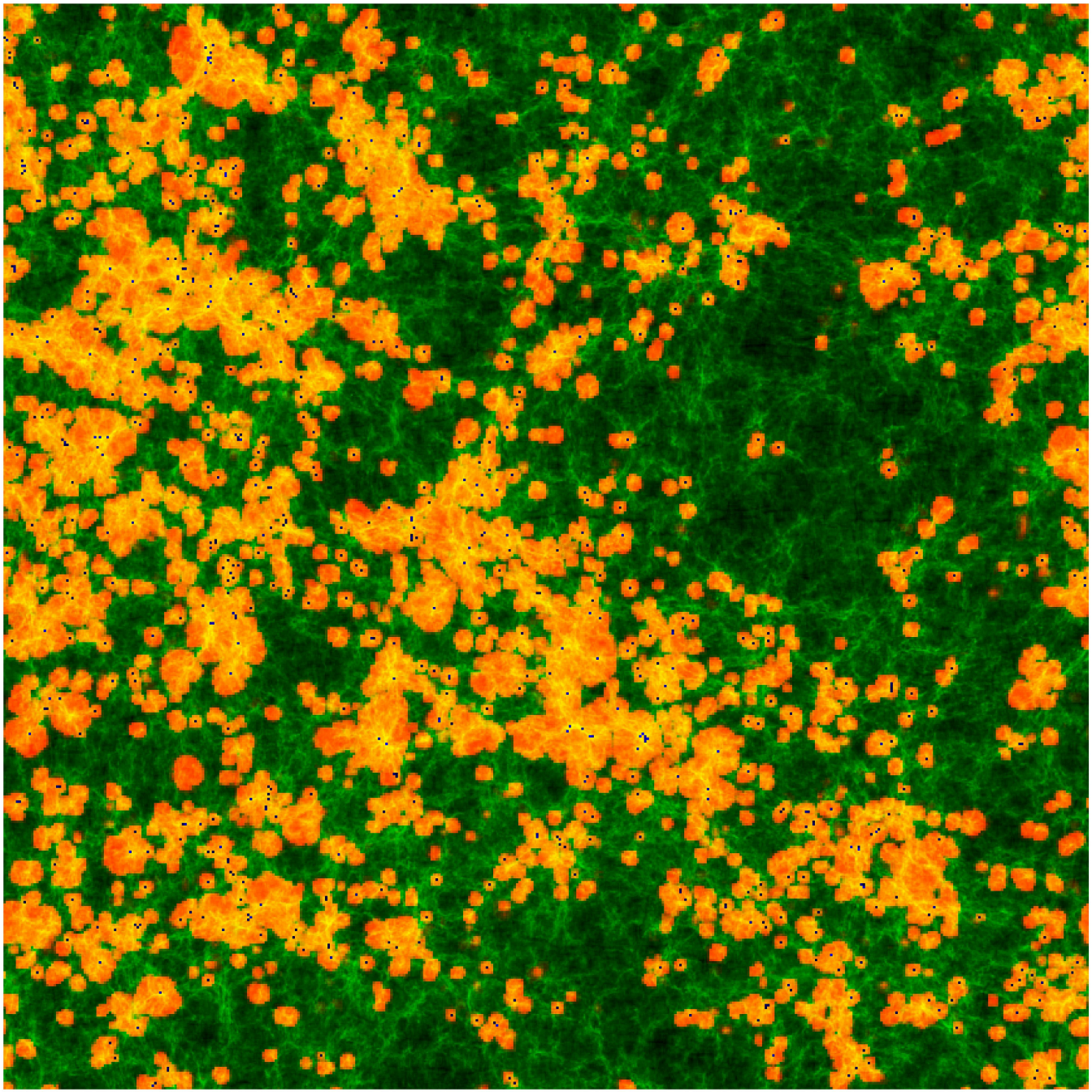

C^2Ray radiative transfer

- RT grid 432^3 cells
- box size = 90 Mpc
- *Ranger*, Texas Sun Constellation Linux Cluster, 700,000 SUs (cores x hours), up to 10,000 cores

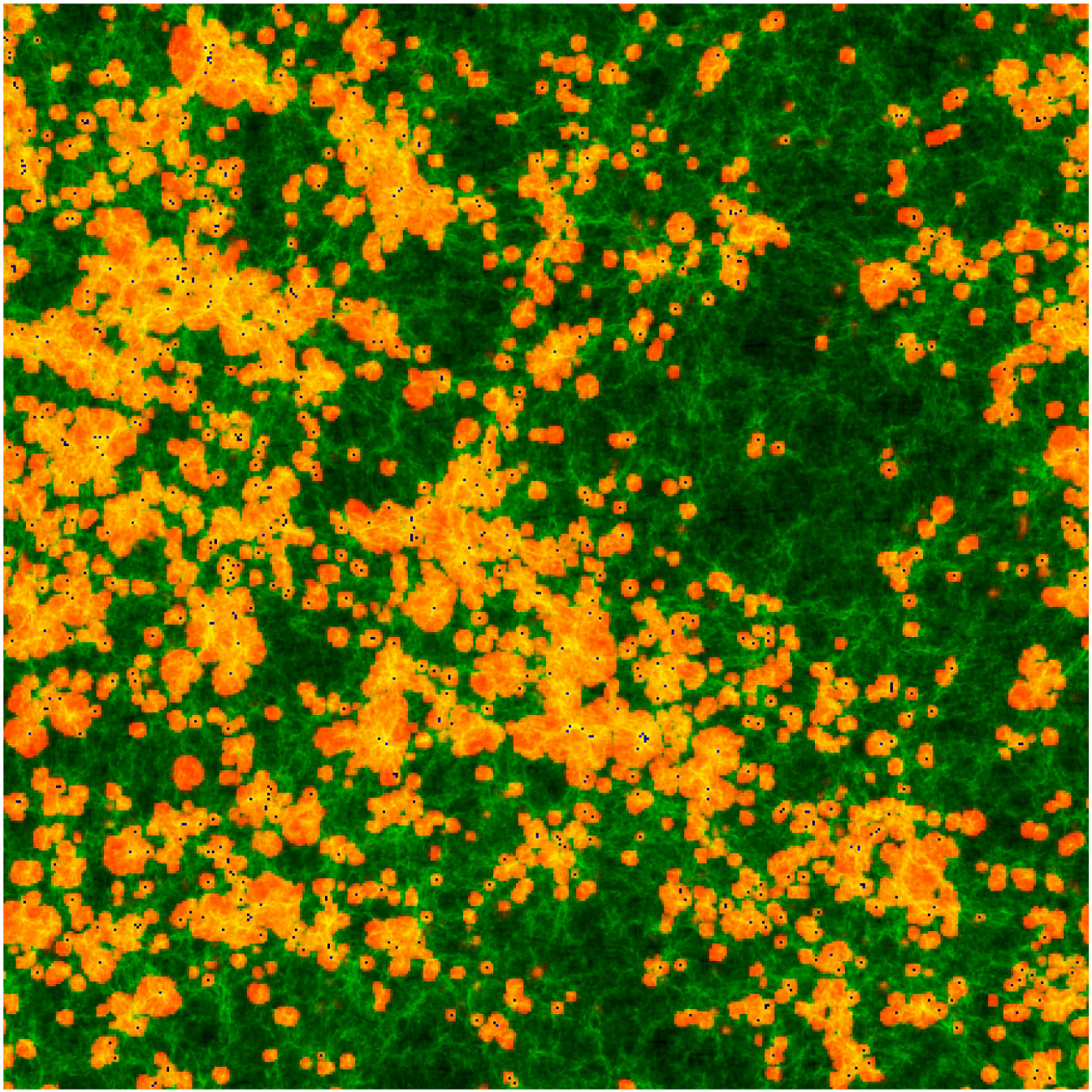

Self-Regulated Reionization in ΛCDM

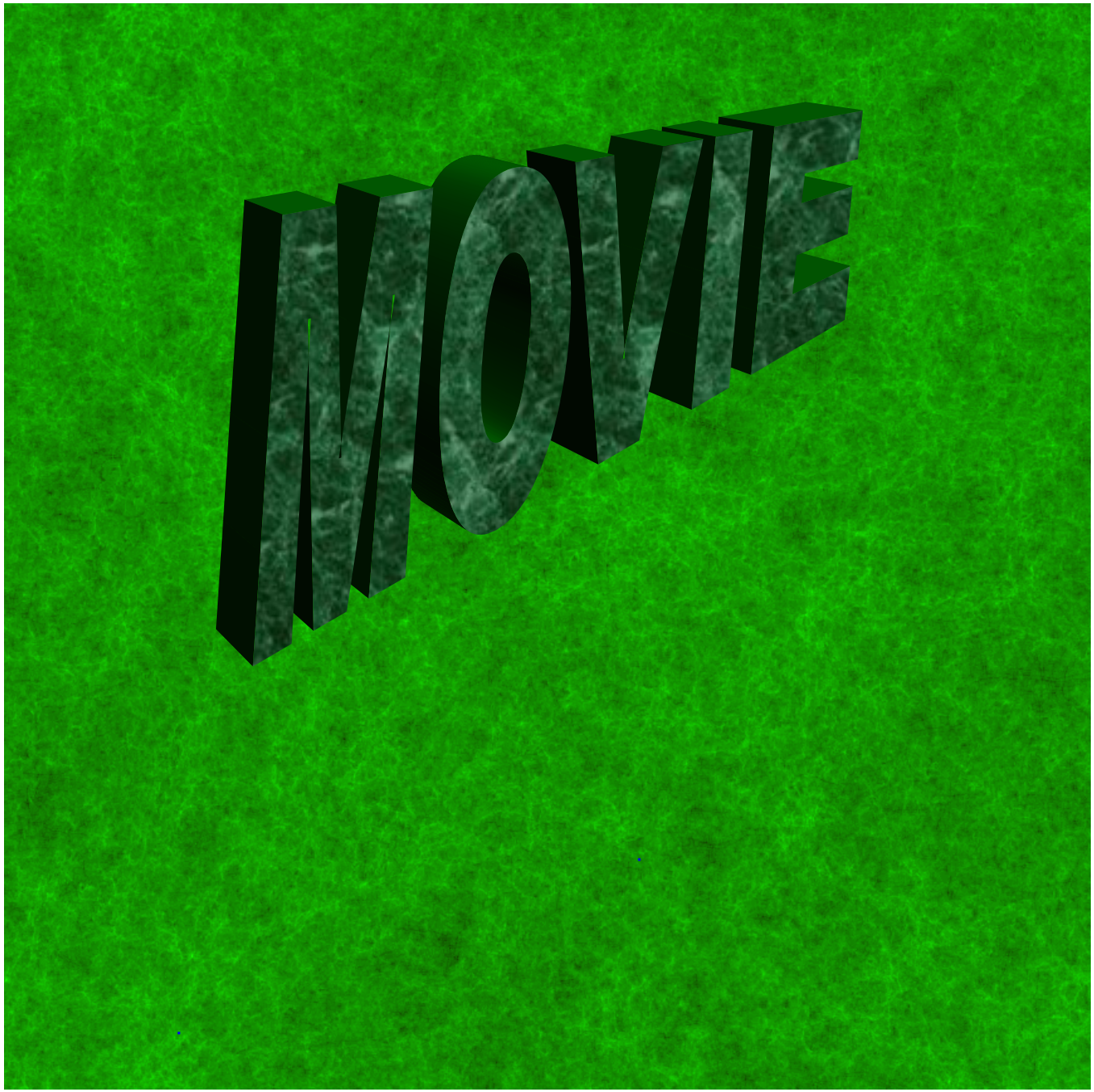

- 90 Mpc box

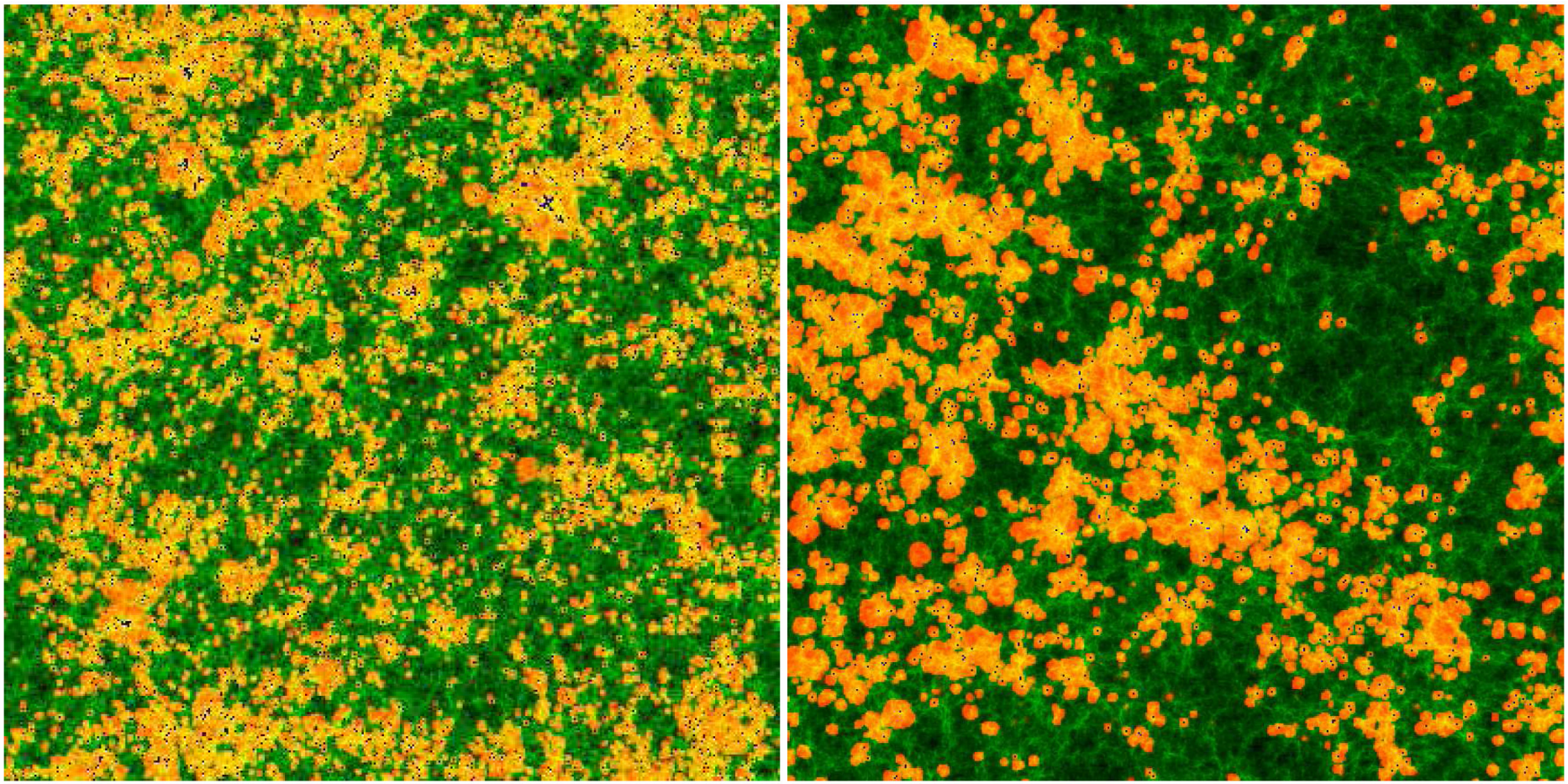

160 Mpc box

90 Mpc box

z = 11.6

z = 11.9

when mass-weighted mean ionized fraction of universe $x_m = 0.3$

Self-regulated halo mass function

- Jeans-mass filtering suppresses formation of sources in small-mass halos which form inside H II regions
- clustering of small-mass halos around density peaks enhances this effect ➔ suppression is strongly biased

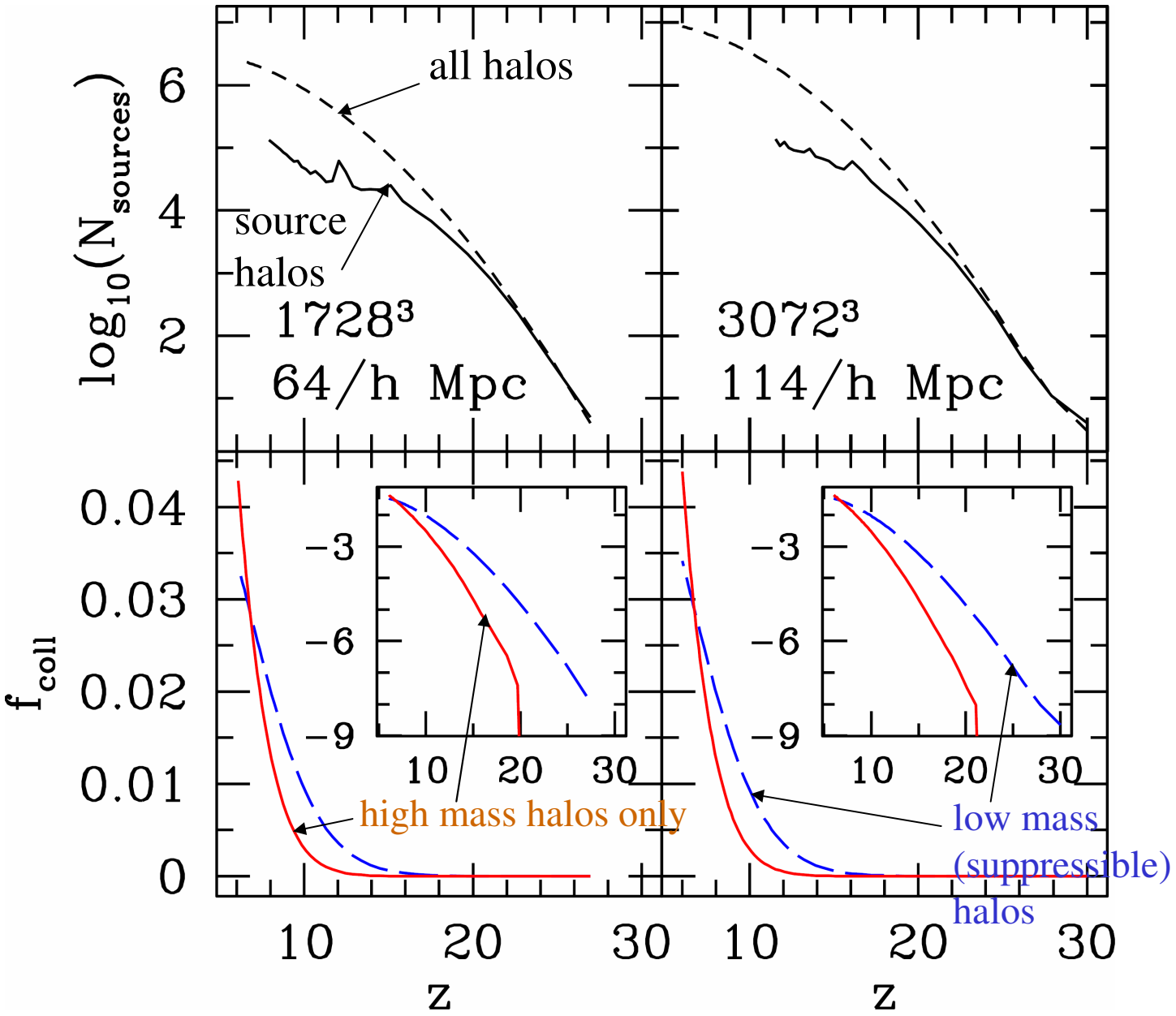

Evolution of the Mean Ionized Fraction of the Universe

- self-regulated reion.
  (i.e. small-mass halos resolved) starts earlier, but ends about the same time ➔
- high-mass halos dominate the end of EOR

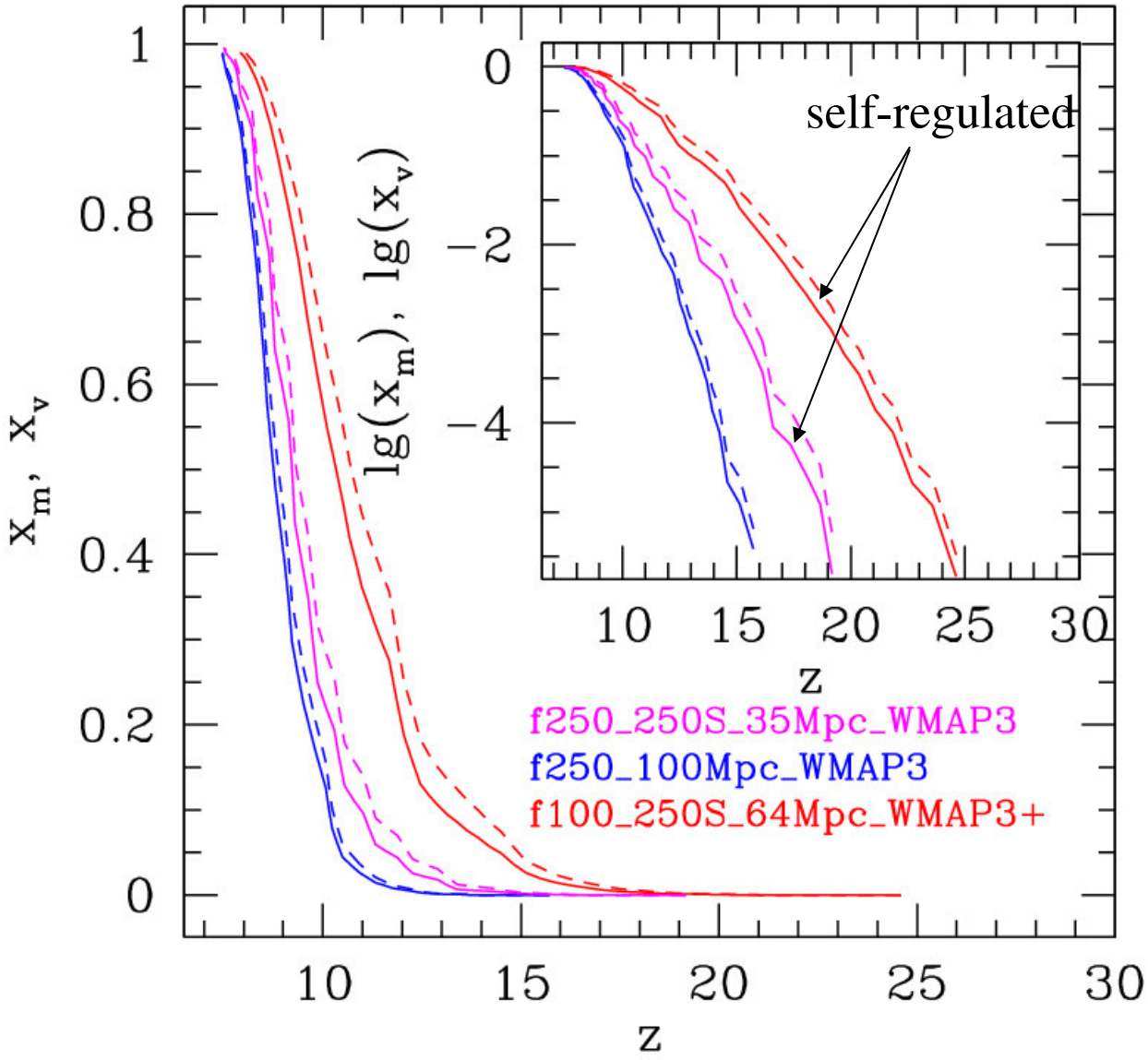

($\delta T/T_{CMB}$) Maps of the Kinetic Sunyaev-Zel'dovich Effect from Radiative Transfer Simulations of Patchy Reionization: Effect of Self-Regulation

- Box size 100/h Mpc comoving
  ➔ 50 ′ x 50 ′
- Source halos > 10^9 solar masses

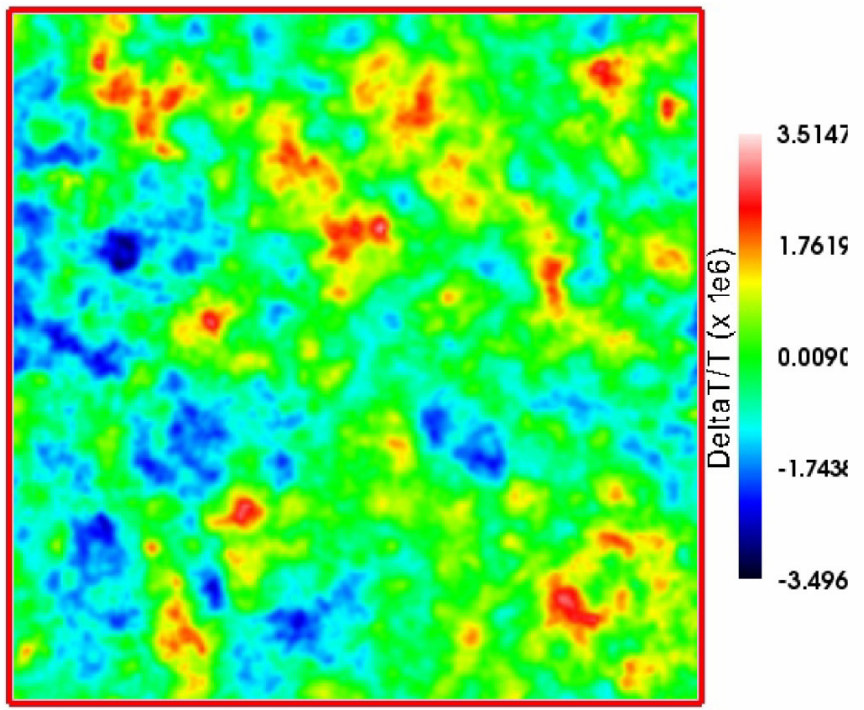

WMAP3

- Box size 114/h Mpc comoving
  ➔ 1^o x 1^o
- Source halos > 10^8 solar masses
- Self – Regulated Reionization

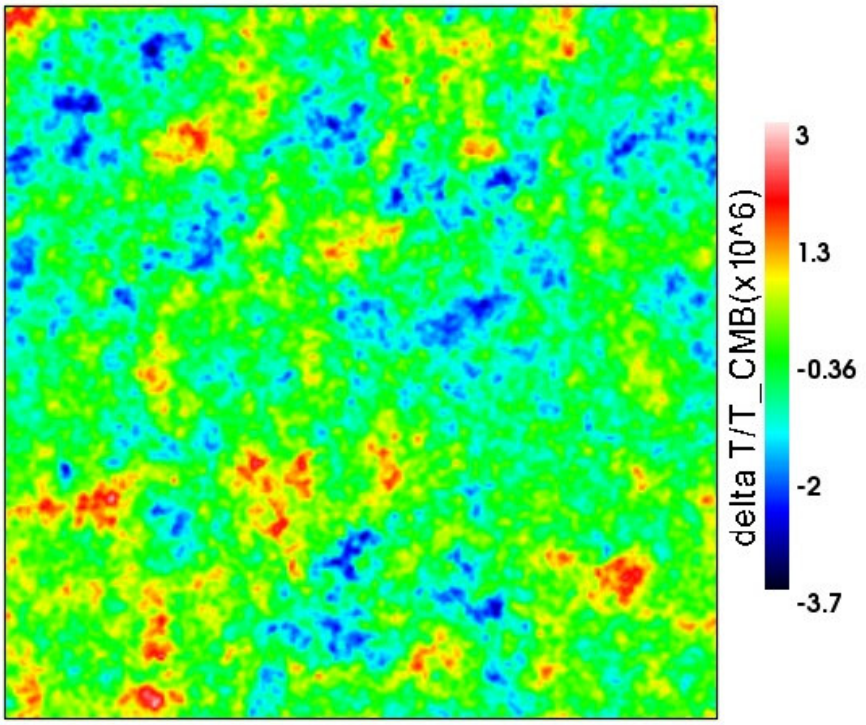

WMAP5

kSZ CMB Anisotropy Signal: Sky Power Spectra of $\delta T_{kSZ} / T_{CMB}$: Effect of Self-Regulation

- Source halos > 10^9 solar masses

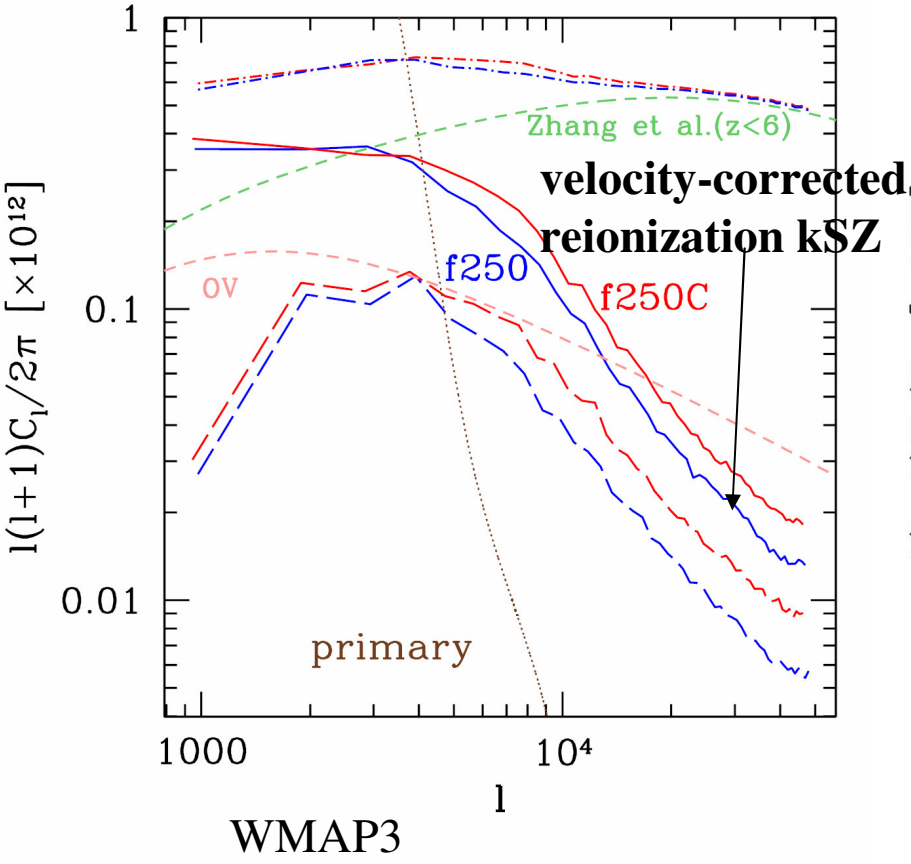

WMAP3

- Source halos > 10^9 solar masses
- Self-regulated reionization

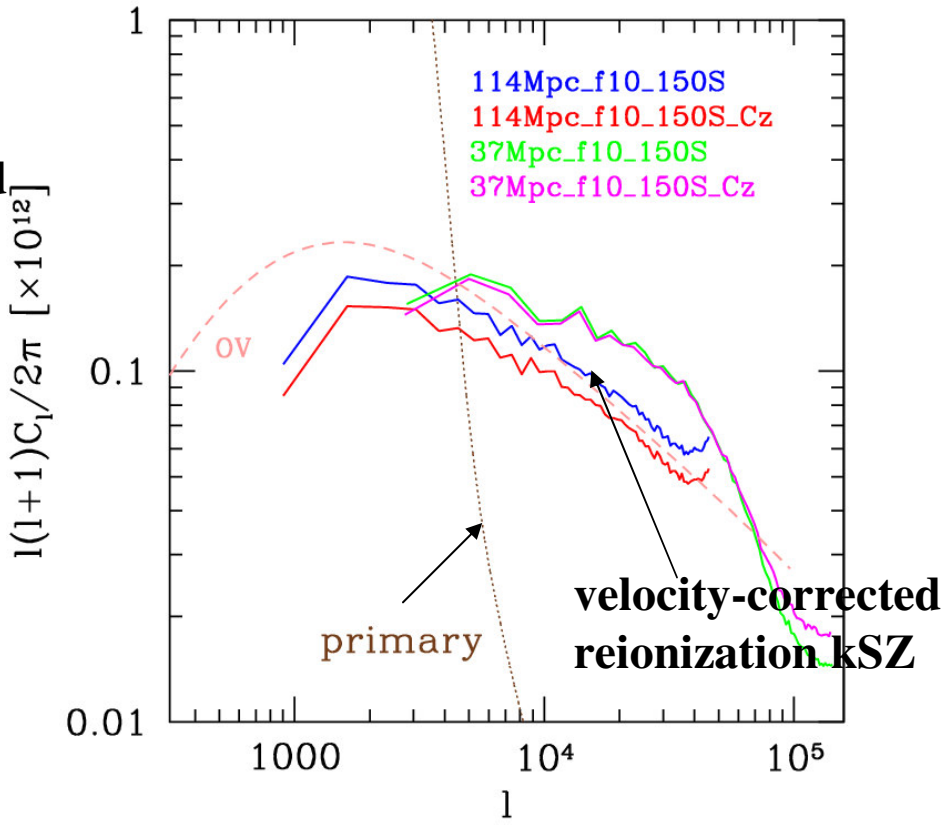

WMAP5

Observability of the kSZ from reionization: sky power spectrum
Effect of Self-Regulation

- Source halos > 10^9 solar masses

- Source halos > 10^9 solar masses
- Self-regulated reionization

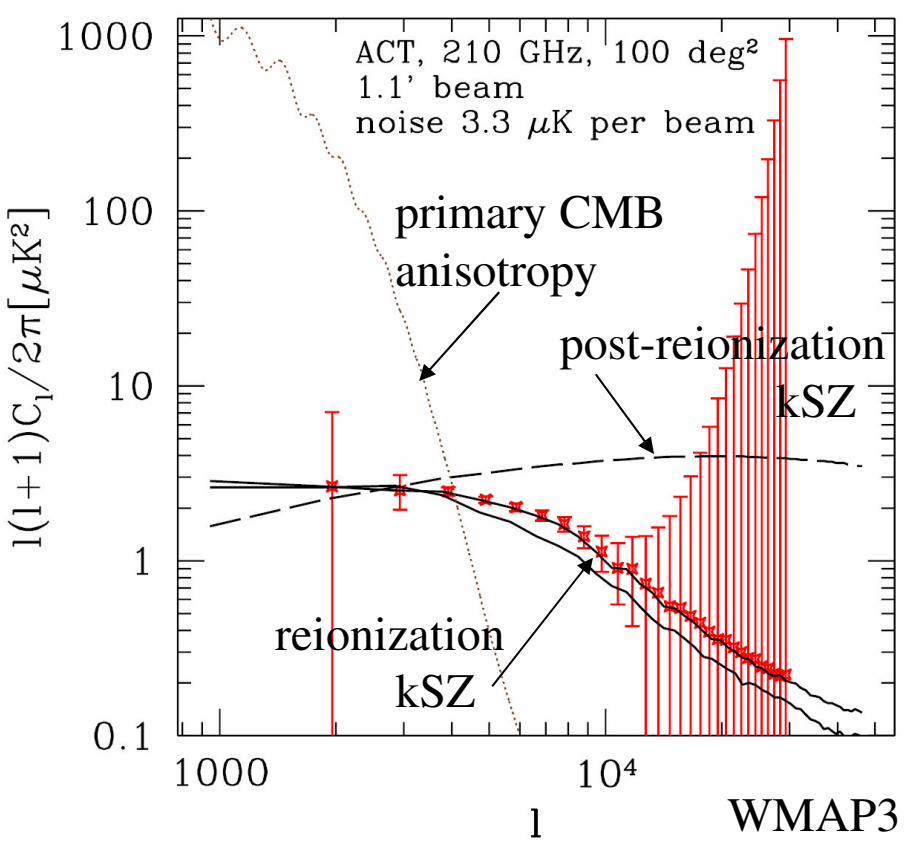

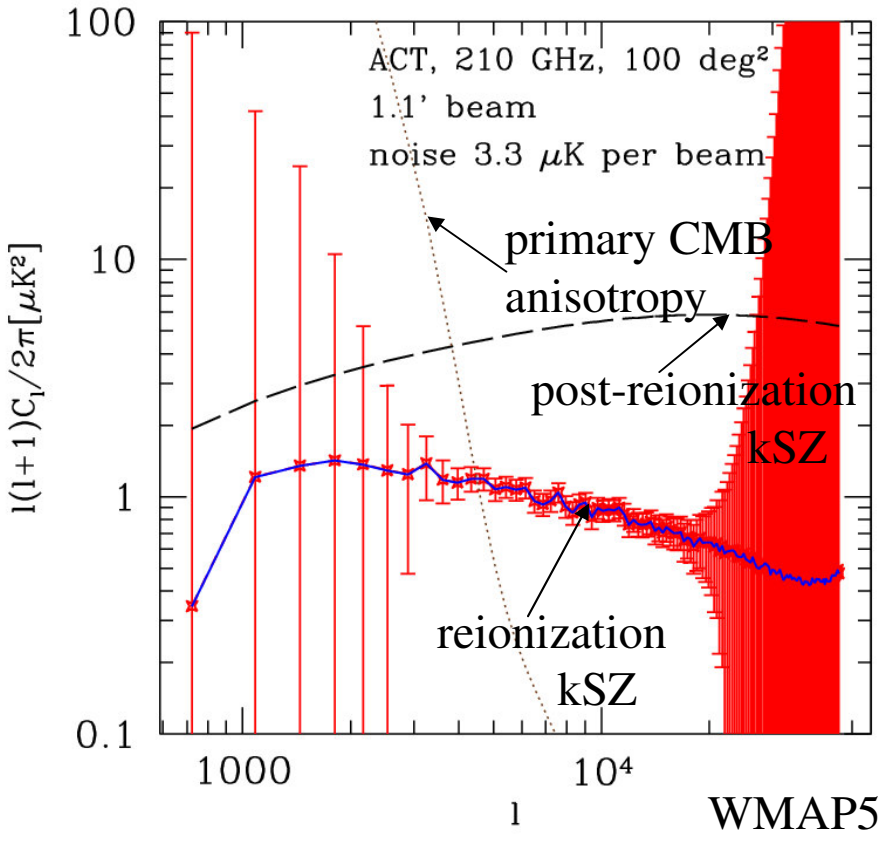

Observability of the kSZ from reionization: sky power spectrum
Effect of Self-Regulation

- Source halos > 10^9 solar masses

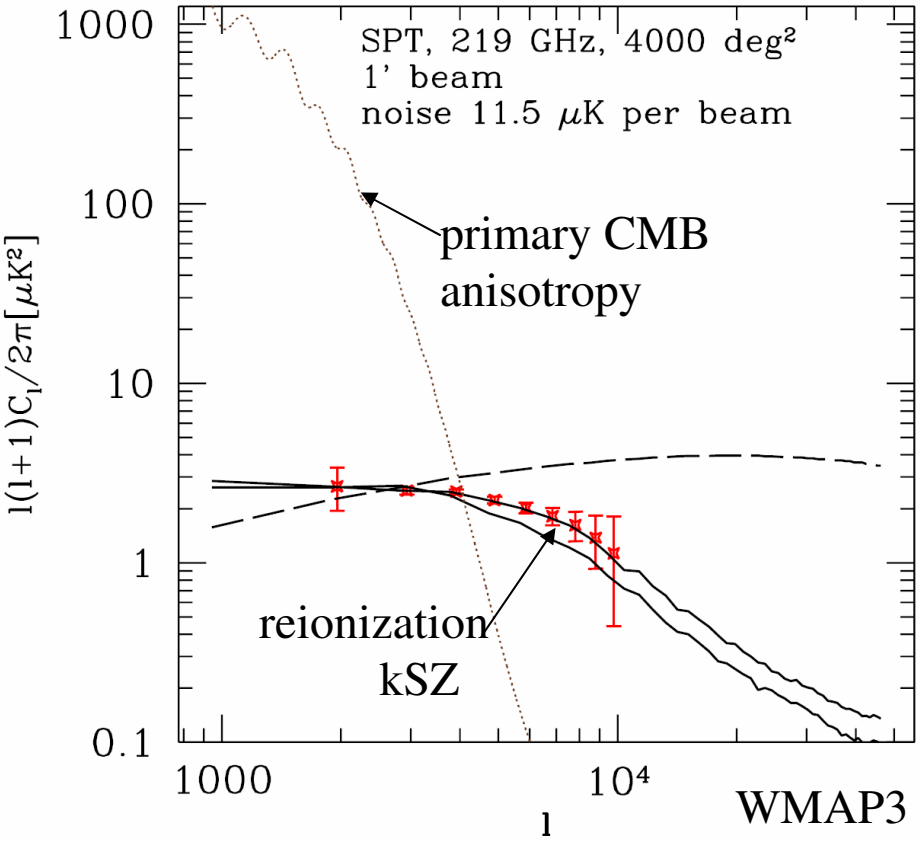

- Source halos > 10^9 solar masses
- Self-regulated reionization

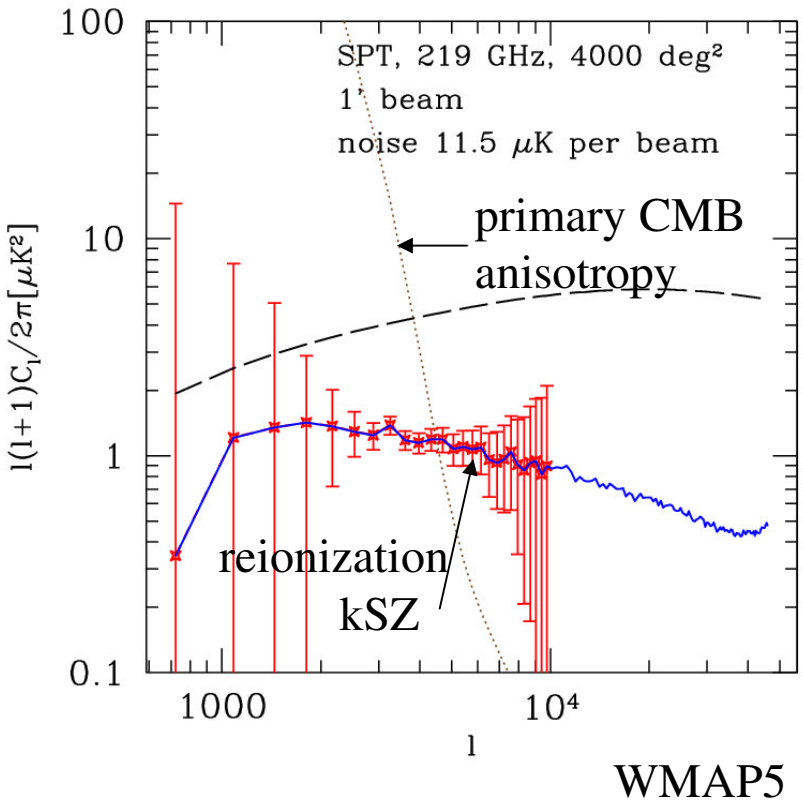

Seeing Invisible Light From the Dark Ages and the Epoch of Reionization that Ended Them

- Hydrogen atoms in the early universe can be detected in absorption or emission against the Cosmic Microwave Background (CMB) at redshifted radio wavelength 21 cm.

- Halos formed during the dark ages are dense and hot enough to appear in emission.

- The intergalactic medium, too, can appear in either emission or absorption.

- Future radio astronomy antenna arrays are being designed and built to detect this 21 cm emission.

Low Frequency Array (LOFAR)

Murchison Widefield Array (MWA)

PrimevAl Structure Telescope (PAST/21CMA)

Prototype Tests, Ulastai, Xin Jiang, China

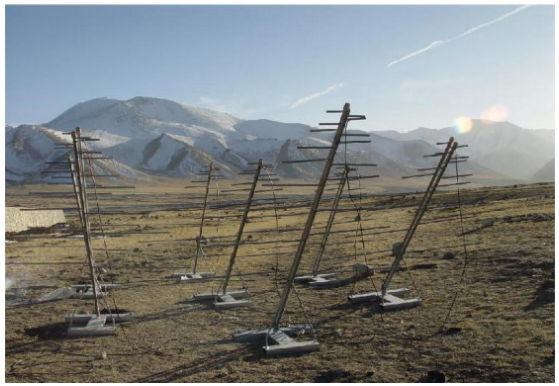

Giant Meterwave Radio Telescope (GMRT)

Square Kilometer Array (SKA)

21-cm Line of Atomic Hydrogen

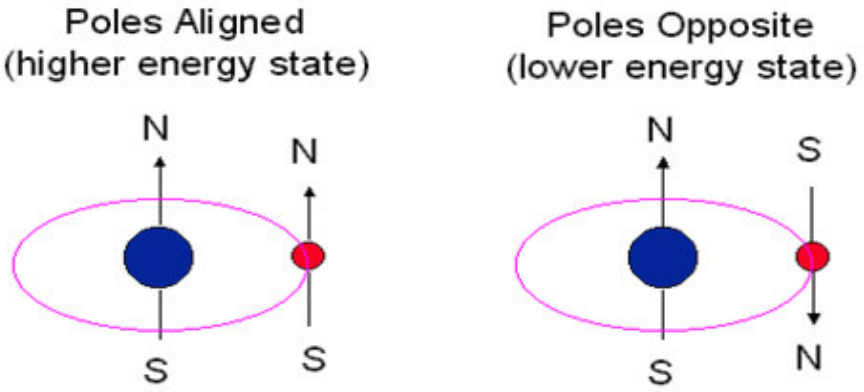

- H atom ground state is split into two energy levels by electron-proton spin interaction.
- Emission or absorption of a photon of 21-cm wavelength and 1.42 GHz frequency will cause transition between these hyperfine levels.

21-cm Level Population of Atomic Hydrogen

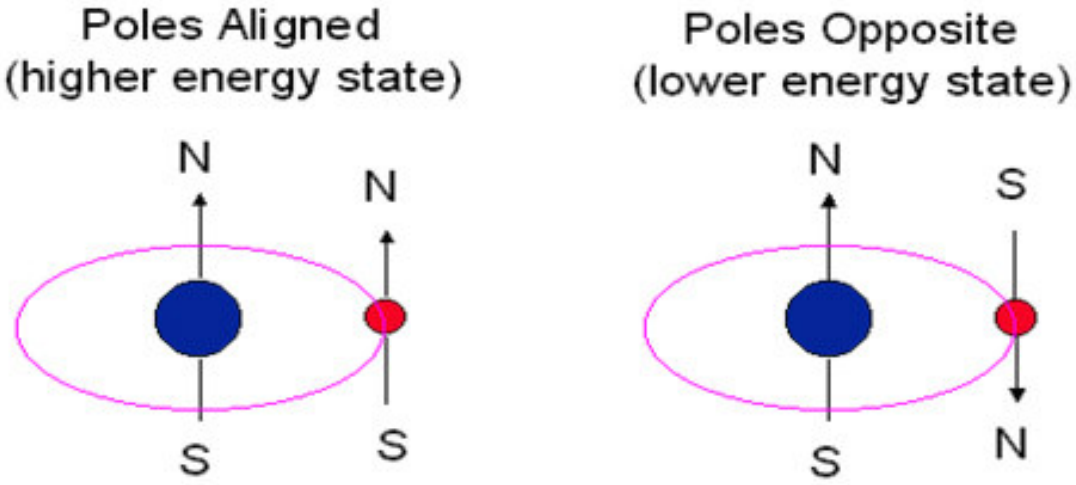

$$\frac{n_2}{n_1} = 3\exp\left(-\frac{h\upsilon_0}{kT_{spin}}\right)$$

21-cm Radiation Background

- Foreground emission or absorption by H atoms at redshift z seen against CMB at redshifted wavelength 21(1+z) cm.

Emission $\leftrightarrow$ $T_{spin} > T_{CMB}$

Absorption $\leftrightarrow$ $T_{spin} < T_{CMB}$

Transparent $\leftrightarrow$ $T_{spin} = T_{CMB}$

3 Ways to Change the 21-cm Level Population

- An H atom can:
  - Absorb a 21-cm photon from the CMB

    (CMB Pumping)
  - Collide with another atom (or an electron or ion)

    (Collisional Pumping)
  - Absorb a UV photon at 1215 Angstrom to make Lyman-α transition of H atom, then decay to one of 21-cm levels ("Wouthuysen-Field Effect")

    (Lyman-α Pumping)

3 Ways to Change the 21-cm Level Population

- An H atom can:
  - Absorb a 21-cm photon from the CMB
    (CMB Pumping)
  - Collide with another atom (or an electron or ion)
    (Collisional Pumping)
  - **Absorb a UV photon at 1215 Angstrom to make Lyman-α transition of H atom, then decay to one of 21-cm levels ("Wouthuysen-Field Effect")**
    (Lyman-α Pumping)

Stages of 21-cm Background

- Dark Ages
  - $z \geq 150$, $T_{spin}=T_{CMB}$ → nothing
  - $20 \leq z \leq 150$, $T_{spin}<T_{CMB}$ → absorption
  - $z \leq 20$, $T_{spin}>T_{CMB}$ in minihalos → emission
- Epoch of Reionization ($6 \leq z \leq 20$)
  - $T_{spin}>T_{CMB}$ in minihalos → emission
  - After sources turn on, Lyman-α pumping →
    - Without heating, $T_{spin}<T_{CMB}$ → IGM in absorption
    - With heating, $T_{spin}>T_{CMB}$ → IGM in emission

Stages of 21-cm Background

- Dark Ages
  - $z \geq 150$, $T_{spin}=T_{CMB}$ → nothing
  - **$20 \leq z \leq 150$, $T_{spin}<T_{CMB}$ → absorption**
  - **$z \leq 20$, $T_{spin}>T_{CMB}$ in minihalos → emission**
- Epoch of Reionization ($6 \leq z \leq 20$)
  - $T_{spin}>T_{CMB}$ in minihalos → emission
  - After sources turn on, Lyman-α pumping →
    - Without heating, $T_{spin}<T_{CMB}$ → IGM in absorption
    - With heating, $T_{spin}>T_{CMB}$ → IGM in emission

The 21-cm Background from the Cosmic Dark Ages: Minihalos and the Intergalactic Medium Before Reionization : Collisionally Pumped Spin Temperature

- Iliev, Shapiro, Ferrara & Martel 2002, ApJL, 572, L123
- Iliev, Scannapieco, Shapiro, & Martel 2003, MNRAS, 341, 81
- Shapiro, Ahn, Alvarez, Iliev, Martel & Ryu (2006), ApJ, 646, 681; (astro-ph/0512516)

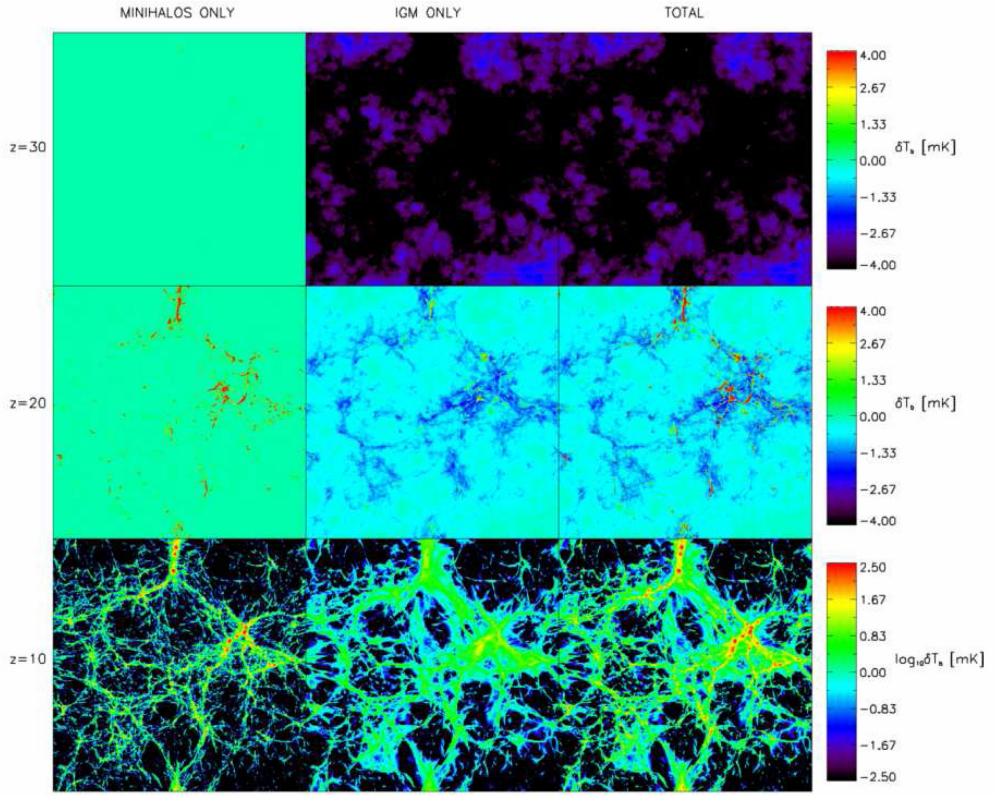

Minihalos vs. IGM

- Mean brightness temperature dominated by minihalos for z < 20.
- For z > 17, IGM contribution changes from emission to absorption.
- At z > 20, IGM absorption dominates over minihalo emission.
- At z > 20, mean brightness temperature same as uniform IGM

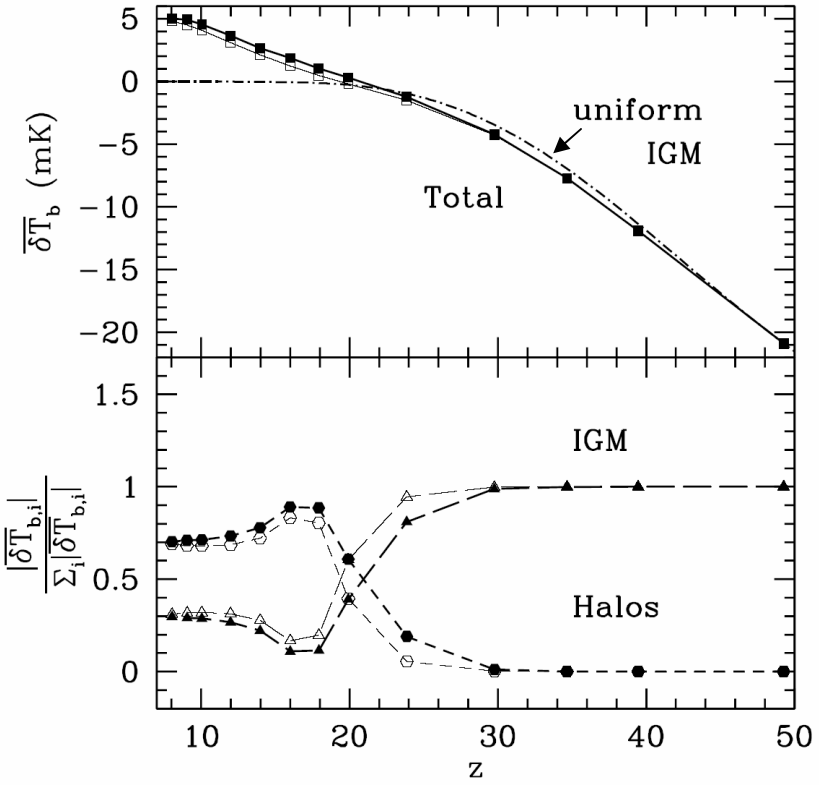

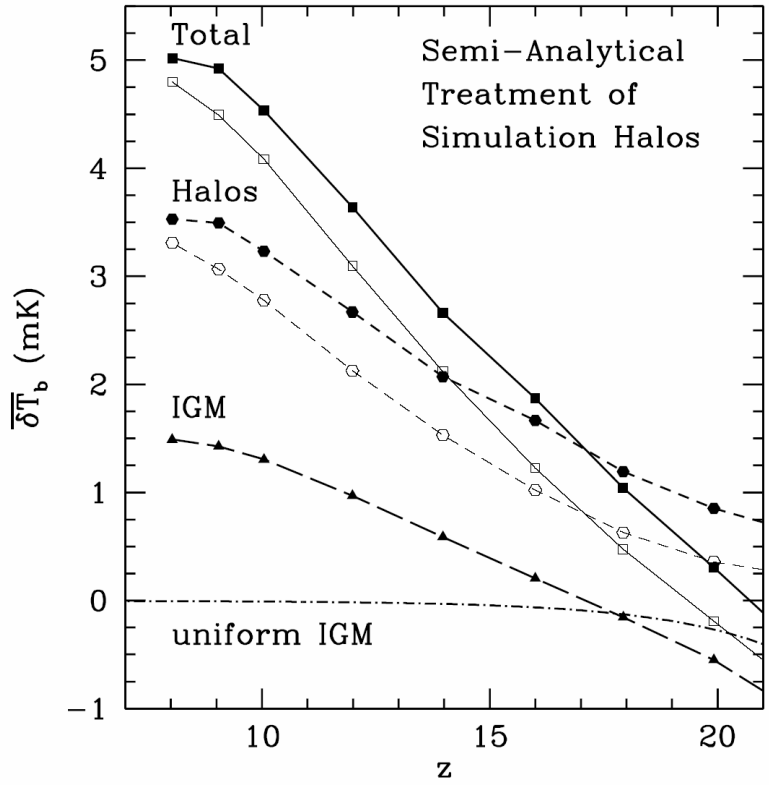

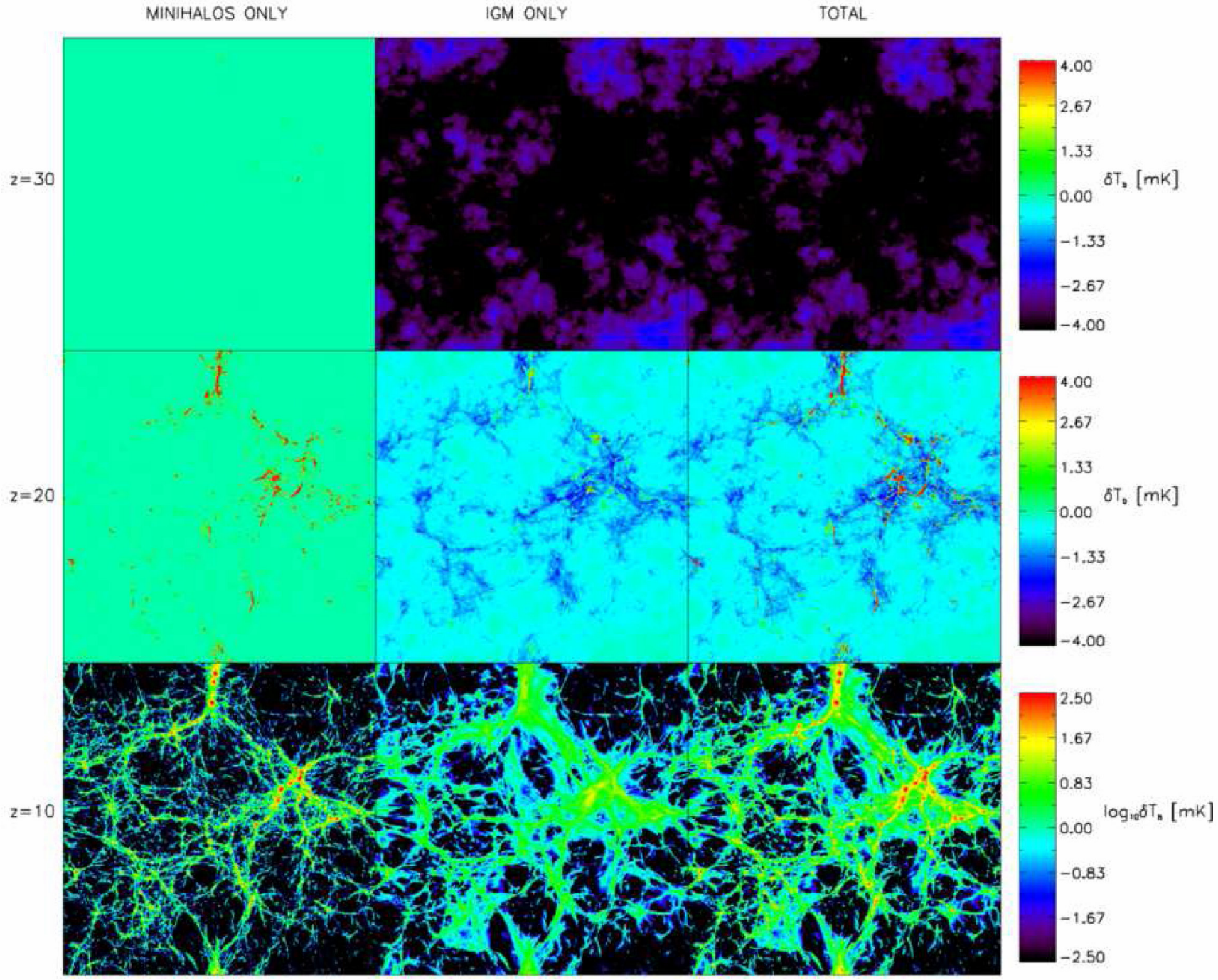
MINIHALOS ONLY
IGM ONLY
TOTAL
z=30
z=20
z=10
4.00
2.67
1.33
0.00
−1.33
−2.67
−4.00
δT_b [mK]
4.00
2.67
1.33
0.00
−1.33
−2.67
−4.00
δT_b [mK]
2.50
1.67
0.83
0.00
−0.83
−1.67
−2.50
log10δT_b [mK]

Stages of 21-cm Background

- Dark Ages
  - $z \geq 150$, $T_{spin}=T_{CMB}$ → nothing
  - $20 \leq z \leq 150$, $T_{spin}<T_{CMB}$ → absorption
  - $z \leq 20$, $T_{spin}>T_{CMB}$ in minihalos → emission
- **Epoch of Reionization ($6 \leq z \leq 20$)**
  - $T_{spin}>T_{CMB}$ in minihalos → emission
  - **After sources turn on, Lyman-α pumping →**
    - Without heating, $T_{spin}<T_{CMB}$ → IGM in absorption
    - With heating, $T_{spin}>T_{CMB}$ → IGM in emission

Stages of 21-cm Background

- Dark Ages
  - $z \geq 150$, $T_{spin}=T_{CMB}$ → nothing
  - $20 \leq z \leq 150$, $T_{spin}<T_{CMB}$ → absorption
  - $z \leq 20$, $T_{spin}>T_{CMB}$ in minihalos → emission
- **Epoch of Reionization ($6 \leq z \leq 20$)**
  - $T_{spin}>T_{CMB}$ in minihalos → emission
  - **After sources turn on, Lyman-α pumping →**
    - **Without heating, $T_{spin}<T_{CMB}$ → IGM in absorption**
    - With heating, $T_{spin}>T_{CMB}$ → IGM in emission

Decoupling the spin temperature of the 21-cm transition of H I from the CMB

(Chuzhoy and Shapiro 2006, ApJ, 651, 1; astro-ph/0512206)

- Spin temperature

$$T_{\rm s} = \frac{T_{\rm CMB} + y_\alpha T_\alpha + y_{\rm c} T_{\rm k}}{1 + y_\alpha + y_{\rm c}},$$

where $y_\alpha = (P_{10}\, T_*)/(A_{10}\, T_\alpha)$

$P_{10} \propto J_\alpha$ = mean intensity at Ly α

(Field 1958, 1959)

- <u>Standard assumption</u>:

scattering ➔ atomic recoil ➔ $T_\alpha = T_k$

and

$J_\alpha = J_{\alpha,0}$ = background level

- But there is a backreaction of the Ly α scattering :

hyperfine splitting + atomic recoil
===>

(1) $T_\alpha \neq T_k$
(T_α between T_k and T_{CMB})

(2) $J_\alpha \neq J_{\alpha,o}$
(Chen and Miralda-Escude 2004; without hyperfine splitting)

(3) T_α , J_α both depend on local departure from Hubble flow
===> small-scale structure affects mean 21-cm signal

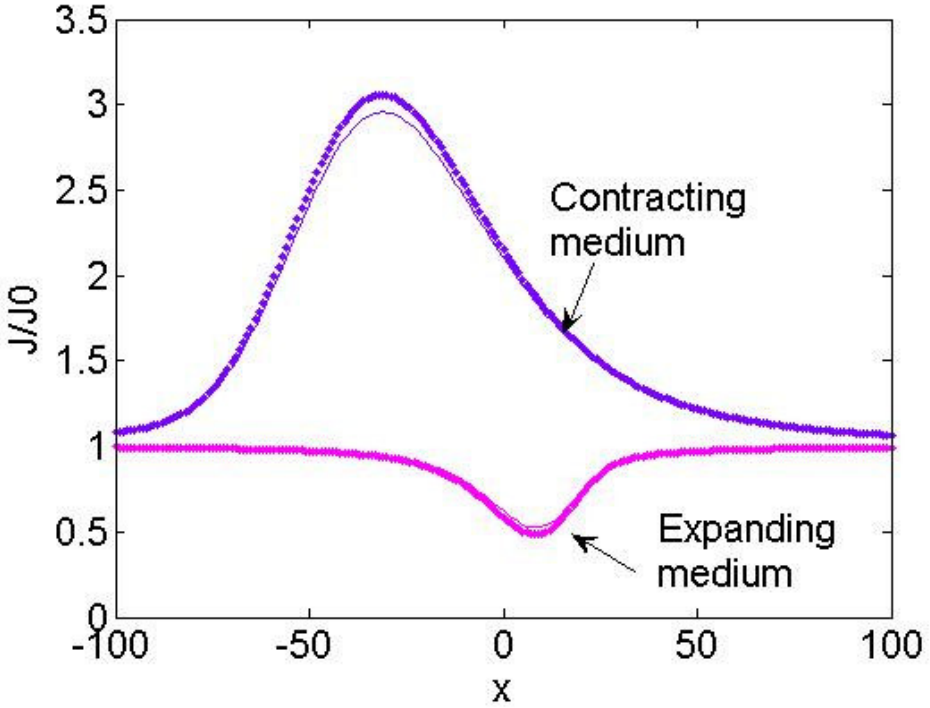

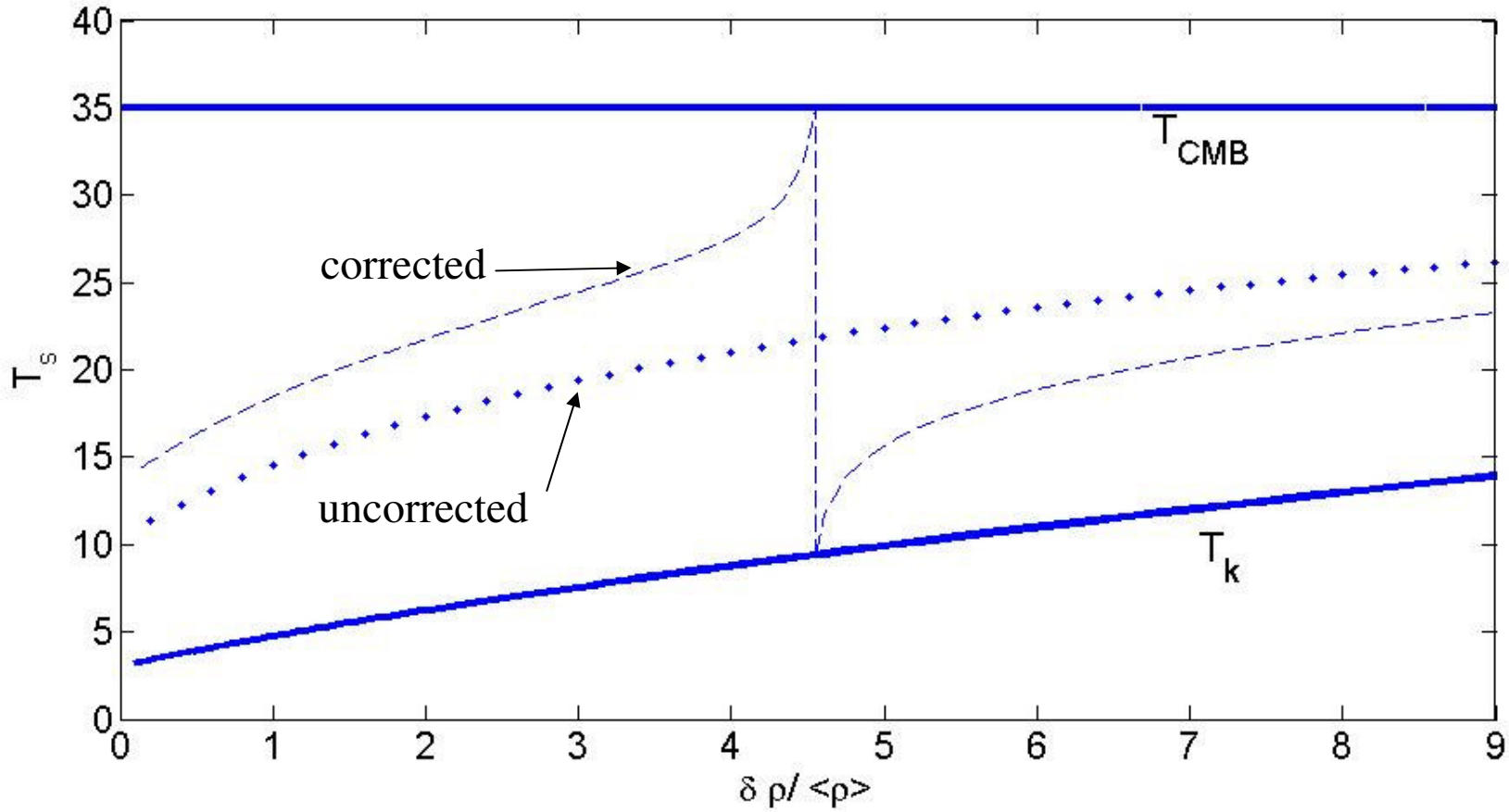

Hydrogen spin temperature at z ~ 12 for an illustrative radiation intensity, for different overdensities

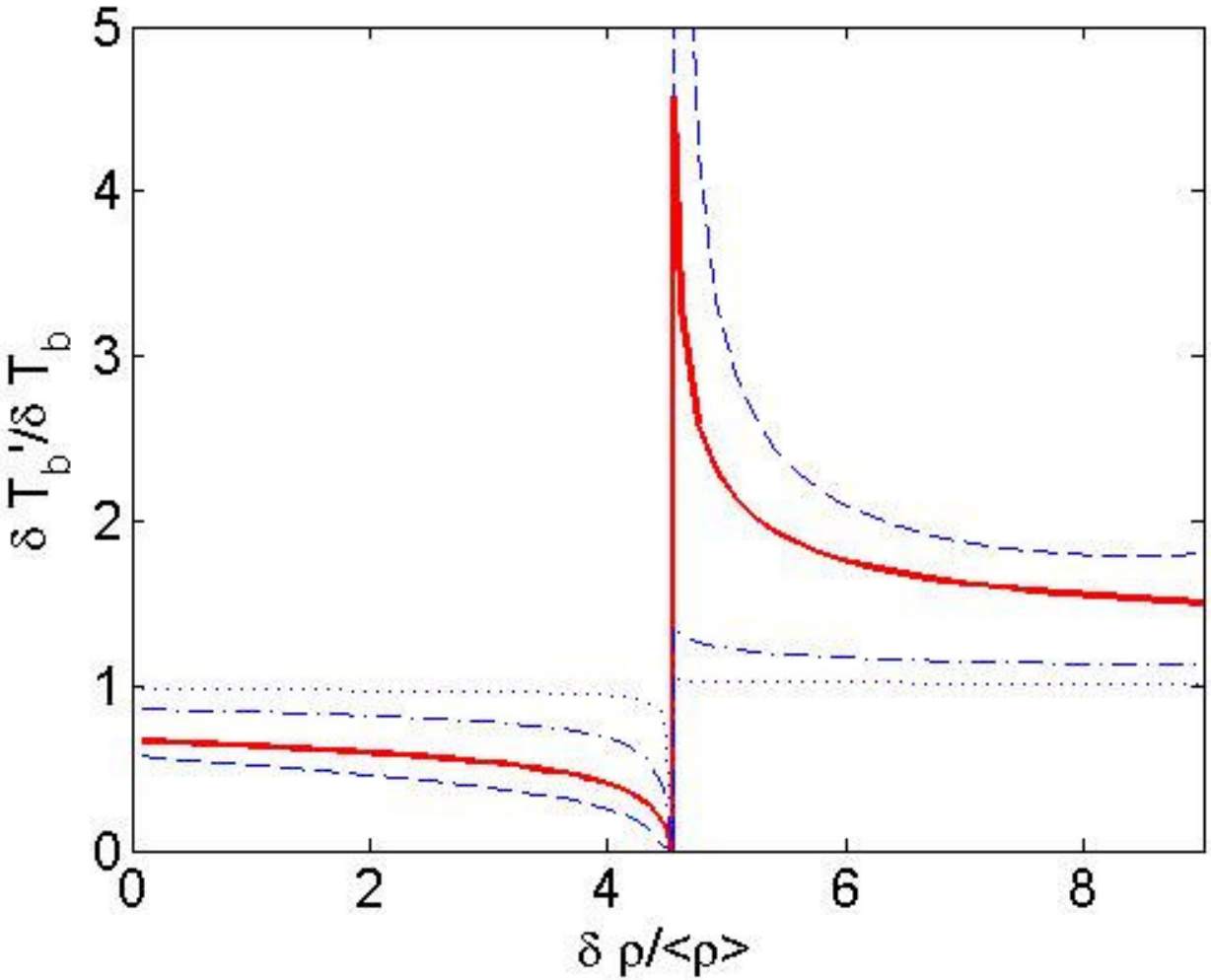

The correction factor to the differential brightness temperature (the 21-cm absorption signal) for different radiation intensities, for different overdensities

Recognizing the First Radiation Sources Through Their 21-cm Signature :

Brightness temperature vs. comoving radius around a radiation source at z =20

a. X-ray source,
L = 5e40 erg/s,
@ t (Myrs) ,
10 (solid),
20 (dash-dot),
40 (dotted);

b. UV source,
L (Ly α to LL)
in erg/s =
5e41 (dashed),
5e42 (dash-dot),
5e43 (solid);

c. Galactic wind,
Lα (erg/s) =
1e41 (solid),
1e40 (dashed),
1e39 (dash-dot).

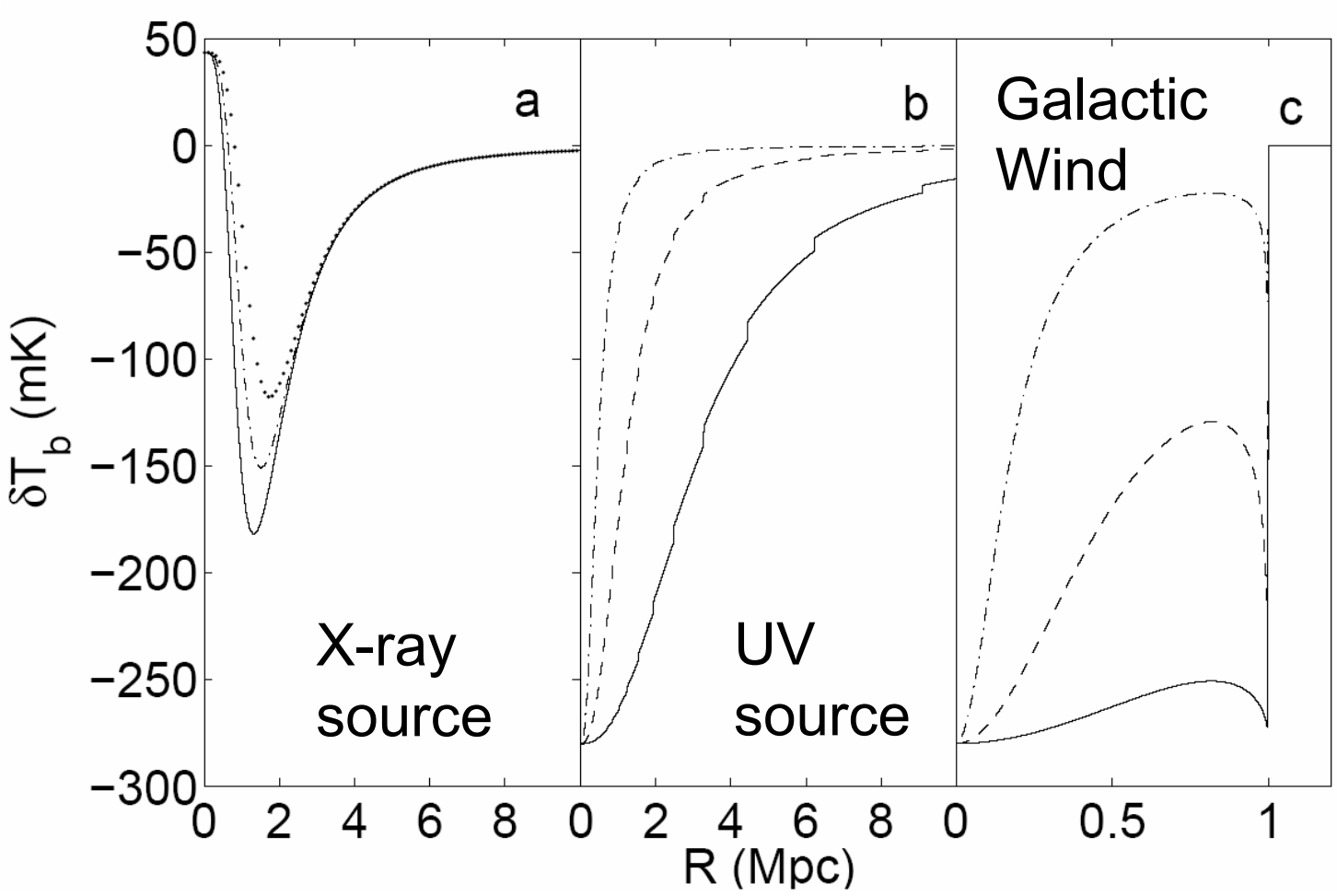

(Chuzhoy, Alvarez & Shapiro 2006, ApJL, 648, L1; astro-ph/0605511)

Recognizing the First Radiation Sources Through Their 21-cm Signature

(Chuzhoy, Alvarez & Shapiro 2006, ApJL, 648, L1; astro-ph/0605511)

Power spectrum of fluctuating 21-cm signal at z = 20

- Ly α pumping is by halo sources clustered in space
- Assume each halo is either an X-ray source or a UV source from Pop III stars
- X-ray sources influence smaller regions than Pop III stellar sources, typically, so they yield greater fluctuations on small scales
- Future radio arrays plan to detect the 21-cm background and may be able to distinguish this.

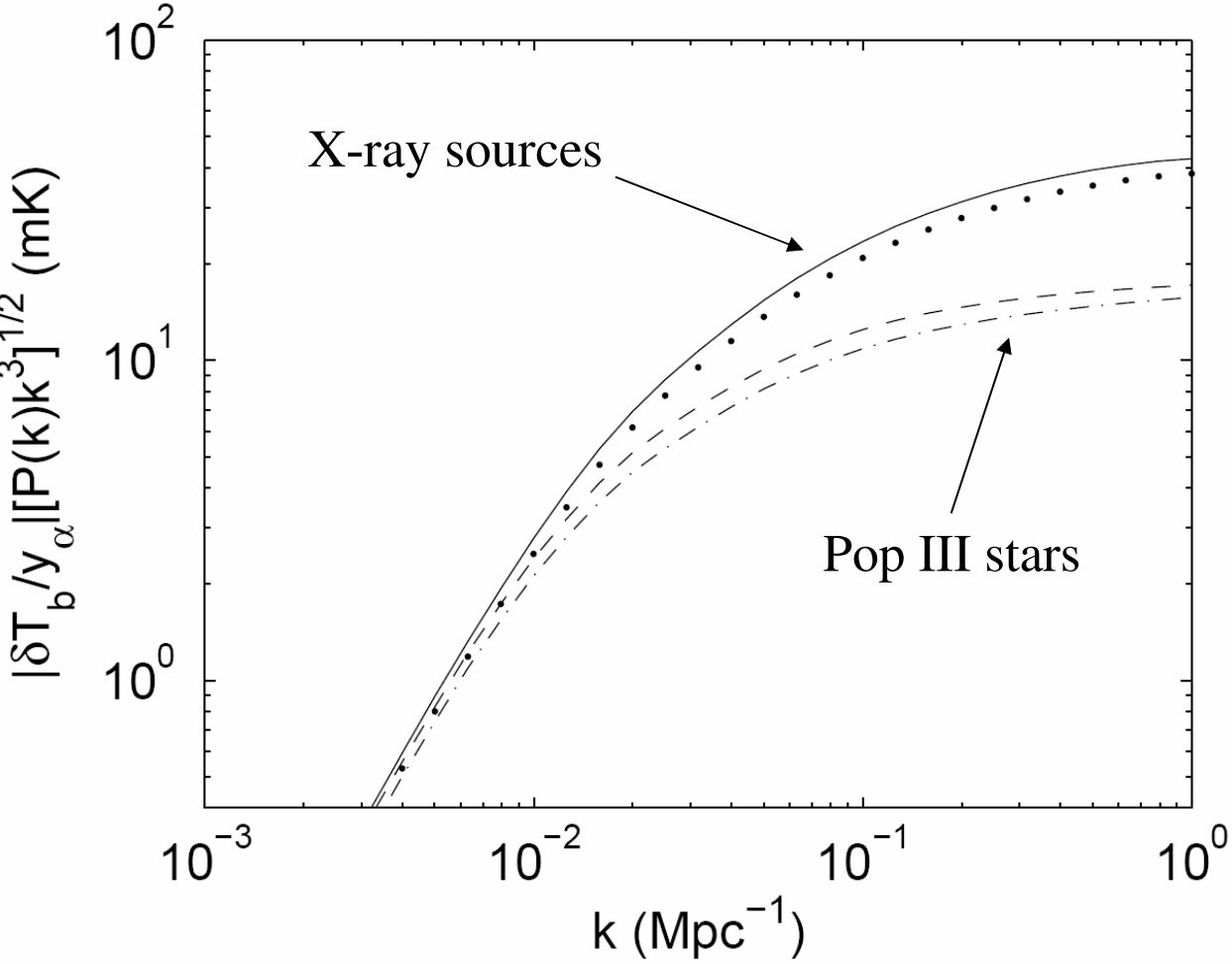

Stages of 21-cm Background

- Dark Ages
  - $z \geq 150$, $T_{spin}=T_{CMB}$ → nothing
  - $20 \leq z \leq 150$, $T_{spin}<T_{CMB}$ → absorption
  - $z \leq 20$, $T_{spin}>T_{CMB}$ in minihalos → emission
- **Epoch of Reionization ($6 \leq z \leq 20$)**
  - $T_{spin}>T_{CMB}$ in minihalos → emission
  - **After sources turn on, Lyman-α pumping →**
    - Without heating, $T_{spin}<T_{CMB}$ → IGM in absorption
    - **With heating, $T_{spin}>T_{CMB}$ → IGM in emission**

The Redshifted 21cm Signal From the EoR

- The measured radio signal is the differential brightness temperature
- $\delta T_b = T_b - T_{CMB}$: $$\delta T_b \approx 25\, x_{\rm HI}(1+\delta)\left(\frac{1+z}{10}\right)^{1/2}\left[1-\frac{T_{\rm CMB}(z)}{T_S}\right]\left[\frac{H(z)/(1+z)}{{\rm d}v_\parallel/{\rm d}r_\parallel}\right]\ {\rm mK}$$

(for WMAP3 cosmological parameters).

- Depends on:
  - x_{HI}: neutral fraction
  - δ: overdensity
  - T_s: spin temperature
- For $T_s \gg T_{CMB}$, the dependence on T_s drops out
- The signal is a spectral *line*: carries spatial, temporal, and velocity information.

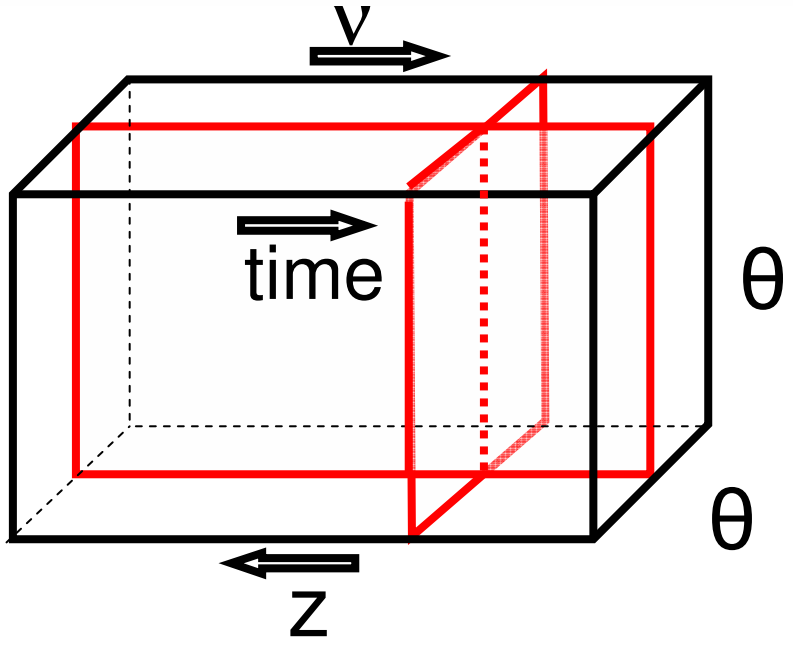

The image cube: images stacked in frequency space

$$\delta T_b \approx 25\, x_{\rm HI}(1+\delta)\left(\frac{1+z}{10}\right)^{1/2}\left[1-\frac{T_{\rm CMB}(z)}{T_S}\right]\left[\frac{H(z)/(1+z)}{{\rm d}v_\parallel/{\rm d}r_\parallel}\right]\ {\rm mK}$$

• For $T_s >> T_{CMB}$, the dependence on T_s drops out and brightness temperature fluctuations then depend only on L.O.S. velocity gradient & H I density fluctuations,

$$\delta_{\rho_{\rm HI}} = (1+\delta_\rho)(1+\delta_{x_{\rm HI}}) - 1 = \delta_\rho + \delta_{x_{\rm HI}} + \delta_\rho \delta_{x_{\rm HI}}$$

• For *linear* perturbations in the matter density, the *peculiar* velocity gradient and density perturbation are related in Fourier space as follows:

$$(aH)^{-1}\frac{dv_\parallel}{dr_\parallel}(\mathbf{k}) = -\mu^2\delta_\rho(\mathbf{k})$$

$\mu = \hat{\mathbf{k}}\cdot\hat{\mathbf{r}}$ = cosine of angle between the wavevector k and the line of sight

• To lowest order, we can then write in Fourier space,

$\delta T_b\,(k) \approx (\delta T_b)_{\rm average}\,(\ \delta_{\rho_{\rm HI}} + \mu^2\delta_\rho\ )$

• the 21cm 3D Power Spectrum can then be decomposed as follows:

$$P_{\Delta T}(\mathbf{k}) = P_{\mu^0}(k) + P_{\mu^2}(k)\mu^2 + P_{\mu^4}(k)\mu^4$$

where

$$\begin{aligned} P_{\mu^0} &= \overline{\delta T_b}^2 \, P_{\delta_\zeta,\delta_\zeta} \\ P_{\mu^2} &= 2\,\overline{\delta T_b}^2 \, P_{\delta_\zeta,\delta_\rho} \\ P_{\mu^4} &= \overline{\delta T_b}^2 \, P_{\delta_\rho,\delta_\rho} \end{aligned}$$

(where $\delta_\zeta \equiv \delta_{\rho_{\rm HI}}$)

• In that case, there is a separation in powers of the angle cosine which makes it possible to use 21cm survey data to solve for the power spectrum of matter density fluctuations ===> can solve for cosmological parameters

• When reionization patchiness must also be taken explictly into account, too, then one can still do this, but requires knowledge of the patchiness and cross-correlations from simulations, to find the best fit for reionization terms, too.

The Redshifted 21cm Signal From the EoR

- The measured radio signal is the differential brightness temperature
- $\delta T_b = T_b - T_{CMB}$: $$\delta T_b \approx 25\, x_{\rm HI}(1+\delta)\left(\frac{1+z}{10}\right)^{1/2}\left[1-\frac{T_{\rm CMB}(z)}{T_S}\right]\left[\frac{H(z)/(1+z)}{{\rm d}v_\parallel/{\rm d}r_\parallel}\right]\ {\rm mK}$$

  (for WMAP3 cosmological parameters).
- Depends on:
  - x_{HI}: neutral fraction
  - δ: overdensity
  - T_s: spin temperature
- For $T_s \gg T_{CMB}$, the dependence on T_s drops out
- The signal is a spectral *line*: carries spatial, temporal, and velocity information.

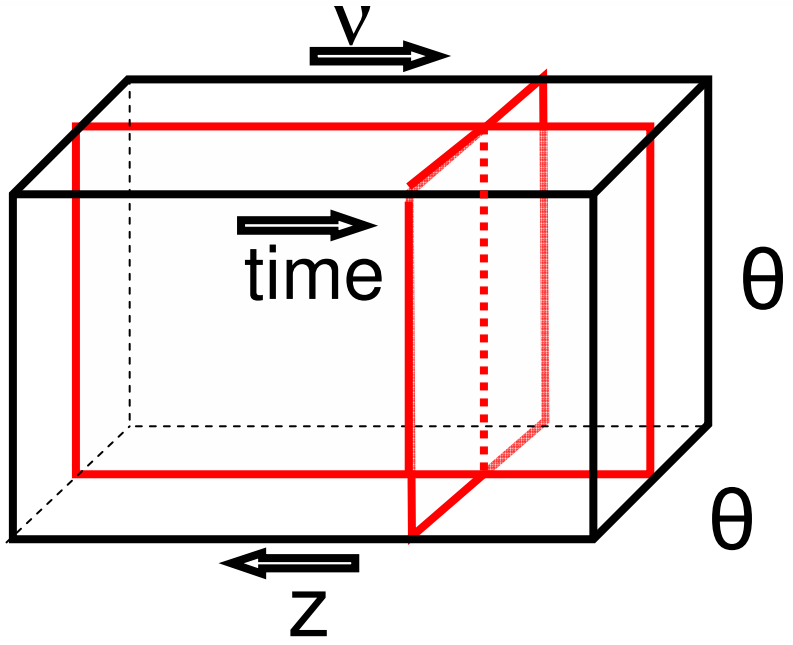

The image cube: images stacked in frequency space

Reionization topology revealed by fluctuations in 21-cm brightness temperature, δT_b , along the line of sight

Iliev, Mellema, Pen, Bond, & Shapiro (2008), MNRAS, 384, 863 (astro-ph/0702099)

- mapping the sky along the LOS: high-resolution cuts in position-redshift space

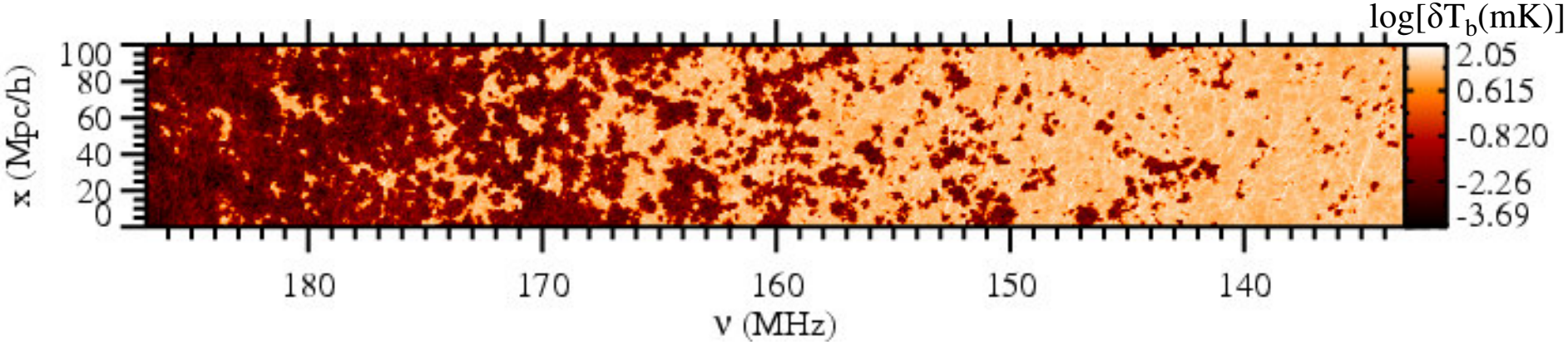

- beam- and bandwidth-smoothed : 3 arcmin, 0.2 MHz (e.g. LOFAR)

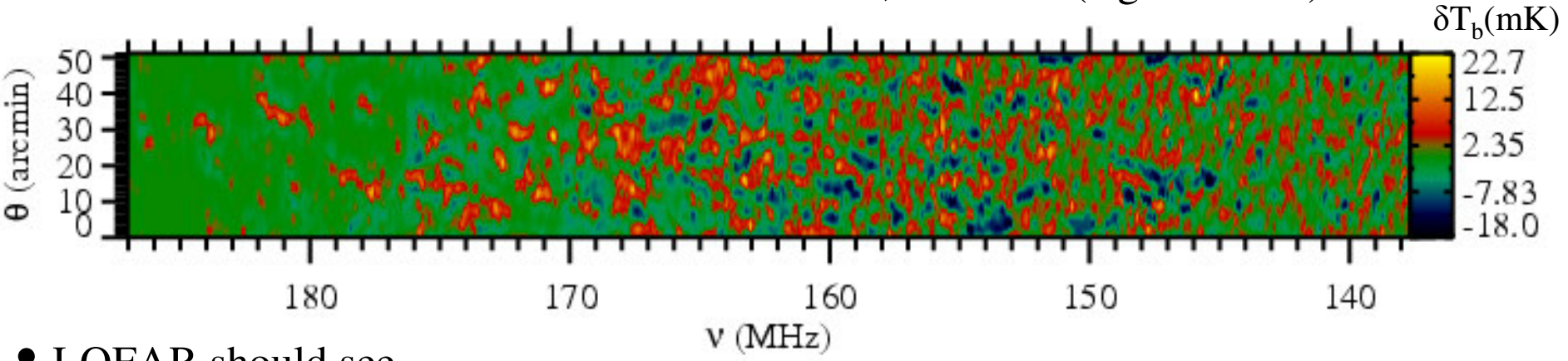

- LOFAR should see large ionized bubbles!

Case: $f_\gamma = 250$, subgrid clumping factor C(z), WMAP3

Reionization topology revealed by fluctuations in 21-cm brightness temperature, δT_b , along the line of sight : Effect of Self-Regulation

(Shapiro, Iliev, Mellema, Pen, and Merz 2008, AIP 1035, 68; astro-ph/0806.3091)

- mapping the sky along the LOS: high-resolution cuts in position-redshift space

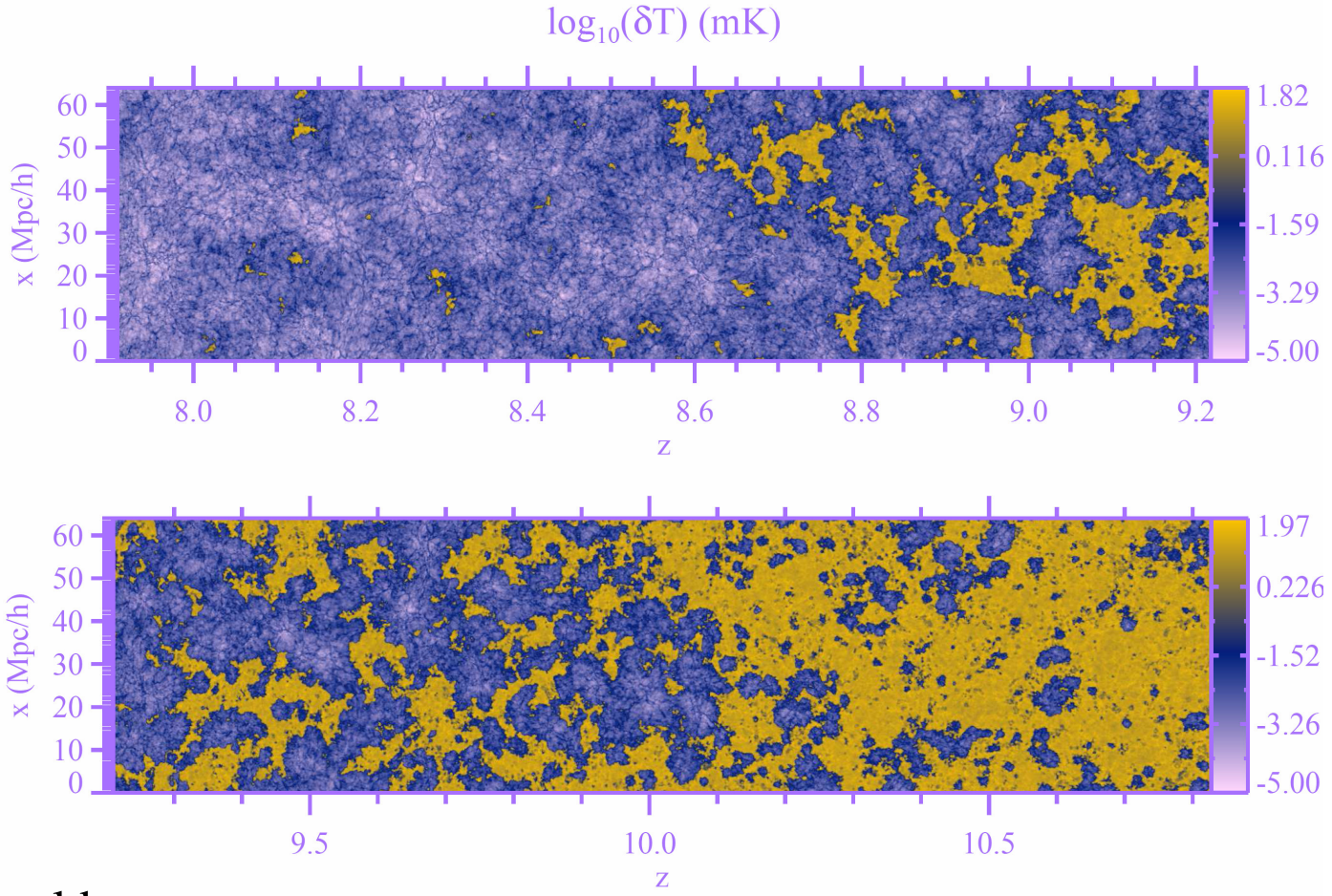

- LOFAR should see large ionized bubbles!

90 Mpc box, WMAP3+

Sky Maps of 21cm Background Brightness Temperature Fluctuations
During Epoch of Reionization : Travel through Time

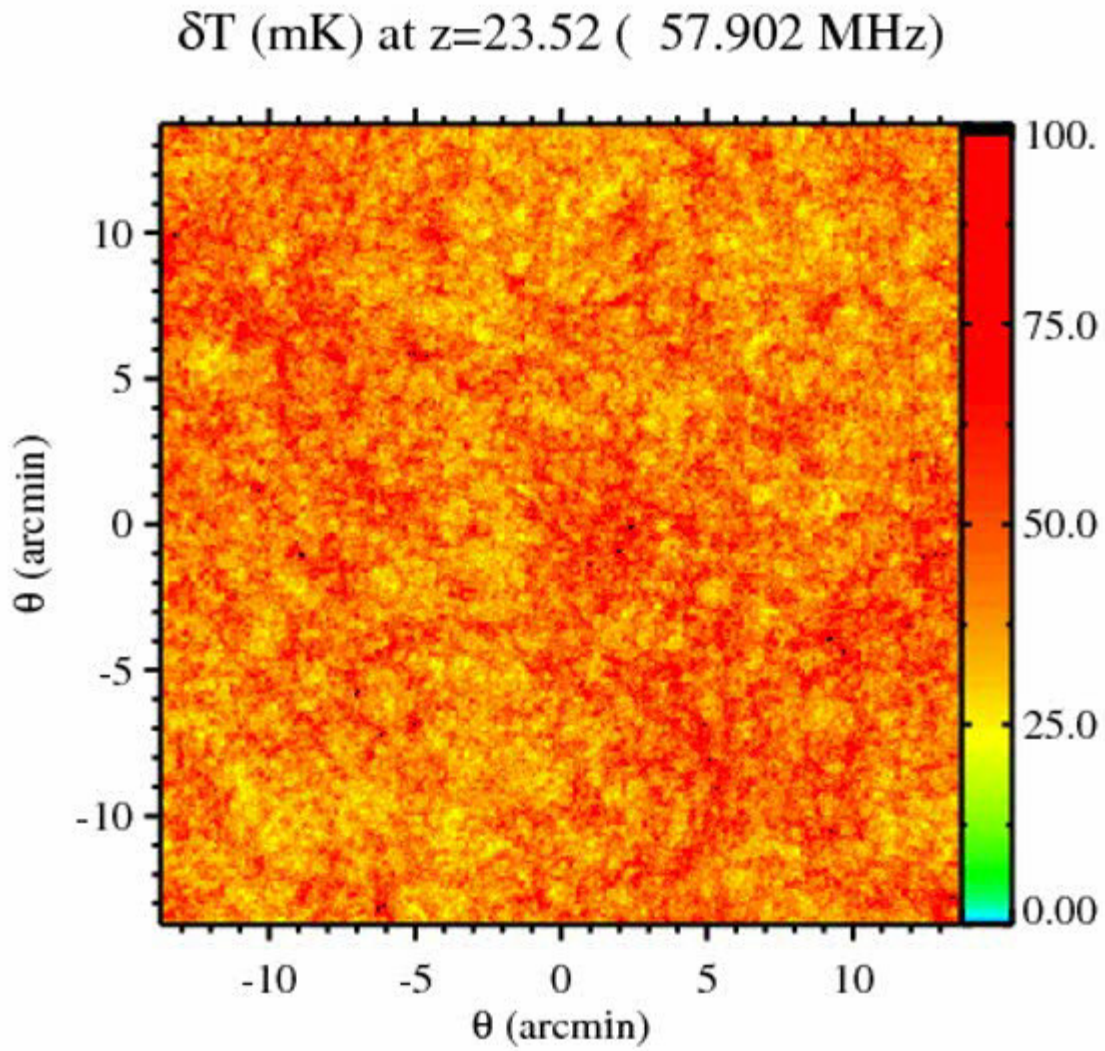

Sky Maps of 21cm Background Brightness Temperature Fluctuations
During Epoch of Reionization : Travel through Time

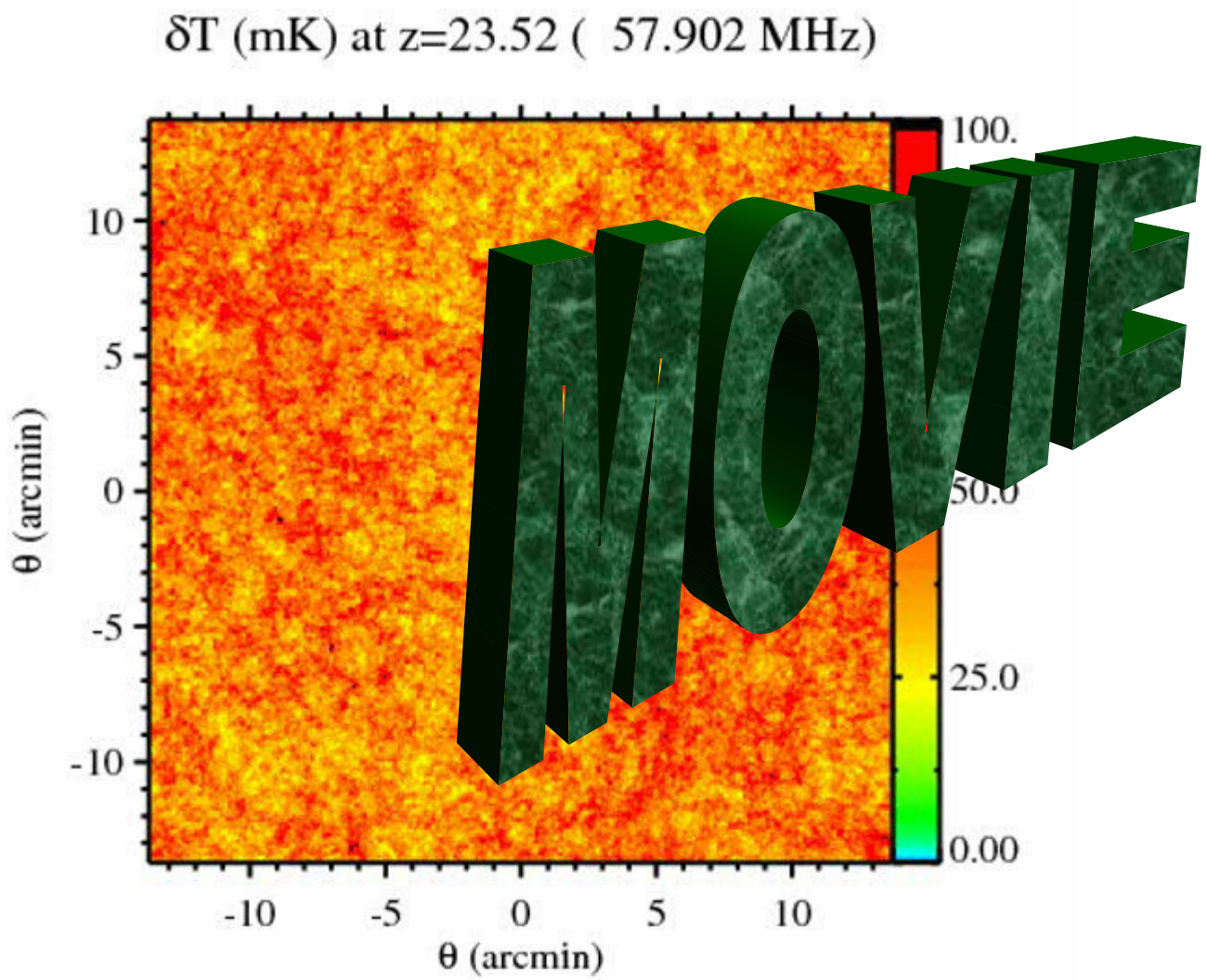

Notation

- Our simulations are characterized by

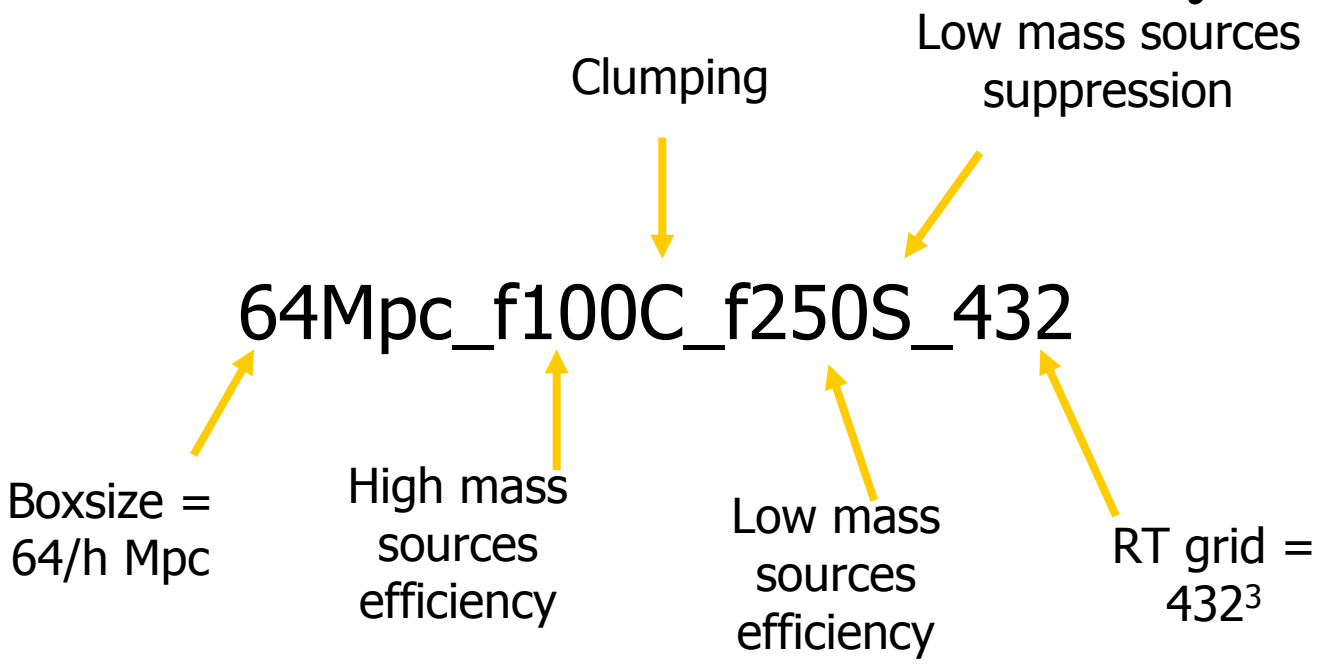

Statistical Measurements of the 21cm Background During the EoR

- The sensitivity of the upcoming EoR experiments will be too low to image 21cm from reionization pixel by pixel: Statistical measurements needed.
  - **First goal**: to reliably detect signatures from reionization (and separate them from foreground and instrumental effects).
  - **Second goal**: to interpret them in terms of astrophysics (source population and properties).
- Luckily, the 21cm line signal is rich in properties:
  1. Global signals: mean signal, fluctuations.
  2. Angular properties: power spectra
  3. Frequency properties: correlation length, Kaiser effect
  4. Non-Gaussianity.

EDGES (Mileura Station, Western Australia)
Bowman, Rogers, and Hewitt (2008)

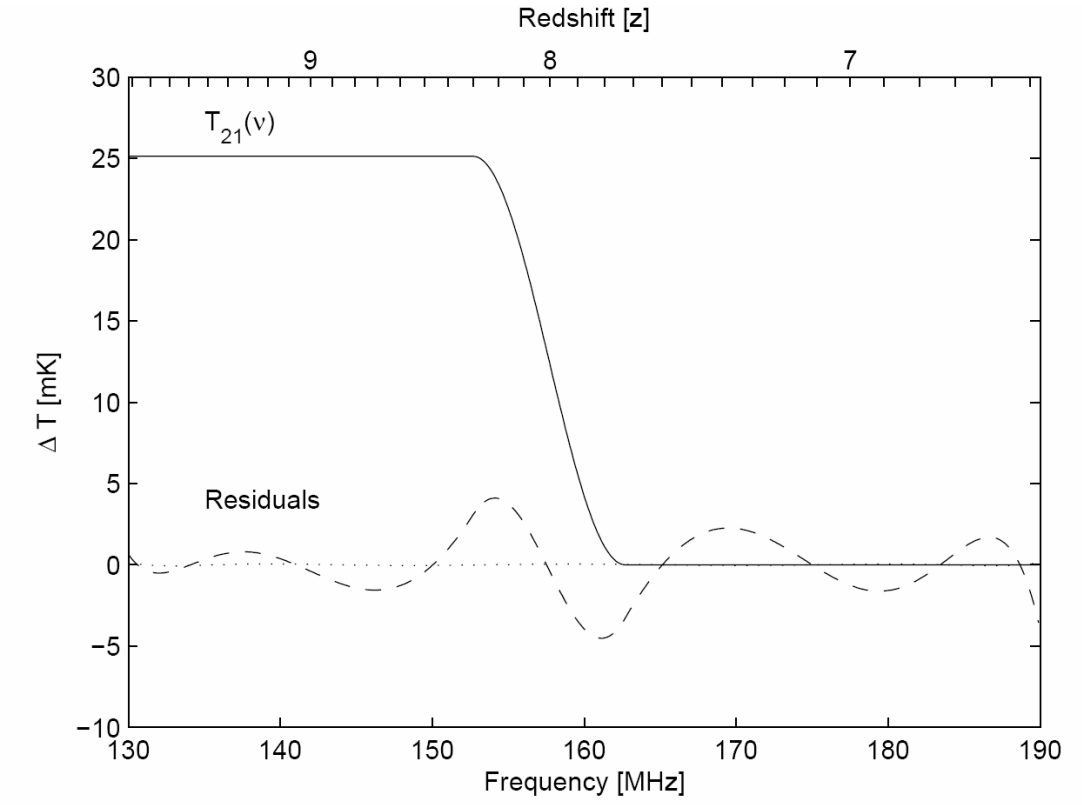

- Search for a "jump" in the global mean brightness temperature when reionization ends

EDGES (Mileura Station, Western Australia)
Bowman, Rogers, and Hewitt (2008)

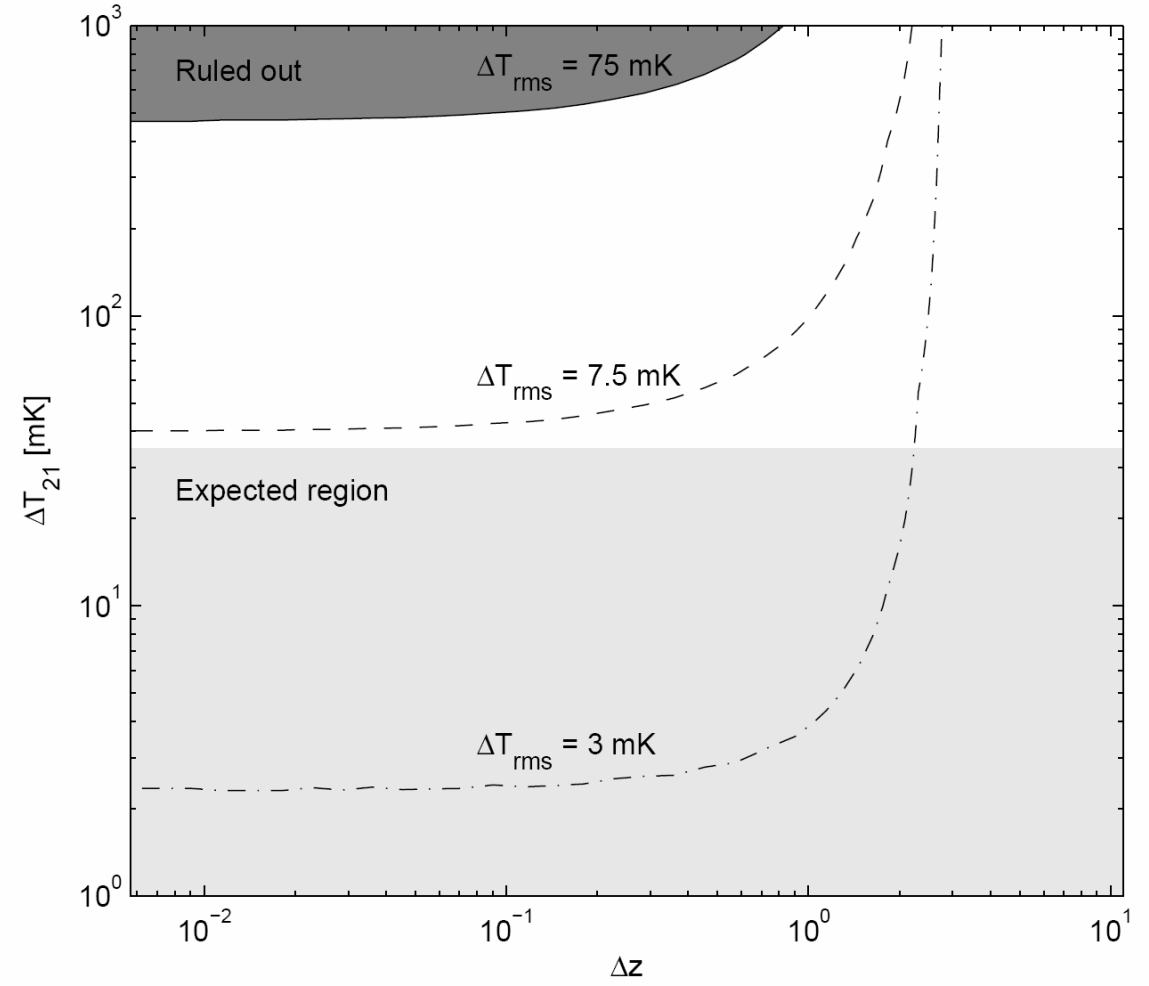

- First results only rule out extreme cases.

Global Signals

- In principle, a single dish telescope could measure the change of the global signal with frequency: contrary to early expectations, however, simulations do not show a sharp transition.
- The corresponding measurement by an interferometer would be the change of the 21cm (rms) fluctuations.
- Simulations: 64Mpc_f100_f250S_432 and 64Mpc_f100_f250S_216

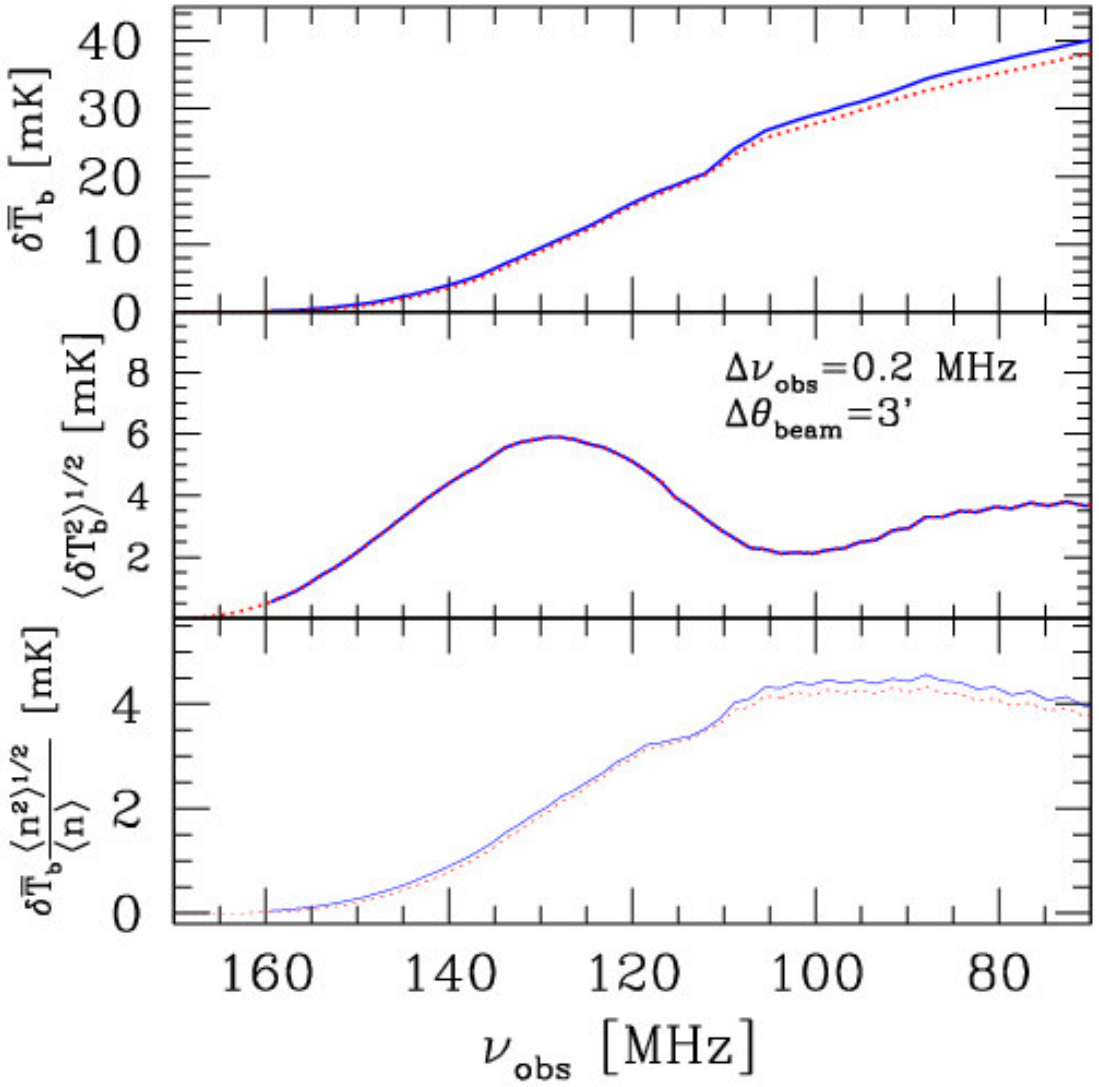

Evolution of 21cm Brightness Temperature Fluctuations

- When plotted against the mean mass-weighted ionization fraction x_m(H II), the evolution of fluctuations shows roughly similar behaviour for different (simulation) resolution and source parameters, but the amplitude differs.
- Peak around x_m(HII)~0.6-0.7 (shifts to lower values for higher angular resolution).

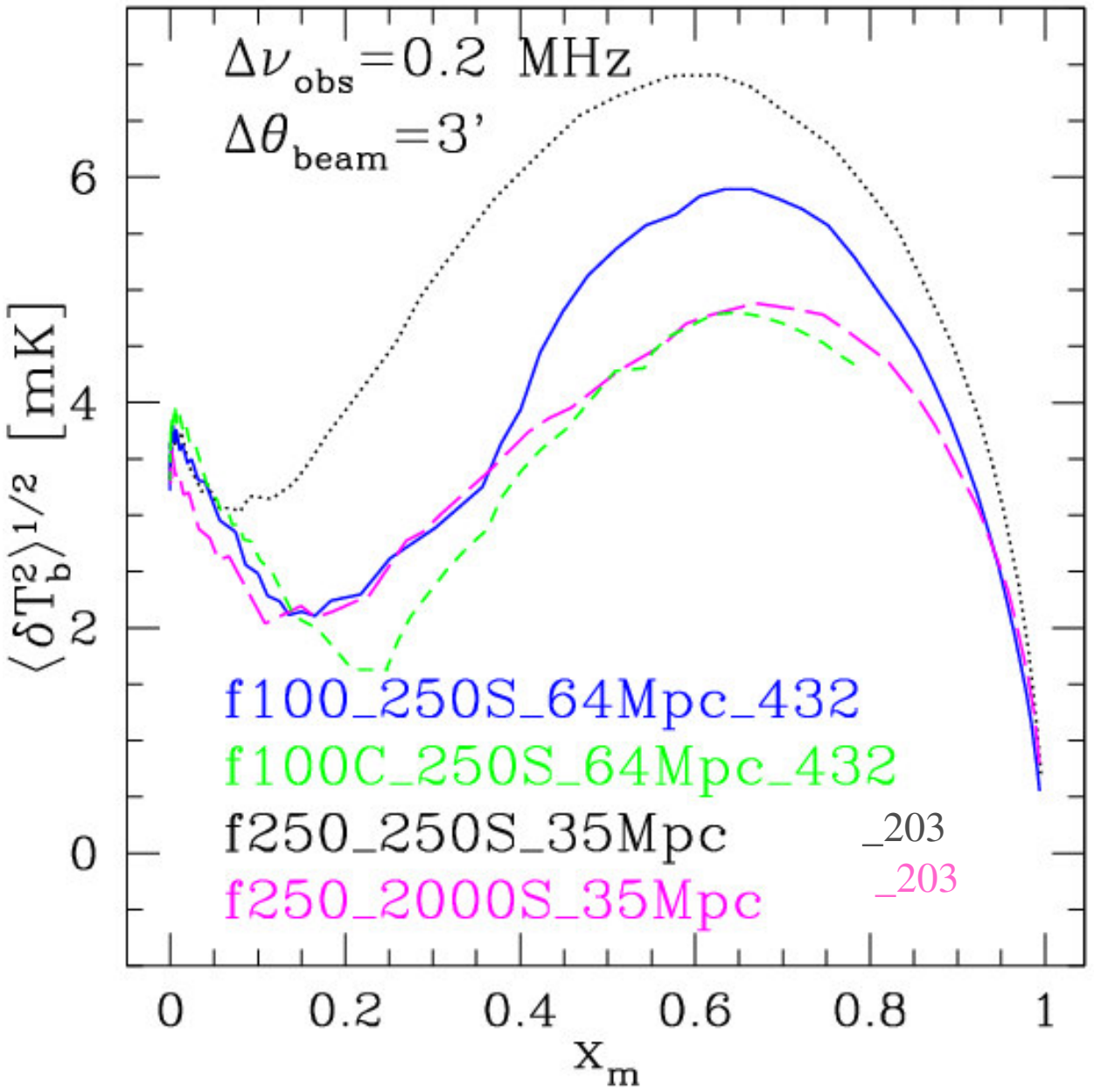

21cm Brightness Temperature Fluctuation Power Spectra

- Information about the length scales can be obtained from the power spectra.
- Power shifts to larger scales as reionization progresses, and the power spectrum flattens.
- Note that the angular power spectrum is measured directly by an interferometer, the multipole l is equivalent to $\sqrt{(u^2+v^2)}$ in a visibility map.

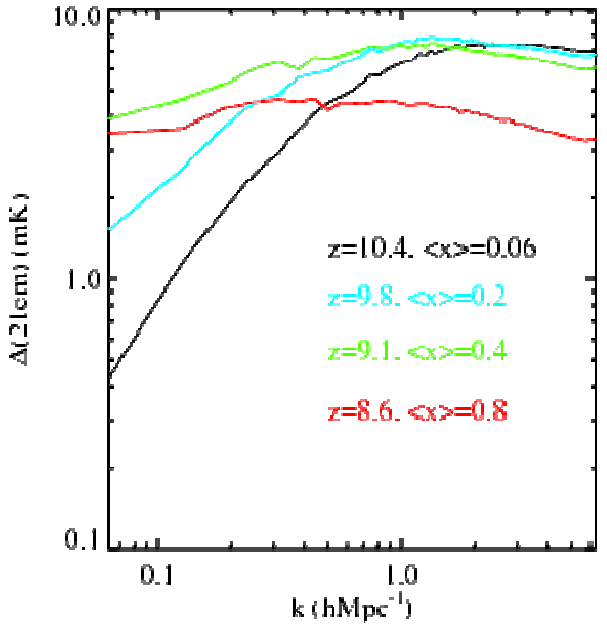

100Mpc_f250C_f0_203

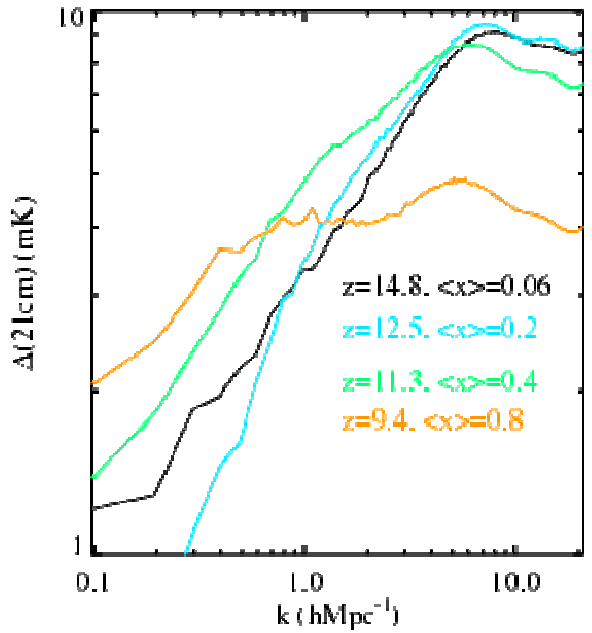

64Mpc_f100_f250S_432

Observability of the 21-cm signal : 3D power spectrum of the neutral hydrogen density

- We show our predicted 21-cm signal at z = 8.6 (x ~ 0.5) for case with z_{ov} = 6.6, with GMRT sensitivity, for 100 hrs integration, 15 MHz bandwidth and T_{sys} = 480 K, pointing at zenith.

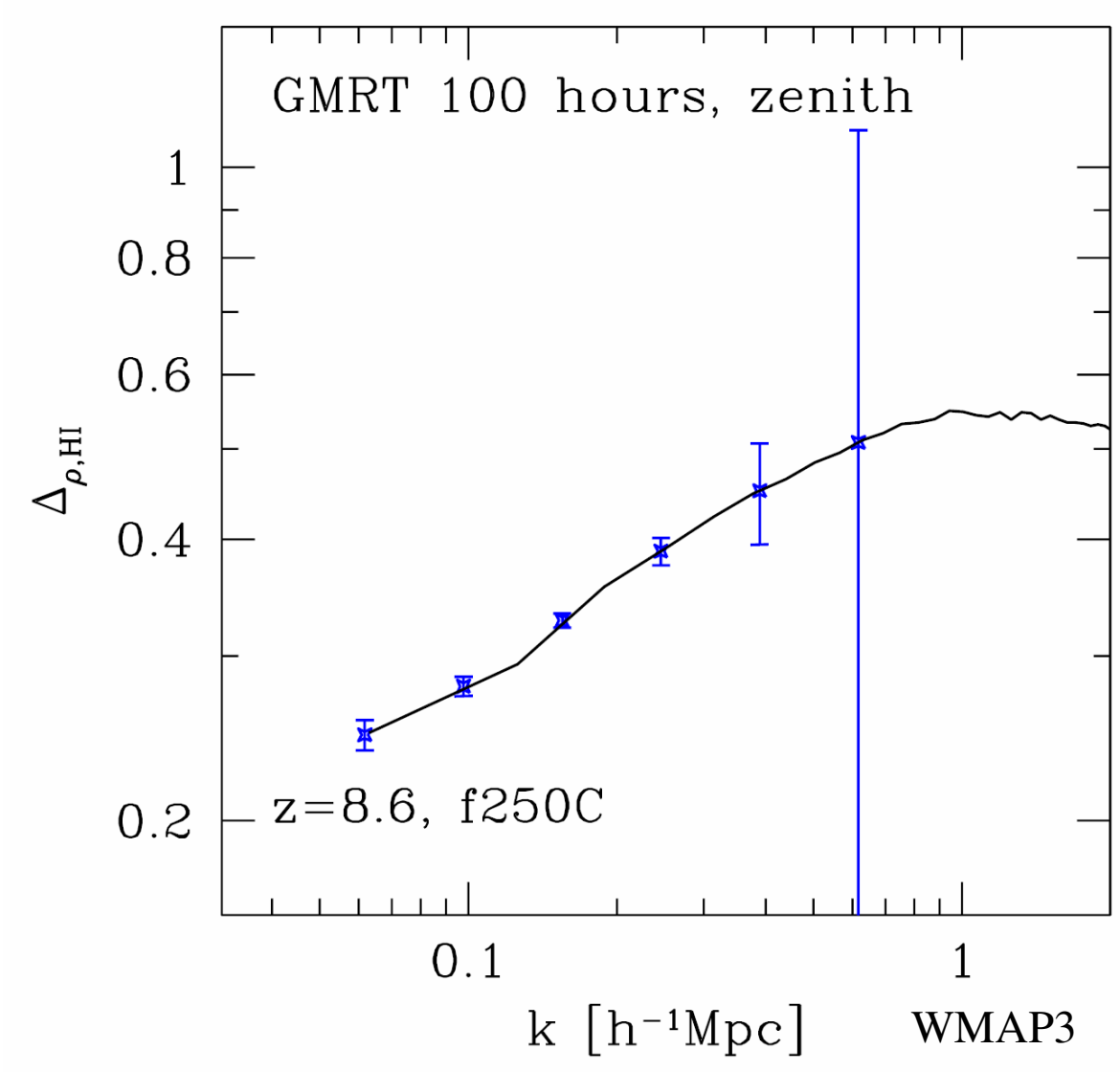

Measuring the History of Cosmic Reionization Using the 21cm PDF

Ichikawa, Barkana, Iliev, Mellema & Shapiro 2009, MNRAS, submitted (astro-ph/0907.2932)

- The **P**robability **D**istribution **F**unction (PDF) of 21-cm differential brightness temperature is a highly nonGaussian signature of the evolving patchy reionization during the EOR.
- Two peaks in PDF:

  $\delta T_b = 0$ mK (ionized regions)

  ≈ 20 mK (neutral regions)
- We use our reionization simulation of large volume 100/h comoving Mpc to predict this 21cm PDF and propose a simple empirical fit
- For the simplest parameterization, upcoming 21cm radio surveys like MWA can recover the reionization history to 1 – 10% accuracy at middle to late stages of EOR
- More realistic fits with more free parameters ➔ 2nd generation surveys

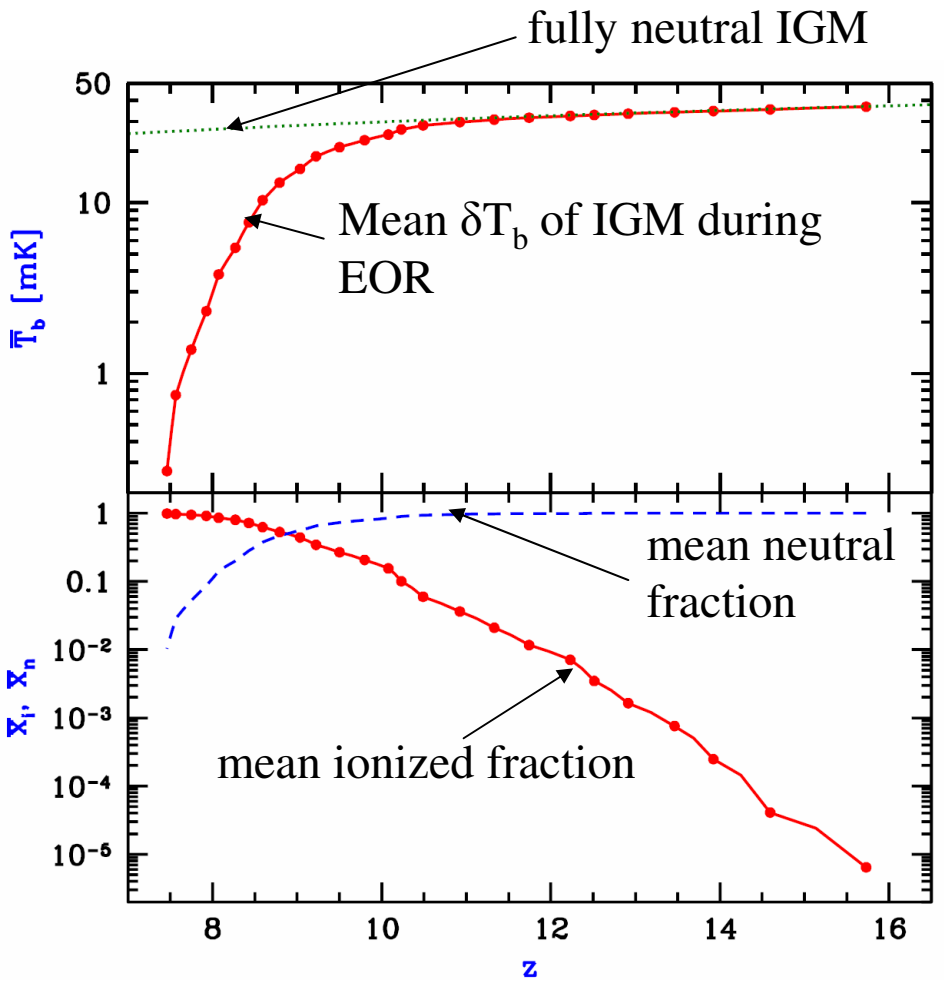

Measuring the History of Cosmic Reionization Using the 21cm PDF

Ichikawa, Barkana, Iliev, Mellema & Shapiro 2009, MNRAS, submitted (astro-ph/0907.2932)

- The **P**robability **D**istribution **F**unction (PDF) of 21-cm differential brightness temperature is a highly nonGaussian signature of the evolving patchy reionization during the EOR.
- Two peaks in PDF:

  $\delta T_b = 0$ mK (ionized regions)

  ≈ 20 mK (neutral regions)
- We use our reionization simulation of large volume 100/h comoving Mpc to predict this 21cm PDF and propose a simple empirical fit
- For the simplest parameterization, upcoming 21cm radio surveys like MWA can recover the reionization history to 1 – 10% accuracy at middle to late stages of EOR
- More realistic fits with more free parameters ➔ 2nd generation surveys

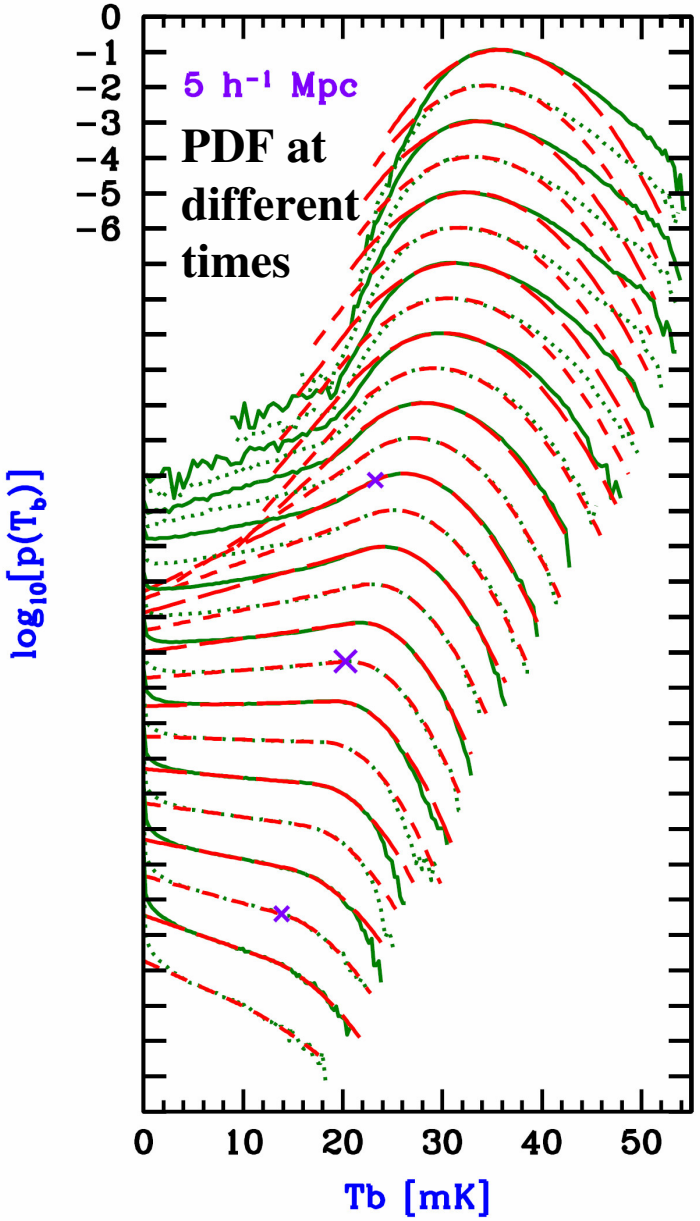

redshift slices from z = 15.7 to z = 7.5 (top to bottom)

x = 50 % at z = 8.8

simulation data smoothed in 5/h Mpc windows

Measuring the History of Cosmic Reionization Using the 21cm PDF

Ichikawa, Barkana, Iliev, Mellema & Shapiro 2009, MNRAS, submitted (astro-ph/0907.2932)

- The **P**robability **D**istribution **F**unction (PDF) of 21-cm differential brightness temperature is a highly nonGaussian signature of the evolving patchy reionization during the EOR.
- Two peaks in PDF:

  $\delta T_b = 0$ mK (ionized regions)

  ≈ 20 mK (neutral regions)
- We use our reionization simulation of large volume 100/h comoving Mpc to predict this 21cm PDF and propose a simple empirical fit
- For the simplest parameterization, upcoming 21cm radio surveys like MWA can recover the reionization history to 1 – 10% accuracy at middle to late stages of EOR
- More realistic fits with more free parameters ➔ 2nd generation surveys

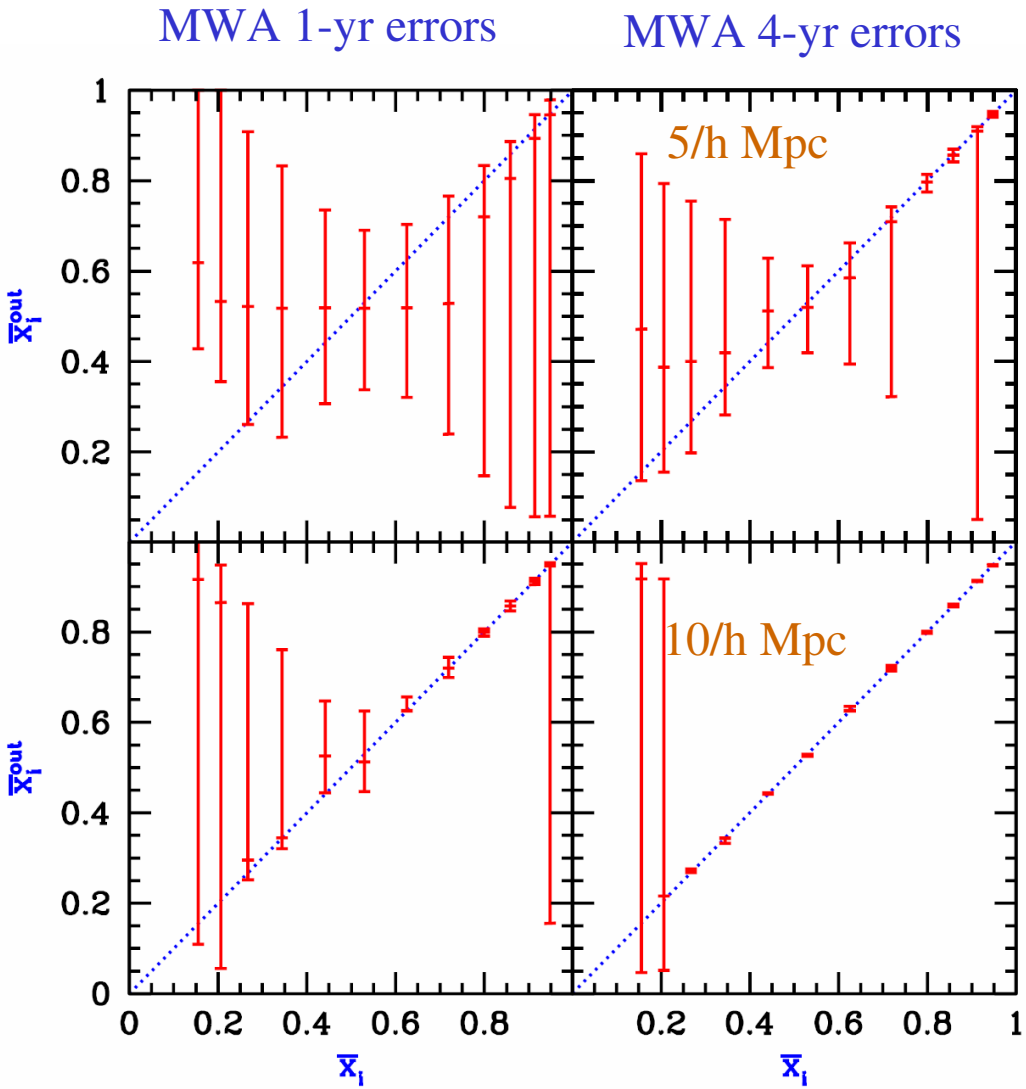

Median values measured by MWA for ionized fraction of universe (and 16 and 84th percentiles)